The long-term impacts of glacier retreat on runoff in the Waitaki Catchment, New Zealand

Joanna D. Borzecki

A thesis submitted to the Victoria University of Wellington
in fulfillment of the requirements for the degree of
Master of Science in Geophysics

School of Geography, Environment, and Earth Sciences
Victoria University of Wellington
2022

ABSTRACT

Runoff from the Waitaki catchment is relied upon for hydroelectricity generation and long-term water storage. The Waitaki catchment holds some of the country's largest glaciers. Ice melt contributes to runoff, along with snow melt and rainfall. Understanding the implications of climate change and glacier retreat on downstream hydrology is important for long-term water resource planning. Using an enhanced temperature index model coupled with an ice flow model, glacier mass balance within the Waitaki was projected through the 21st century for four future climate scenarios based on CMIP5.

Glacier volume in the Waitaki catchment is projected to decrease over the 21st century for all future climate scenarios by up to 86%. Average ablation is projected to begin earlier in spring and continue later into autumn by the end of the century. Conversely, average accumulation is projected to start later in autumn and end earlier in spring. These shifts become more pronounced with increasing severity of climate change scenarios. The largest increases in average rainfall and ablation are projected to occur in the winter and spring months when runoff is typically at its lowest, as a result of warmer winter temperatures.

Maximum ice melt contributions to runoff, known as peak water, are projected to occur before 2040 in the Waitaki catchment for all future climate scenarios. Before peak water is reached, increases in total ablation may mitigate the frequency and magnitude of low flow events during dry periods, but may also increase flood risks in and around the summer season when rainfall is high. Once peak water passes and ice melt contributions to runoff decrease, extreme low flow events may be more of a concern during dry periods with reduced rainfall.

Contents

List of Tables

List of Figures

ACKNOWLEDGEMENTS

I would first like to acknowledge my supervisors, Lauren Vargo and Ruschle Dadic for their continued mentorship throughout this past year. Lauren, you have made me feel welcome since my first day at VUW. Thank you for all your kindness, positivity, and support. I appreciate all the time you have spent with me working through modelling code or talking through various concepts and ideas. Thank you for letting me join you for the annual survey of mass balance at Brewster Glacier, that was a highlight I won't soon forget! Ruschle, thank you for sharing your wealth of experience and expertise with me. Your attention to detail and your thought-provoking insight has challenged me and enabled me to grow both as a scientist and as a writer. I would also like to thank Brian Anderson, for allowing me the opportunity to build on your existing research and for providing invaluable knowledge and guidance into the complexities of glacier modeling.

Thank you to the National Institute of Water and Atmospheric Research for providing me with funding to carry out this research through the Ministry of Business, Innovation, and Employment scholarship. Thank you to Antarctic Research Centre and the School of Geography, Environment and Earth Sciences for inviting me into their offices, letting me use their facilities, and welcoming me into their community.

I would also like acknowledge my original mentors, Drew Brayshaw and Eryne Croquet, for first exposing me to the wonderful world of glacier science. You nurtured my curiosity, fostered my professional development, and inspired me to pursue a postgraduate degree. To my parents, thank you for always encouraging me to follow my passions, regardless of the where that path may lead. To my friends, thank you for reminding me of my strengths and helping me celebrate little wins along the way.

Finally, I owe a special thank you to my partner Alex King for being my unwavering pillar of support, for providing me with endless encouragement, and most of all, for being my home and family, when home and family are a world away. Writing a thesis during a global pandemic would not have been possible without you.

Chapter 1

Introduction

Approximately two billion people live in or directly downstream of mountainous areas (Immerzeel et al., 2020), but more than half of the global population indirectly relies on runoff from mountainous regions for water supply (Beniston, 2003; Viviroli and Weingartner, 2004). With future population growth, the pressure on water resources around the world will increase.

Mountain regions are sensitive to climate change (Beniston et al., 1996; Viviroli et al., 2011; Rasouli et al., 2014; Immerzeel et al., 2020). Thus the impacts of climate change on downstream hydrology are likely to have significant repercussions in populated downstream areas that depend on mountain water for domestic, agricultural, energy, and industrial purposes (Arnell, 1999; Beniston, 2005). While runoff generation in mountain catchments is one of the most complex hydrological processes (Wilcox et al., 1991; Jakeman and Hornberger, 1993; Becker, 2005), understanding generating mechanisms and their implications on downstream hydrology is vital for informed planning of long-term water security.

Mountain runoff is generated by rainfall, snow melt, and ice melt, and each mechanism leads to a different downstream hydrological response (Woo and Liu, 1994; Aizen et al., 1996; Shanley et al., 2015). The dominant runoff process within a watershed is dictated by physical geography and climate (Falkenmark and Chapman, 1989). Glacierized catchments have particularly unique hydrological characteristics because glaciers store water in catchments far longer than rainfall or snow. As such, glaciers act as valuable long-term reservoirs of freshwater that exert a strong control on drainage characteristics such as annual and seasonal downstream runoff (Meier and Tangborn, 1961; Lang, 1986; Stenborg, 1970; Jansson et al., 2003; DeBeer et al., 2020). Storage and release of water from glaciers are important for water supply, hydroelectric power, agriculture, flood forecasting, sea level fluctuations, glacier dynamics, sediment transport, and landscape evolution (Jansson et al., 2003). In regions such as the Andes and the Himalayas, runoff from glacierized basins provides consistent flows for agriculture and irrigation, power generation, and ecosystem integrity (Vergara et al., 2007; Akhtar et al., 2008). In other regions like Switzerland, Canada, the United States of America, and New Zealand, many rivers used for hydropower are influenced by meltwater from seasonal snow and glaciers (Filion, 2000; Caruso et al., 2017; Cherry et al., 2017; Schaefli et al., 2019). In addition to their important role as water resources, glaciers are unique indicators of climate change (Oerlemans and Fortuin, 1992; Laumann and Reeh, 1993; Francou et al., 2005). The advance or retreat of a glacier over time is influenced by changes in climate. Glacier mass balance studies have found that rising air temperatures over the past century have driven a reduction in the area and volume of glaciers worldwide (Huss et al., 2017). Glaciers are continuing to exhibit historically unprecedented retreat with extreme mass-loss years becoming more prevalent in recent decades (Vargo et al., 2020). With warming of the global climate, glaciers are expected to change their water storage capacity with potential consequences for downstream water supply (Kaser et al., 2010; Marzeion et al., 2020).

The projected reduction in glacier mass in coming decades will have profound impacts around the globe, with downstream consequences on water resources, sea-level rise, and tourism (Purdie, 2013; Anderson et al., 2021). Changes in timing and volume of ice melt may pose several risks. High flows may cause flooding risks where glacier runoff contributions are still increasing, and low flows may threaten the ability to meet downstream water demands where glacier runoff contributions are waning (Huss and Hock, 2018; DeBeer et al., 2020). Snow and rainfall regimes are also highly sensitive to climate change, and can further complicate downstream hydrological responses by amplifying or dampening the effects of glacier loss (DeBeer et al., 2016). Even in catchments that are not heavily glacierized, the affect of glacier change on catchment runoff can have important consequences for long-term water resource planning (Meier, 1969).

1.1 Purpose and objective of study

In New Zealand, glaciers contain a small but important fraction of the country's water resources. While there are a few thousand individual glaciers across the Southern Alps (Baumann et al., 2020), catchments with the largest glaciers store the greatest volume of water (Chinn, 2001). Located on the southeast side of the Southern Alps of New Zealand, the Waitaki catchment is approximately 11900 km^2 in size and contains some of the country's largest ice masses including the Haupapa/Tasman, Murchison, Mueller, and Hooker Glaciers (Figure 1.1). Numerous smaller glaciers are also located within the basin. Runoff generated from ice melt, snow melt, and rainfall, is used to generate electricity through eight power stations located in the Waitaki catchment. Runoff is also stored in lake reservoirs to supply water to downstream users and agricultural operations throughout the year.

The Waitaki River catchment is one of New Zealand's primary sources of hydro-electricity and water storage. In 2010, hydroelectric power stations in the Waitaki catchment produced 35% to 40% of New Zealand's electricity (Purdie and Bardsley, 2010). The Waitaki catchment consists of three dammed glacial lakes (Pukaki, Tekapo, and Ohau) and three artificial lakes (Benmore, Aviemore, and Waitaki). Water from these lakes flows into the Waitaki River before draining at the east coast near Glenavy. The glacial lakes in the upper Waitaki basin account for nearly 60% of the controllable water storage available in the country (Sirguey, 2010). The glacierized upper Waitaki catchment provides nearly 80% of the inflow to the Waitaki River (Leong and Chesterton, 2005).

Understanding how climate change and glacier recession will affect future ice melt contributions to runoff is particularly important for long-term water resource planning in catchments used for hydro-electricity and water storage like the Waitaki. The aim of this research is to improve this understanding for the upper Waitaki catchment by analyzing projections of future climate and glacier mass balance to determine changes in downstream runoff.

To achieve this aim, the following research objectives are:

1. Investigate the annual changes of total ice volume within the Waitaki catchment through the period 2006 to 2098,

2. Determine how glacier mass balance processes, specifically accumulation and ablation, and rainfall processes will change through the century using daily and monthly time series analysis and,

3. Determine how changes to ablation could affect the timing and magnitude of runoff, and possibly downstream water availability

This thesis is structured into six chapters. Chapter 2 presents a background of catchment hydrology, climate change models, and modeling glacier mass balance. Chapter 3 outlines the methods used in this research and Chapter 4 presents the results. Chapter 5 discusses the findings and the implications to downstream runoff. Lastly, summary, conclusions, and recommendations are presented in Chapter 6.

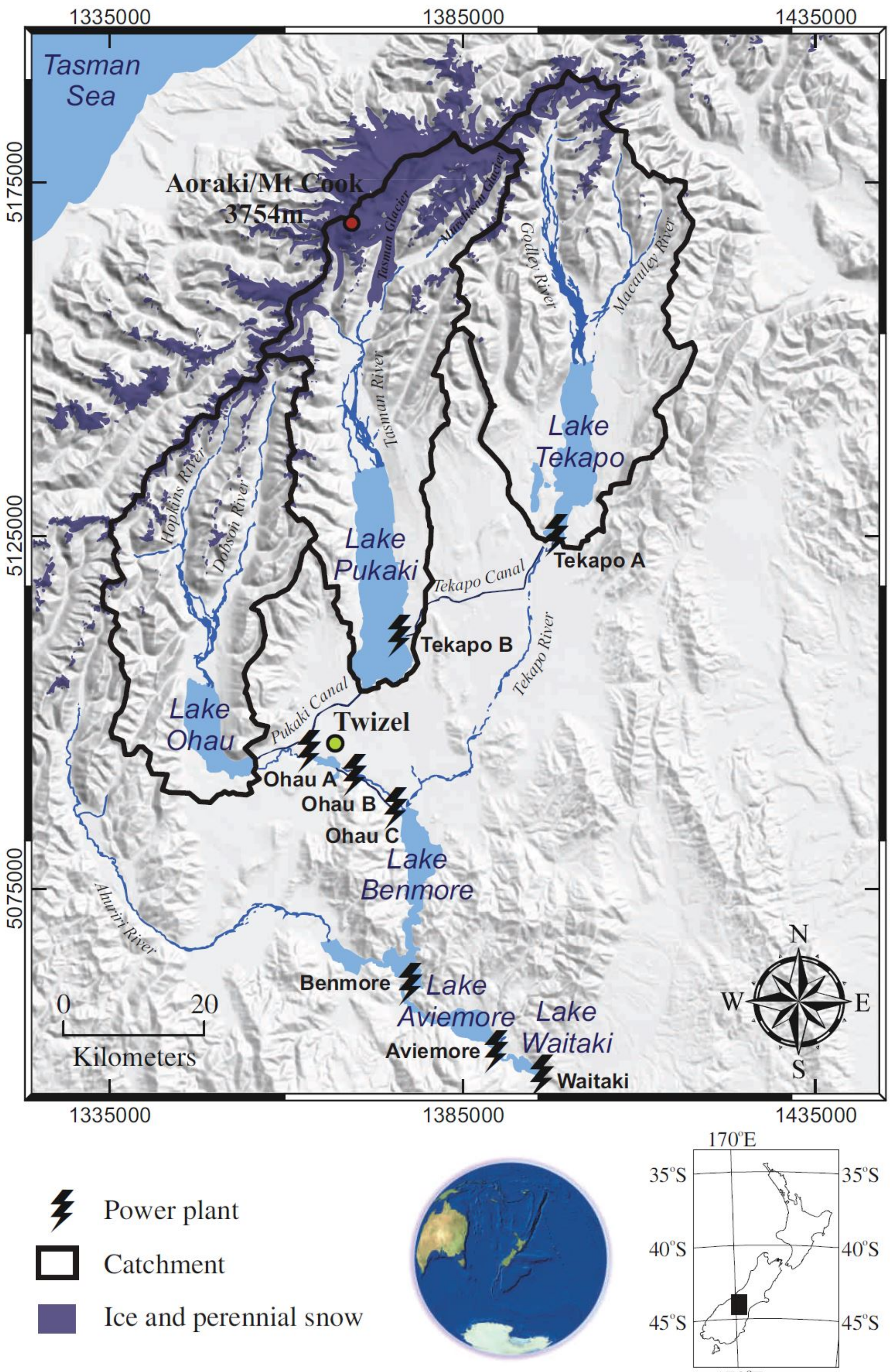

Figure 1.1: The upper Waitaki catchment, located on the South Island of New Zealand. Bold black lines indicate the three glacier lake sub-catchments within the Waitaki basin. Figure from Sirguey (2010).

Chapter 2

Background

To determine how climate change may affect runoff in glacierized catchments in the future, computer models are used to project future climate for different emission scenarios. The response of glacier mass balance to future climate scenarios is then simulated. The first section of this chapter describes runoff mechanism and the effect of glaciers on downstream hydrology. The second section explains climate models and how they are used in this research. The third section describes glacier mass balance and glacier mass balance models. Finally, findings from studies investigating the effect of climate change on glaciers in New Zealand and in the Waitaki catchment are summarised in the fourth section.

2.1 Catchment runoff

Understanding the processes that generate mountain runoff is important for long-term water resource planning. Watershed geography and climate influence what mechanisms generate runoff, whether this is through rainfall, snowmelt, and/or ice melt (Falkenmark and Chapman, 1989). Watershed runoff can therefore be rainfall dominated, snowmelt dominated, ice melt dominated, or a combination of all three processes.

Shanley et al. (2015) describes the characteristics of rainfall, snow melt, and ice melt dominated watersheds in temperate western North America (Figure 2.1). Rain-dominated catchments are low-land or are located in warm climates. Watershed runoff in rain-dominated catchments matches the annual pattern of rainfall. Snow melt-dominated catchments are characterised by a spring snowmelt peak in runoff, and minimum discharge in summer in this region. Interestingly, Figure 2.1 also shows an autumn peak in runoff in snow melt-dominated catchments, which may be a result of the transition in increasing precipitation from rain to snow. High elevation or cold climate watersheds that are highly glacierized export little water during winter and early spring, with main peak discharge occurring late spring to early fall (Shanley et al., 2015). The potential influence of large-scale atmospheric circulation seasonality could also be a factor that influences these hydrographs, especially in rain-dominated catchments (Manabe, 1969).

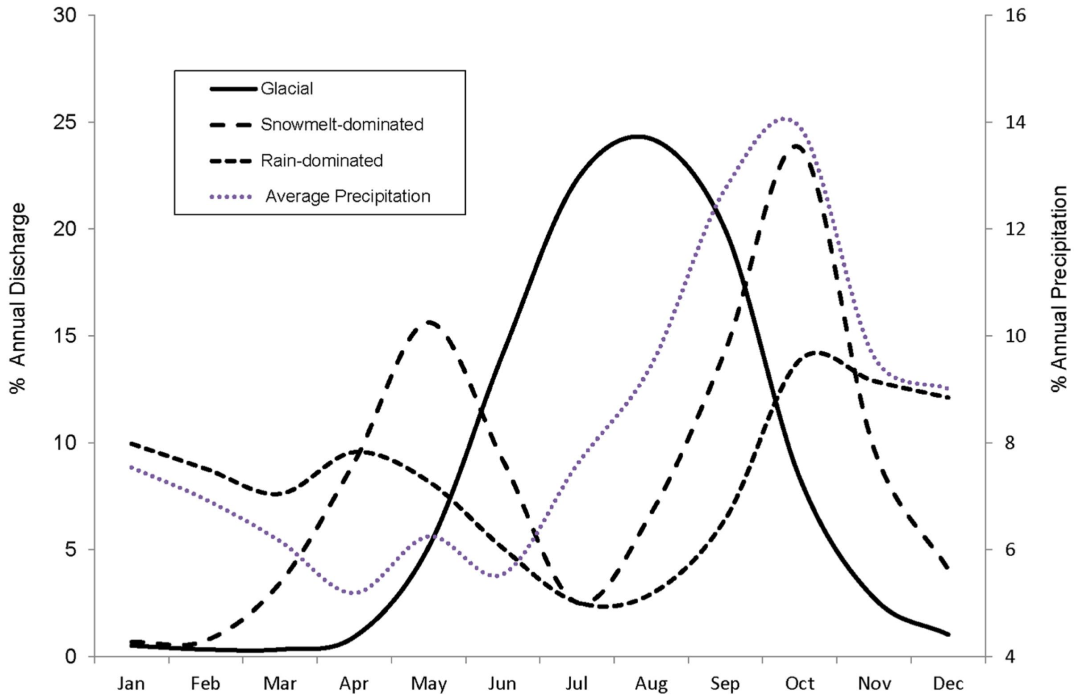

Figure 2.1: Characteristic hydrographs for the three watershed types (rain-dominated, snowmelt-dominated, and ice melt-dominated) during a northern hemisphere hydrological year. Hydrographs are long-term averages (30-60 years) from three individual representative streams in temperate western north America, compared to long-term average precipitation. Figure from (Shanley et al., 2015).

Glaciers affect catchment hydrology, such as annual and seasonal runoff (Meier and Tangborn, 1961; Fountain and Tangborn, 1985; Lang, 1986; Stenborg, 1970). In larger basins with sufficient elevation range to include ice melt- and rainfall dominated runoff, glacier runoff compensates for otherwise decreasing summer discharge (Fountain and Tangborn, 1985; Young and Hewitt, 1993; Jansson et al., 2003; Sirguey, 2010). As such, glaciers can help to sustain runoff during dry periods (Hopkinson and Young, 1998; Sirguey, 2010). Glaciers can also mitigate peak flows by delaying the time of maximum seasonal runoff, as spring melt water can be temporarily stored in glaciers and released later in the summer (Fountain and Tangborn, 1985).

New Zealand has a temperate maritime climate, with alpine climates on the South Island that support snow and ice cover, and extreme orographic effects (Collins, 2020; Salinger et al., 2004). As such, rainfall, snow melt, and ice melt contribute to the downstream hydrological response of watershed runoff in many catchments on the South Island. Specifically, melt from snow and ice compose up to 17% of runoff from catchments on the South Island (Kerr, 2013). As climate changes, runoff contributions for any given watershed may shift. With increasing temperature, snow melt contributions to runoff may decrease while rainfall contributions to runoff increase. The contribution of ice melt to runoff in a glacierized catchment will decrease as glaciers recede or disappear (Jansson et al., 2003; Huss and Hock, 2018). As a result, seasonal shifts and changes in magnitude of peak and low flows may occur that have otherwise been uncharacteristic to that catchment.

The change in glacier mass and the downstream hydrological response is influenced by changes in climate (Oerlemans and Fortuin, 1992; Laumann and Reeh, 1993; Francou et al., 2005; Vargo et al., 2020). To understand how glacier retreat and downstream runoff will respond to climate change in the future, computer models are used. Climate models are fundamental in providing projections of future glacier mass and ice melt contributions to runoff over the next century.

2.2 Climate change projections

2.2.1 General circulation models

Climate models are fundamental tools of modern climate science (Edwards, 2011) and are a critical component of projecting future changes in glaciers. As climate research progresses, numerous organisations around the globe continue to develop and advance these models to better simulate future environments. Since the 1950s, computer models have simulated global general circulation patterns that distribute heat and energy across Earth (Edwards, 2011). General Circulation Models (GCMs) are representations of Earth's energy balance fluxes which influence global climate (Figure 2.2).

The atmosphere, ocean, land surface, and cryosphere are components of the energy balance that affects the distribution of energy and heat around the globe (Trenberth et al., 2009). The energy balance is affected by clouds and aerosols concentrations in the atmosphere, currents in the ocean, changes to land-use or vegetation cover on the land surface, and the amount of radiation absorption or emission influenced by snow and ice cover in the cryosphere (Kiehl and Trenberth, 1997; Trenberth et al., 2009; Wild et al., 2013). Earth's temperature is stable when the incoming and outgoing energy is balanced. Due to the increase of greenhouse gases in the atmosphere, Earth is experiencing an energy surplus with an extra 0.5 to 1 watts per meter squared presently being absorbed (Trenberth et al., 2009; Hansen et al., 2011; Trenberth et al., 2014).

GCMs use large three-dimensional grids or a mesh to simulate energy balance

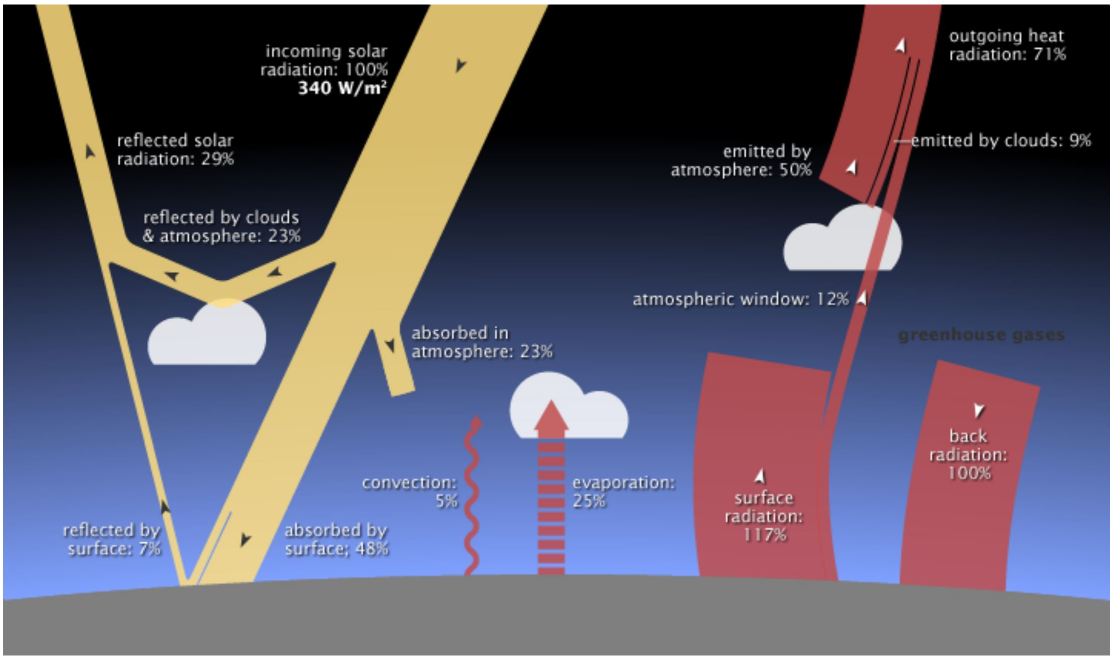

Figure 2.2: Global energy balance showing the balance of incoming and outgoing of radiation. Figure from Lindsey (2009).

processes in the atmosphere, ocean, land, and cryosphere on a global scale. GCMs models are the most advanced tools currently available for simulating the global climate system's response to increasing greenhouse gas concentrations (IPCC Data Distribution Centre, n.d.).

Due to the number of organisations or groups producing climate models, a standardised framework was developed to allow GCMs to be analysed, validated, and improved. As a result of this need, the Coupled Model Intercomparison Project (CMIP) was established by the Working Group of Coupled Modelling (WGCM) within the World Climate Research Programe (WCRP) in 1995 to study and intercompare climate simulations made by GCMs (Meehl et al., 2000). The CMIP provides boundary conditions for GCMs so that outputs can be compared. Since its creation, CMIP has evolved over six phases and has held a central place in reports from the Intergovernmental Panel on Climate Change (IPCC) (Touzé-Peiffer et al., 2020).

The Intergovernmental Panel on Climate Change is the United Nations body for assessing the science related to climate change. The IPCC was created to provide policymakers with regular scientific assessments, on climate change, its implications and potential future risks, as well as to put forward adaptation and mitigation options (IPCC, n.d.). These findings are summarised in comprehensive "Assessment Reports" that are periodically released by the IPCC as climate science progresses. This research uses GCMs comprising CMIP5, relating to the IPCC Fifth Assessment Report, for climate change projections.

2.2.2 Representative concentration pathways

Within CMIP5, GCMs simulate four possible future climate scenarios. These scenarios are referred to as Representative Concentration Pathways (RCPs) and they describe four different 21st century trajectories of greenhouse gas emission concentrations (Stocker et al., 2013). The different pathways represent variations in population growth, technology advancements, energy consumption, land use patterns, and adherence to climate policy. The four CMIP5 scenario runs are used as the basis for exploring climate change impacts and policy to society (Taylor et al., 2012).

Radiative forcing is a change in energy flux resulting from different natural and anthropogenic factors that affect or drive climate change (Forster et al., 2007). The RCPs represent the amount of possible radiative forcing by the end of the century relative to pre-industrial levels, measured in watts per meter squared (W/m^2) (Van Vuuren et al., 2011).

The RCP2.6 scenario indicates an increase in global absorbed energy, with a radiative forcing peak of approximately 3.0 W/m^2 before 2100, then declines and stabilises at 2.6 W/m^2 by 2100 (Stocker et al., 2013). The RCP2.6 scenario is representative of stringent measures with high compliance aimed to keep global warming below 2°C above pre-industrial temperatures (Van Vuuren et al., 2011). The RCP4.5 and RCP6.0 scenarios represent a stabilization of radiative forcing of 4.5 W/m^2 and 6.0 W/m^2 after 2100. The RCP8.5 scenario represents an environment where radiative forcing is larger than 8.5 W/m^2 by 2100, and continues to rise afterward (Stocker et al., 2013). Scenarios without additional efforts to constrain present emissions rates lead to pathways ranging between RCP6.0 and RCP8.5. The effect of these changes on global temperature and sea level rise are shown in Table 2.1.

Table 2.1: The IPCC's fifth assessment report on climate change shows the change in temperature and sea level relative to pre-industrial times (between 1850-1900) that would result under each of the four RCP scenarios modelled in CMIP5 (Edenhofer et al., 2014).

		2046–2065		2081–2100	
	Scenario	**Mean**	***Likely* range [c]**	**Mean**	***Likely* range [c]**
Global Mean Surface Temperature Change (°C) [a]	RCP2.6	1.0	0.4 to 1.6	1.0	0.3 to 1.7
	RCP4.5	1.4	0.9 to 2.0	1.8	1.1 to 2.6
	RCP6.0	1.3	0.8 to 1.8	2.2	1.4 to 3.1
	RCP8.5	2.0	1.4 to 2.6	3.7	2.6 to 4.8
	Scenario	**Mean**	***Likely* range [d]**	**Mean**	***Likely* range [d]**
Global Mean Sea Level Rise (m) [b]	RCP2.6	0.24	0.17 to 0.32	0.40	0.26 to 0.55
	RCP4.5	0.26	0.19 to 0.33	0.47	0.32 to 0.63
	RCP6.0	0.25	0.18 to 0.32	0.48	0.33 to 0.63
	RCP8.5	0.30	0.22 to 0.38	0.63	0.45 to 0.82

Determining which RCP scenario is most plausible is dependent on how socio-economic parameters evolve or improve and thus is the subject of ongoing research. One recent study suggests that most plausible scenarios project emissions trajectories to 2100 are consistent with 3.4 W/m^2 or 2.0°-2.4°C of warming (Pielke et al., 2021).

2.2.3 Regional climate model

Due to the low spatial resolution (approximately 200 km) of GCMs, meaningful high-resolution climate data cannot be provided for New Zealand from GCM output. However, understanding regional variability is important for local government in developing climate change response plans (Ackerley et al., 2012). Two methods were developed to increase the resolution of the GCM output so that it can be applied on smaller, regional scales: statistical downscaling and dynamical downscaling.

Statistical downscaling involves using techniques like regression equations to determine relationships between large-scale climate circulation and local-scale climate variations using historical data (Ackerley et al., 2012). GCM data is used as boundary conditions together with the regression equations to interpolate small-scale model output. Dynamical downscaling uses Regional Climate Models (RCMs) to interpolate higher-resolution climate data from GCMs. GCM data (such as temperature, moisture, wind circulation, and sea surface temperature) is supplied to RCMs as boundary conditions, and then regional-scale climate is modelled (Rummukainen, 2010).

The National Institute of Water and Atmospheric Research (NIWA) uses both statistical and RCM dynamical downscaling to simulate climate over New Zealand. For statistical downscaling, NIWA generates regression equations and then uses forty-one GCMs, stratified by season, to describe how monthly temperature and precipitation vary with large-scale climatic and circulation features (Ministry for the Environment, 2018). Out of those forty-one GCMs, six representative GCMs were selected to drive the RCM over New Zealand (Table 2.2).

The six GCMs used in RCM dynamical downscaling were selected to validate well on present climate and to be as different as possible to capture a range of model sensitivities (Ministry for the Environment, 2018). Model output data is downscaled to a five kilometre grid and bias-corrected relative to a 1986–2005 climate (Ministry for the Environment, 2018). Bias correction and downscaling procedures are performed separately on regional climate model (RCM) data for the primary climate variables of minimum and maximum temperature and precipitation (Ministry for the Environment, 2018).

Table 2.2: The six CMIP5 General Circulation Models used to generate NIWA's Regional Climate Models.

1	BCC-CSM1.1
2	CEM1-CAM5
3	GFDL - CM3
4	GISS-E2-R
5	HadGEM2-ES
6	NorESM1-M

Using these downscaling techniques, the four RCP projections from six representative GCMs can be used to determine how climate change may affect New Zealand on a regional scale.

2.3 Glacier mass balance

Glacier mass balance is the change in the mass of a glacier over a given time period (Cogley et al., 2010). Glacier mass balance can provide information about the amount of water stored or released by a glacier over that given time frame. Glaciers are known indicators of climate change (Oerlemans and Fortuin, 1992; Laumann and Reeh, 1993; Francou et al., 2005) and thus one of the main motives of early mass-balance studies was to further understand the relationship between the glaciers and the climate (Braithwaite and Zhang, 1999).

Mass balance describes the change in mass of a glacier driven by accumulation and ablation process over a given time (Cogley et al., 2010). The accumulation area of a glacier is where there is a net increase in mass for a given mass balance year (Figure 2.3). In this research, snow fall is considered the only input to the accumulation area. Other mechanisms for gaining mass can include avalanche deposition and wind blown snow (Benn and Lehmkuhl, 2000; Dadic et al., 2010; Laha et al., 2017). The ablation area is where a net decrease in mass occurs as a result of ice melt in a given time period. The two areas are separated by the Equilibrium Line Altitude (ELA) (Hambrey et al., 2004). The ELA represents the location and elevation where annual mass balance is equal to zero. The position of the ELA is different every year, and its movement up or down a glacier indicates the trend toward a positive or negative mass balance over time.

Several methods to measure glacier mass balance have been developed over time. These methods range from physical measurements of ice surface changes, snow depth, or water inflow and outflow, to using remote technology designed to capture changes in ice elevation, and to models that simulate physical and climatic processes. One of the original methods of measuring glacier mass balance

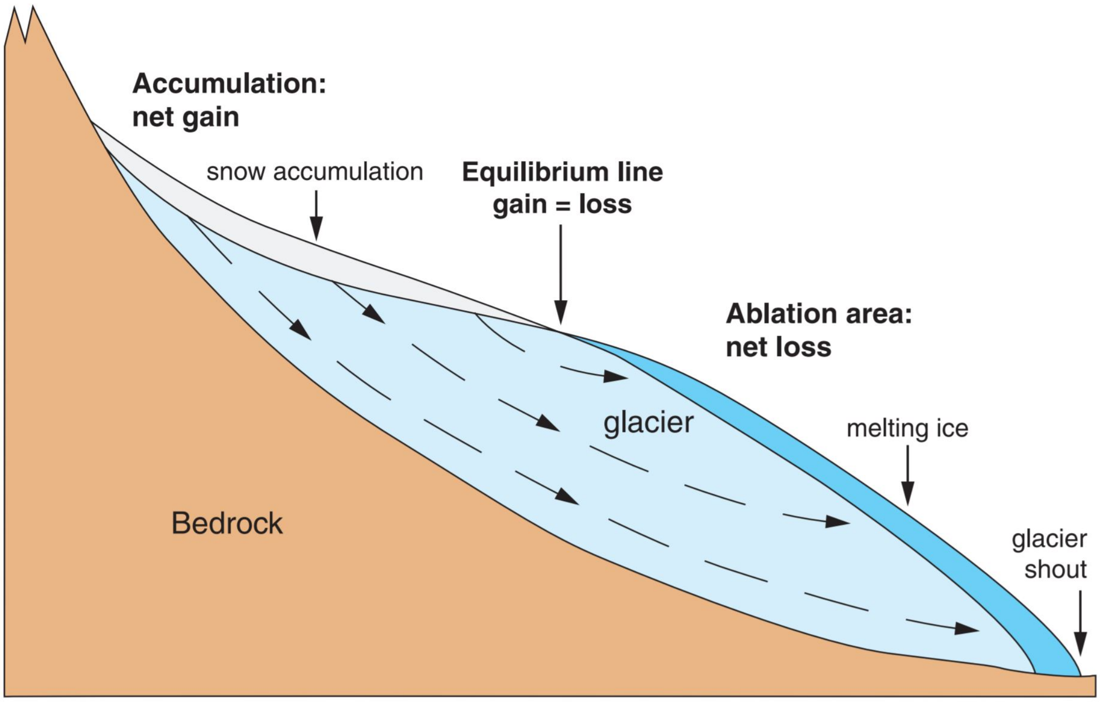

Figure 2.3: The processes of glacier surface mass balance. The accumulation area is where there is a net gain in glacier mass, and the ablation area is where there is a net loss. The two areas are delineated by the Equilibrium Line Altitude (ELA). Figure from Hambrey et al. (2004).

is the classic glaciological method (Østrem and Brugman, 1966). The glaciological method estimates the loss or gain in mass over the whole glacier surface from field measurements obtained from stakes in the ablation area and snow pits, drilled cores, or stakes in the accumulation area (Soruco et al., 2009). Typically, field measurements are taken twice per year: once at the end of winter when the glacier is at its maximum annual mass, and once at the end of summer when the glacier is at its minimum annual mass. During the winter measurements, ablation stakes are drilled into the ice. Snow pits are dug to measure snow depth and density in various representative locations. During the summer measurements, the portion of the ablation stakes that was exposed from melt is measured from the new ice surface. Annual accumulation and ablation can then be extrapolated across the rest of the glacier surface by using elevation gradients to determine annual surface mass balance. In New Zealand there are only two glaciers with ongoing measurements using the glaciological method: Brewster Glacier (Figure 2.4) and Rolleston Glacier (Vargo et al., 2020).

Other common methods for measuring glacier mass balance include the hydrological method, the geodetic method, the ELA method, and the process-model method (Cuffey and Paterson, 2010). The hydrological method measures water flowing to and from the glacier (as precipitation and runoff, respectively) to

Figure 2.4: Photos from the 2021 end-of-summer mass balance survey of Brewster Glacier using the glaciological method.

calculate a water balance. The water balance of a glacier can then be used to calculate the glacier mass balance (Bhutiyani, 1999; Braithwaite, 2002). The geodetic method uses techniques to measure changes in the glacier surface altitude by comparing two measurements made at two different times (Cogley, 2009; Soruco et al., 2009). The geodetic method techniques include repeat photogrammetry, ground surveys, airborne or satellite laser altimetry and satellite interferometric radar (Cuffey and Paterson, 2010). The ELA method uses aerial reconnaissance techniques to determine snowline at the end of the glacier melt season (Kulkarni, 1992; Chinn, 1995, 2001; Chinn et al., 2012). The known correlation between snowline and annual mass balance is used to calculate glacier mass balance (Østrem, 1975). Lastly, the process-model method uses meteorological models for explicit calculations of the surface mass exchanges that are driven by observations of local climatic variables (Cuffey and Paterson, 2010).

2.4 Modelling glacier mass balance

This research aims to understand the impact of climate change on glaciers using the process-model approach to project mass balance into the future. To accurately model glacier mass balance, the climatic processes and variables that drive or influence mass changes must be defined. Precipitation, radiation, and air temperature are important factors in modeling mass balance (Hock, 1999). Other important factors include turbulent fluxes of heat and moisture, and energy used for heating up the upper snow or ice layers (Oerlemans and Fortuin, 1992). The type of mass balance model used depends on the desired complexity, and what climatic information is available. As a result, two models have evolved in recent years: temperature index models (also known as degree day models) and energy balance models (Paul et al., 2008).

A temperature index or energy balance model can either be a point-scale model, or a distributed model which is comprised of many point models (Arnold et al., 1996; Carenzo, 2012). Point-scale models estimate the change in mass balance or melt on a single point on the glacier surface often where data is available, like a climate station (Arnold et al., 1996). Distributed models use a grid or mesh system to calculate changes at multiple locations across the glacier. The foundation of all distributed mass balance models is a Digital Elevation Model (DEM) that allows the "distribution" of point measurements (like climate data from weather stations) across the glacier surface (Paul et al., 2008). Distributed models are preferred as they take account of the special distribution of mass balance over the whole glacial area (Braithwaite and Zhang, 1999). There has been much effort focused on enhancing spatial and temporal resolution of melt models by moving from point-scale to distributed modelling (Hock, 2005).

2.4.1 Energy balance models

Energy balance models use a physically based approach to compute melt which involves the assessment of energy fluxes to and from the glacier surface (Arnold et al., 1996). Surplus energy at the surface is used to raise the temperature, then once ice or snow reaches 0°C, any remaining energy drives melt (Hock, 2005). The energy balance method requires a large amount of meteorological input data (Paul et al., 2008). Cuffey and Paterson (2010) expresses the energy balance of a glacier as:

$$E = E_{Sin} + E_{Sout} + E_{Lin} + E_{Lout} + E_G + E_H + E_E + E_P \tag{2.1}$$

Where E is the energy available for melting. E_{Sin} and E_{Sout} are incoming and outgoing shortwave (solar) radiation, and E_{Lin} and E_{Sout} are ingoing and outgoing longwave radiation. E_G is the subsurface or ground heat flux, i.e., the change in heat of a vertical column from the surface to the depth at which vertical heat transfer is negligible (Hock, 2005), and E_H and E_E represent the sensible and latent heat fluxes due to turbulent mixing of air adjacent to the surface. Lastly, E_P represents the heat flux from precipitation (Cuffey and Paterson, 2010).

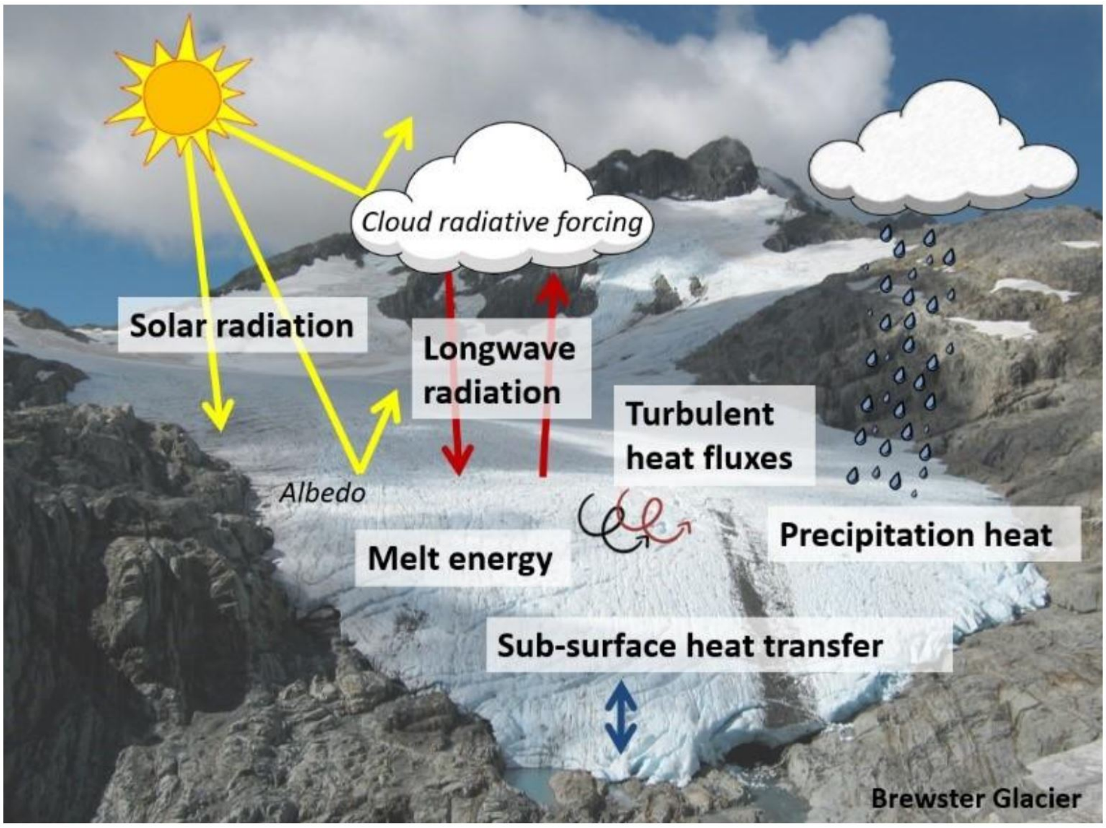

Figure 2.5: The components of the energy balance represented on Brewster Glacier (Conway, 2019).

Shortwave radiation is energy supplied to the glacier surface from the sun and varies depending on the albedo of glacier ice or on debris cover over ice. Shortwave radiation consists of direct radiation and diffuse radiation. Direct solar radiation is shortwave radiation that reaches the glacier surface unobstructed. Direct radiation reaching a glacier varies considerably in space and time. The slope and aspect of the glacier, along with the relief of the surrounding topography may affect how shaded a glacier is through the year (Corripio, 2003). The location and angle of the sun throughout the year also affect direct radiation (Hock, 2005). Conversely, diffuse radiation is shortwave radiation that is scattered by clouds, aerosols, or by surrounding slopes (Gu et al., 2002).

Longwave radiation originates from the atmosphere or terrain surrounding a glacier (Hock, 2005). Longwave radiation can originate from adjacent valley or rock walls, or from cloud cover or air above a glacier. Humid air emits more longwave radiation than dry air. As such, glaciers in temperate climates will therefore experience more longwave radiation than glaciers or ice sheets located in unconfined areas or in dry climates (Hock, 2005; Sicart et al., 2006). The sum of all incoming and outgoing shortwave and longwave radiation is called the net radiation (Cuffey and Paterson, 2010).

Sensible heat flux is energy transferred from one material to another, or from the atmosphere to ice. Temperature and wind play a role in the amount of sensible heat available for transfer. Latent heat is the energy released or absorbed during a change of state (melting, freezing, sublimation, or condensation). Together, sensible and latent heat fluxes are also known as turbulent heat fluxes. Lastly, the energy supplied by precipitation, such as rain, may affect the melt of a glacier.

The main advantage of energy balance models is that their strict, process-based physical rules allow their application to large regions. Their major disadvantage is the large amount of (meteorological) input data they require (Hock, 2003).

2.4.2 Temperature index models

Temperature index or degree-day models use the relationship between ice melt and air temperature to determine glacier mass balance (Braithwaite, 1984; Reeh, 1991; Jóhannesson et al., 1995; Hock, 2003). Temperature index models use temperature to calculate snow and ice melt across a glacier (Braithwaite and Zhang, 1999). The melting of snow and ice is assumed to be related to air temperature as long as air temperature is above a threshold of 0°C, representing the melting point of ice (Braithwaite, 1984).

The classic degree day model is often expressed as:

$$M = \begin{cases} f_m(T_d - T_0), & T_d > T_0 \\ 0 & T_d \leq T_0 \end{cases} \tag{2.2}$$

Where M is daily melt, T_d is daily mean temperature, T_0 is a threshold temperature (0°C) beyond which melt is assumed to occur, and f_m is a melt factor (Hock, 2003), otherwise known as the melt coefficient, degree-day factor, or temperature factor (mm day^{-}1 °C^{-}1).

In this case where T_0 is 0°C, the relationship between T_d and T_0 represents a positive degree day (PDD). Positive degree day is a derived unit equal to the difference between the daily temperature above the threshold temperature and the threshold temperature itself, averaged over one day (Cogley et al., 2010). Therefore, the positive degree day sum is the sum of all average daily temperatures above T_0 for a given time period, often over a year. The PDD or PDD sum represents the potential energy for melting (Huybrechts and Oerlemans, 1990).

The degree day factor (f_m) is the amount of melt that occurs per positive degree day (mm day^{-}1 °C^{-}1). This value is different for any given glacier and sometimes any given site on a particular glacier. There are two ways of obtaining the degree day factor, the first is from direct measurements using snow lysimeter outflow or ablation stakes, and the second being through energy balance computation (Kustas et al., 1994; Braithwaite et al., 1998; Hock, 2003). Variations in degree day factors can be attributed to the variations in energy components providing energy for melt (Hock, 2003). For example, maritime environments are likely to have lower degree-day factors than continental climate regions and vice versa (Ambach, 1988; Hock, 2003). It should also be noted that while daily time intervals are most commonly used to determine degree day factors, other time intervals (such as hourly or monthly intervals) can also be used (Hock, 2003).

The above degree day equation can be further simplified to:

$$M = M_T T \tag{2.3}$$

Where M is the daily melt, M_T represents the melt factor, and T is the daily sum of positive air temperatures.

The simplicity of the classic temperature index model makes it easy to apply because it does not require large amounts of input data, but there are also drawbacks to this approach. Hock (1999) noted that the classic temperature index approach does not capture the diurnal variations of glacial runoff. In addition, the model calculated an unrealistic rate of melt for glaciers in complex terrain because the influence of topography (slope, aspect, and shading of glacier) is not considered.

2.4.3 Enhanced temperature index models

Hock (1999) described a new enhanced approach to the classical temperature index method to overcome the shortcomings with respect to spatial and daily variability of glacial melt rates. Shortwave radiation strongly influences melt rates, but is also largely affected by atmospheric conditions and by local topography, particularly in high mountainous regions (Hock, 1999). Enhanced temperature index models therefore incorporate solar radiation into their computations by using DEMs. In doing so, enhanced degree day models combine the lower data requirement of degree day models with the high accuracy of energy balance models (Carenzo et al., 2010).

The enhanced degree day method used in this research, as described by Anderson et al. (2021) and Vargo et al. (2020), is expressed as:

$$M = M_T T + M_R (1 - a) Q \tag{2.4}$$

Where M is glacial melt, M_T is a temperature (degree day, or melt) factor, T is the daily sum of positive air temperatures, M_R is a radiation factor, a is albedo, and Q is the clear sky incoming shortwave radiation which combines diffuse and direct components (Anderson et al., 2021; Vargo et al., 2020). As in the classic degree day model, melt is calculated only when daily temperature is above 0°C.

Several variations of enhanced degree day models exist as more variables from the energy balance method are added. For example, in some enhanced degree day models, reduction of potential clear-sky direct radiation due to clouds is neglected to avoid the need for additional meteorological input (Hock, 1999). The model used in this research includes a cloud cover factor.

In summary, the ideal model for any given scenario, whether it is the energy balance, degree-day, or enhanced degree day approach, depends on the type of meteorological information available, the scale of research (one glacier versus regional scale), and the desired complexity.

2.4.4 Accumulation

Energy balance models, temperature index models, and enhanced temperature index models are three common methods to model the melt of a glacier. Regardless of which melt model is used, accumulation must be factored into compute glacier mass balance.

Cogley et al. (2010) defines accumulation as the rise of the surface level of a glacier relative to its summer surface level, multiplied by the density of the added mass. The added mass can take multiple forms, such as snow, hail, freezing rain, wind-blown snow, avalanche deposits, or hoar frost. Accumulation data to inform melt models can therefore be obtained using the glaciological method of stakes and snow pits as described by Østrem and Brugman (1966), and extrapolated across the glacier. Another method to determine accumulation involves the use of automated weather stations located on or near the glacier (Oerlemans and Klok, 2004; Vargo et al., 2020; Anderson et al., 2021). From the meteorological data collected from the weather station, solid precipitation can then be identified based on a threshold temperature (Paul et al., 2008). Accumulation information from the weather station can be extrapolated across each cell of a DEM, including a glacier surface.

2.5 Glacier flow models

While degree day or energy balance models can estimate historic and present-day mass balance, an additional component is needed to project future mass balance. Modelling the future extent and thickness of a glacier, known as its geometry, is done through glacier flow models. These flow models have been used for large scale ice sheets in polar regions (Rignot et al., 2011), as well as smaller scale alpine glaciers (Le Meur and Vincent, 2003; Anderson et al., 2021). Ice flow models have been developed to gain better insight on key processes controlling glacier behaviour and to predict glacier response to external climate forcing (Huybrechts, 2007).

There are two common types of glacier flow models. The most simplistic type is the flowline or flow band model which studies the dynamics of a selected one-dimensional flowline of a glacier (Huybrechts, 2007). The flowline represents a sequence of columns of infinitesimal cross section extending vertically from base to surface of a glacier (Cogley et al., 2010). One by one, these columns gain mass or lose mass, representing the movement of ice driven by accumulation and ablation. The second type of glacier flow model is the distributed model. This type of model simulates flow over the horizontal extent of a glacier using a grid or a mesh system, while averaging ice dynamic processes over the vertical extent (Huybrechts, 2007). These models are referred to as two-dimensional models. Both one-dimensional and two dimensional models are vertically known as vertically integrated models. Distributed models can also factor in a third dimension when modeling ice flow.

As these models represent the flow of ice, there are several established methods of varying complexity to calculate the stresses and strains that cause ice deformation and movement. A model calculating all relevant ice flow dynamics is known as a full Stokes model, and is considered to be the most accurate flow model available (Kirchner et al., 2016). Full Stokes models account for all stresses that affect ice flow, such as drag, compression or extension, vertical stresses within the ice, and gravitational forces (Seddik et al., 2012). Simpler versions, such as the shallow ice approximation discards small mathematical terms in the full Stokes equation (Kirchner et al., 2016). In this research, ice flow is simulated using a two-dimensional, vertically integrated shallow ice approximation model.

Paired with future climate change projections, glacier mass balance and flow models can be used to estimate glacier response to climate change. This is the approach taken in this research to understand the effect of climate change on the Waitaki catchment runoff.

2.6 Climate change in glacierized catchments

A recent study on global hydrologic response to glacier mass loss has started to identify regions across the world where long-term water security may be threatened (Huss and Hock, 2018). Though glacier retreat can lead to an increase in meltwater contributing to runoff, this phase is often short, lasting only a few years or decades (Orlove, 2009). The temporary increase in ice melt contributions from receding glaciers is called “peak water” (Huss and Hock, 2018). After peak water is reached, ice melt contributions steadily decrease as glaciers become smaller or disappear completely (Jansson et al., 2003; Huss and Hock, 2018). Huss and Hock (2018) illustrate peak water characteristics in Figure 2.6.

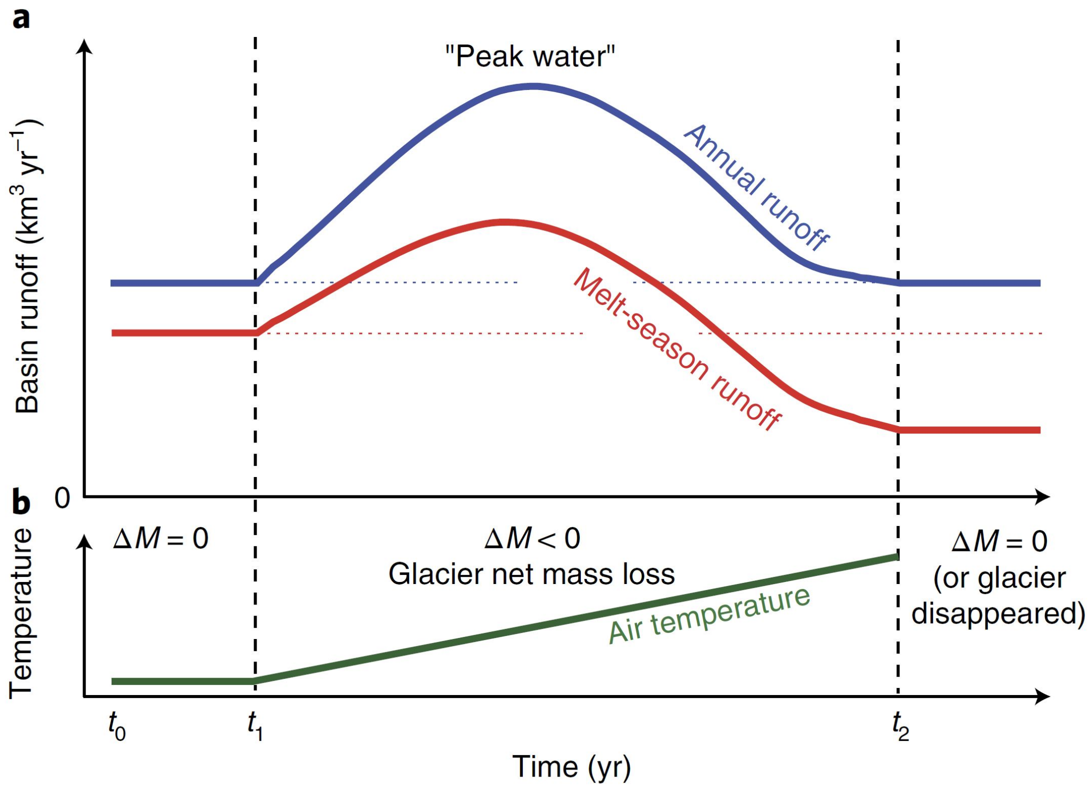

Figure 2.6: Schematic illustration of the changes in runoff from a glacierized catchment in response to continuous atmospheric warming, as seen in Huss and Hock (2018). The figure shows a glacier in equilibrium with a mass balance of zero until time t_1 when temperature begins to increase. Peak water is achieved past t_1, which corresponds with a temporary increase in melt season runoff. Past time t_2, melt runoff is now less than the initial amount, as the glacier has either reduced in size and reached equilibrium or has vanished.

Milner et al. (2009) also depicts glacier recession, peak flow, and the effect on daily downstream discharge through a hydrograph. In their schematic, glacier volume decreases, and overall runoff temporarily increases to a peak during recession (Figure 2.7). Once the glacier reaches a new equilibrium and volume stabilizes, runoff also stabilises but at a reduced rate. The figure shows how the downstream hydrograph changes during the stages of glacier recession in a northern hemisphere hydrological year. Initial melt during the early summer season remains roughly the same, but runoff significantly changes depending on how much glacier mass is present and melting.

Using a temperature index model, Huss and Hock (2018) define glacier runoff as the sum of glacier melt (melt from ice, firn, and snow) and rain, less refreezing,

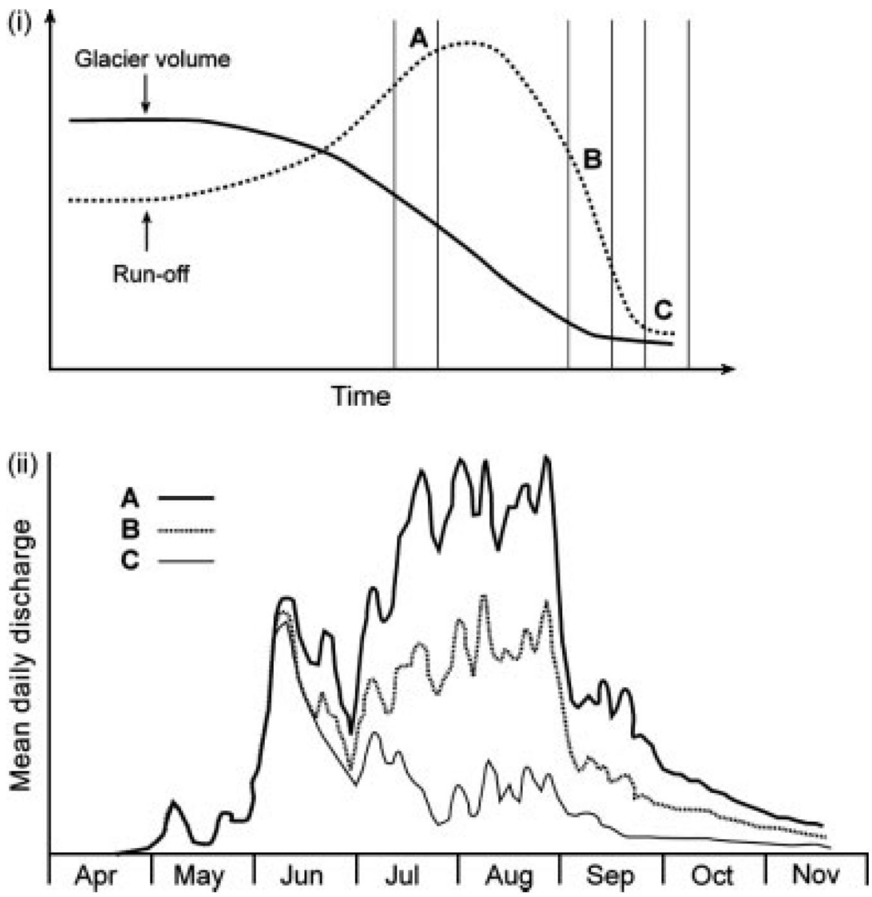

Figure 2.7: The theoretical relationship between glacier volume loss and daily run off at different stages of recession, represented in a northern hemisphere hydrological year. Figure from Milner et al. (2009).

that originates from the initially glacierized area as given by the Randolph Glacier Inventory (a global inventory of glacier outlines). While this study reviewed glacier runoff and peak water globally, only the Clutha watershed was selected to represent the hydrological response to glacier retreat in New Zealand. The Clutha watershed is one of the largest catchments on the South Island, though the volume of ice it holds is less than the volume present in the Waitaki catchment. The study suggests that peak flow is not as distinct in the Clutha catchment as in other regions globally, but with most significant reductions occurring in the latter half of the century for an RCP4.5 scenario.

Another global glacier runoff and peak water study by Bliss et al. (2014) also used a temperature index model but instead analysed runoff from all glaciers across New Zealand for an RCP4.5 scenario, forced by 14 GCMs. The study concluded that in all glacierized regions of the world including New Zealand, glacier runoff exhibited a strong seasonality with pronounced peaks in summer and negligible runoff amounts in winter. Maximum monthly runoff is significantly greater than the seasonal maxima of snow accumulation or rain, and summer flows are strongly reduced by the end of the century. (Bliss et al., 2014). The study also suggests that the loss of glaciers will shift the downstream hydrograph to an earlier peak flow, as seen in unglacierized basins with winter snow that melts in late spring or early summer (Bliss et al., 2014).

The effect of receding glaciers on downstream water resources, such as peak water, and changes to the timing and magnitude of runoff is particularly important for catchments on the South Island of New Zealand, like the Waitaki catchment. The Waitaki catchment is a nationally important watershed for hydroelectricity generation and water supply storage (Purdie and Bardsley, 2010; Sirguey, 2010; Kerr, 2013), and holds some of the country's largest glaciers.

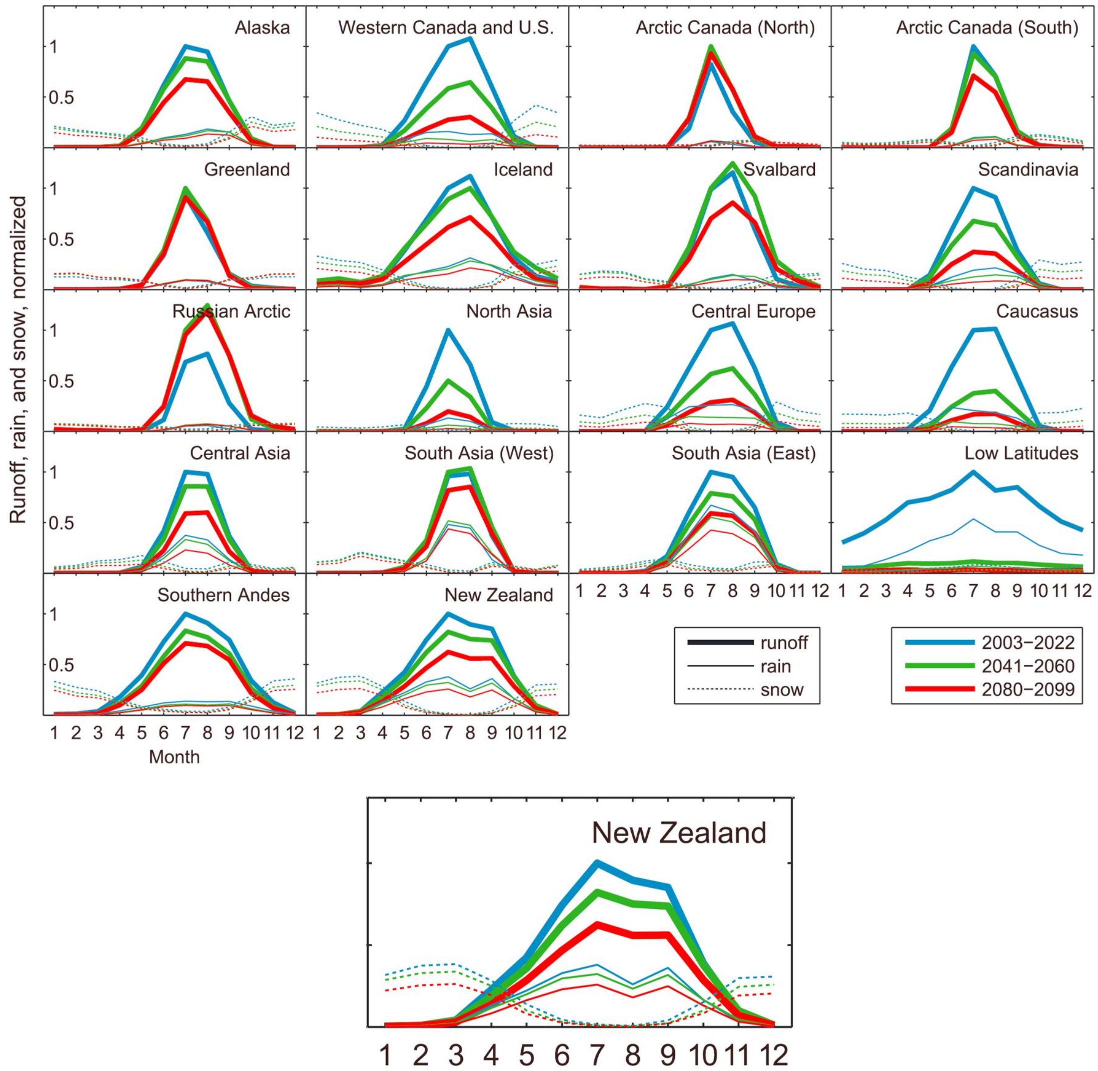

Figure 2.8: Projected monthly glacier runoff, snow accumulation, and rain averaged for three periods. Month 1 in New Zealand represents July instead of January. Extract of New Zealand results provided for clarity. Figure from Bliss et al. (2014)

2.6.1 Past hydrological research in the Waitaki watershed

The upper Waitaki basin is a prime example of an important glacierized catchment where changes in peak water and long-term water resources may impact power generation, reservoir storage levels, and other downstream water users. Previous studies have recognised the importance of understanding water resources in the Waitaki catchment and various aspects of the catchment have been researched over time. Many studies have focused on the specific glaciers within the catchment, namely the Haupapa/Tasman Glacier, being the largest in New Zealand (Quincey and Glasser, 2009; Kirkbride and Warren, 1999; Hochstein et al., 1995).

Purdie and Fitzharris (1999) investigated the processes and rates of ice loss at the terminus of the Haupapa/Tasman Glacier during the summer of 1995 and the resulting effect on the downstream proglacial lake. They concluded that 6% of the annual inflow into Lake Pukaki that year came from ice loss in the catchment, including Haupapa/Tasman Glacier.

Sirguey (2010) expanded on this work and completed a study quantifying contributions of snow melt and ice melt within the upper Waitaki basin between 2000 and 2007. The study primarily focused on snow cover but did include an approximate consideration of glacier melt. Due to the difficulties in partitioning seasonal snow and glacier melt contributions, it was suggested that contributions from glaciers would need to be addressed in a more deterministic way (Sirguey, 2010). Regardless, this study provides insight into possible ice melt contributions to runoff in the upper Waitaki catchment over several years (Figure 2.9).

Of particular note in the study by Sirguey (2010) is the hydrological response to a drought that occurred in and around the 2005 hydrological year. Sirguey (2010) suggested that inflows were largely mitigated by ice melt from glaciers in the Pukaki basin. Specifically, contributions to runoff from glacier melt "much larger than usual" were believed to have sustained the discharge to within 17% of the mean annual flow, despite precipitation being reduced by 34% (Sirguey, 2010). This phenomenon was less pronounced in the other glacier lake catchments with less glacier volume. The results highlight the importance of glacier melt contributions to runoff during dry periods, as dry periods may become more frequent with increasing global temperatures (Mullan et al., 2005).

One recent study using climate change projections to understand future runoff into the three glacial lakes of the upper Waitaki was completed by Caruso et al. (2017). This study used the TopNet hydrologic model developed by the National Institute of Water and Atmospheric Research (NIWA). The TopNet hydrological model was used to estimate catchment runoff and lake inflows in the 2040s and the 2090s by using climate projected from 12 GCMs based on the IPCC 4th assessment

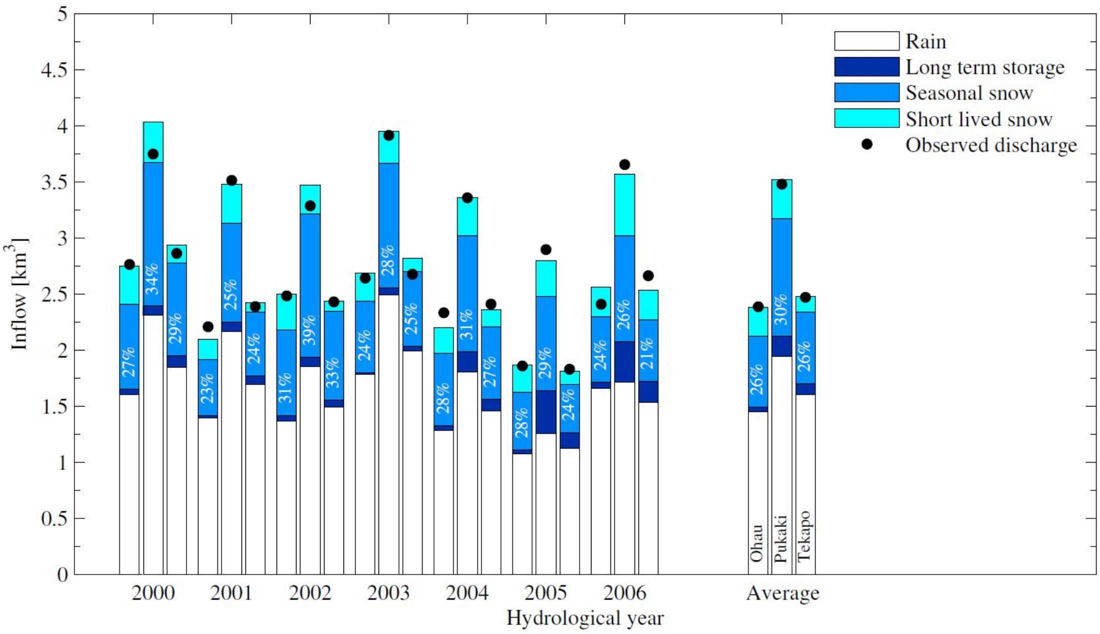

Figure 2.9: The components of runoff into each of the three upper Waitaki glacial lakes (Ohau, Pukaki, and Tekapo) over 2000 to 2006. Ice melt contributions are termed "long term storage". Short-lived snow is defined as snow that does not last more than 30 days on the ground. Figure from Sirguey (2010).

report. The study mainly focused on hydrologic response to climate change and did not explicitly consider ice melt contributions to runoff. Caruso et al. (2017) concluded that annual lake inflows would increase under future climate scenarios but seasonal changes in the hydrograph would result in potential shortfalls of water for energy generation and storage in summer and autumn seasons. Additionally, seasonal shifts could result in increased risks of flood and drought for downstream areas.

Limited studies have explicitly addressed glacier change and ice loss contributions to runoff in the Waitaki under future climate scenarios. A recent study by Anderson et al. (2021) included projections of glacier volume change around the Aoraki Mt Cook region, which includes portions of the Waitaki catchment. The study used an energy balance coupled with a 2D vertically integrated shallow ice approximation model to simulate glacier change up to the year 2099 (Anderson et al., 2021). Additionally, the study investigated whether debris-covered glaciers and debris-free (clean) glaciers responded the same to climate change projections, and finally if volume loss is controlled by debris cover or lake-calving events at the toe of glaciers.

Anderson et al. (2021) showed that glaciers in the region are projected to continue to melt through the 21st century with different rates depending on the RCP scenario used. By 2099, ice volume is projected to reduce by 50% for an

RCP2.6 scenario, and up to 92% for an RCP8.5 scenario. During experimental runs of the model, the study also showed that removing debris cover from glaciers increased the speed of ice loss, whereas removing lake calving from the simulations slowed ice loss.

While the implications of these glacier change projections on downstream runoff were beyond the scope of the study by Anderson et al. (2021), this thesis aims to build on those findings. Using the same coupled energy balance and shallow ice approximation model as Anderson et al. (2021), this research refines the study area to the Waitaki Catchment and investigates how project glacier change will impact downstream runoff that, in turn, is relied upon for hydropower generation and water supply.

Chapter 3

Methodology

This chapter first explains which models were used to project accumulation, ablation, and rainfall through the 21st century for glaciers located in the Waitaki catchment. Statistical methods used to determine changes in model outputs through the century and between RCP scenarios include calculating and comparing averages, totals, and standard deviations using annual, monthly, and daily model output, and are described in detail in the following sections.

Annual time series of glacier change was analyzed first to understand how ice volume in the Waitaki catchment is projected to change over the century. Next, daily and monthly times series of accumulation, ablation, and rainfall are analyzed to further understand the change of components comprising glacier change and runoff over the century. Lastly, a comparison of statistical methods was completed to determine how the analysis may affect results showing annual runoff volumes.

3.1 Glacier mass balance and ice flow model

This research examines the model outputs from an enhanced temperature index model, coupled with a two-dimensional shallow-ice approximation (SIA) ice flow model. The mass balance model and ice flow model and all components and parameters are the same as that used by Anderson et al. (2021). The glacier simulations used for the analysis in this work are the same simulations from Anderson et al. (2021) but this research focuses on the analysis of daily, monthly, annual, and seasonal trends for water output from glaciers.

A full description of the model components and parameters are described in the study of glacier response to climate change by Anderson et al. (2021). The coupled model uses a dynamic calibration in which a state of glacier equilibrium is defined in late 1800s. The model is run to present (2005) using estimates of historic climate variations and then simulated state glaciers are used as the initial condition for future mass balance projections (Anderson et al., 2021).

For this study, the spatial extent of the coupled models has been refined to project changes of glacier volume and mass balance across glaciers in the Waitaki catchment, rather than the Aoraki Mt Cook region. The Waitaki catchment boundary was obtained through open source GIS data from local government councils in the Canterbury region (Canterbury Maps, n.d.). Glacier volume change and glacier mass balance are projected from 2006 to 2098. Based on the Randolph Glacier Inventory (RGI 6.0) (RGI, 2017), a total of 588 glaciers were identified in the Waitaki catchment. The models calculate catchment-wide changes in glacier mass balance based on each individual glacier. A digital elevation model (DEM) is used to provide surface elevation information. Spatial resolution of the grids across a given glacier is 100 m^2, and the ice flow model updates the grid annually to adjust for decreasing ice extent (Anderson et al., 2021).

Climate input data to the coupled models are temperature, total precipitation, relative humidity, wind speed, and incoming solar radiation (Anderson et al., 2021). Temperature and precipitation are interpolated from local climate station data, relative humidity and solar radiation are sourced from the virtual climate station network (VCSN) with a resolution of approximately 5 kilometers, and wind speed is scaled from reanalysis data. As high elevation climate stations in the Southern Alps are limited, and climate in these areas are not accurately represented by the interpolation of VCSN data, a three-step calibration procedure developed by Huss and Hock (2015) was used to align modelled mass balance with measured mass balance or an accepted regional mass balance value. This method includes a series of adjustments to precipitation, temperature, and degree-day factors applied sequentially until the mass balance for a given glacier is within a small range of a regional mass balance value (Anderson et al., 2021). The model is then validated against mass balance measurements of nearby glaciers (Brewster Glaciers and Rolleston Glacier), as well as RGI glacier outlines from 1978 and 2009.

(Anderson et al., 2021). Projections of future climate are driven by general circulation models (GCMs) which were included in CMIP5. Projections of glacier mass balance were made using climate simulations from six GCMs composing NIWA's Regional Climate Models (RCM), for four RCP scenarios (RCP2.6, RCP4.5, RCP6.0, and RCP8.5) and are listed in Table 2.2. Climate simulations for the six GCMs were used throughout annual, monthly, and daily time series analysis.

The next section labeled "Annual time series" describes the annual time series analysis of glacier volume projections. Glacier volume projections were first made using the six GCMs described above. Then, the temperature index model and the ice flow model were re-run using sixteen statistically downscaled GCMs, as per the methods derived and used by Vargo et al. (2020), for three RCP scenarios (RCP2.6, RCP6.0, and RCP8.5). A comparison was made between the two methods of projections to test the influence of GCMs on results.

The following sections named "Daily time series" and "Monthly time series", describe how mass balance, accumulation, and ablation were calculated. Calculations include using spatial averages that consist of one average value of mass balance, accumulation, and ablation per glacier, for all glaciers in the Waitaki catchment. Average daily and monthly rainfall on a glacier were similarly analysed.

Finally, the last section labelled "Statistical comparison of annual time series analysis" describes how spatially averaged annual ablation volume and total annual ablation volume were calculated for three individual glaciers of differing sizes. These calculations were done to compare and determine how the statistical analysis could affect the results. Lastly, total annual ablation volume for the Waitaki catchment was calculated.

3.2 Annual time series

Changes to total ice volume within the Waitaki catchment were determined through annual time series analysis. Projections of total ice volume were produced by Anderson et al. (2021) and the outputs have been adapted to specifically address the Waitaki Catchment. Projections of glacier mass balance were forced using climate simulations from six GCMs composing NIWA's Regional Climate Models (RCM), for four RCP scenarios (RCP2.6, RCP4.5, RCP6.0, and RCP8.5). The coupled temperature index and ice flow model was re-run and projections of glacier mass balance were made again using sixteen statistically downscaled GCMs, as per the methods used Vargo et al. (2020), for three RCP scenarios (RCP2.6, RCP6.0, and RCP8.5). Annual changes to ice volume were compared from both runs to determine how climate forcing data influences projections of glacier change through the century.

3.3 Daily time series

For daily and monthly time series analysis, future projections of glacier change and rainfall were forced using only the six regional climate model GCMs. Daily time series are analyzed for the hydrological year starting on 1 April and ending on 31 March. Each season lasts three months. March through April is defined as autumn, June through August is defined as winter, September through November is considered spring, and December through February is considered summer.

The coupled mass balance and ice flow models calculated daily mass balance, accumulation, and ablation between 2006 and 2098. The model outputs were analyzed for each glacier within the Waitaki catchment, for each of the four RCP scenarios using six GCMs. As a result, each output had an initial daily data set of 14112 points (588 glaciers x 4 RCP scenarios x 6 GCMs runs). For the 94 year period, the total data set for one process comprised 366 days x 94 years x 14112 points. To account for leap years, 366 days were used to represent one year. For regular non-leap years, a "nan" (not-a-number) value was used in the model instead. Input rainfall data across each glacier for each RCP scenario and for all GCMs was also separated into the same size data sets.

Each output was then divided by RCP scenario. For example, accumulation for all Waitaki glaciers between 2006 and 2098 for an RCP4.5 scenario was separated into a new data set called "acc_day_rcp45". This data set consists of 366 days x 94 years x 3528 points (composed of 588 glaciers x 1 RCP x 6 GCMs runs). This was done for mass balance, accumulation, ablation, rainfall.

Next, three time periods were selected to compare the data through the century. The first time period of 31 years is 2006-2037, the second time period of 31 years is 2037-2068, and the last time period of 30 years is 2068-2098.

For each output and respective RCP scenario, respective GCM runs for all Waitaki glaciers were spatially averaged and each glacier was weighted equally despite large variations in size. Daily data for each time period was averaged. The resulting model output of 366 days represents the average daily data over the selected 30 or 31 year time period. This step was repeated for each data set (mass balance, accumulation, ablation, and rainfall) for every time period (2006-2037, 2037-2068, and 2068-2098). For example, daily accumulation was analysed through a total of 12 different data sets (3 time periods x 4 RCP scenarios).

In every data set the minimum and maximum daily values were determined, along with which day of the year on which they occurred. The difference between the maximum or minimum values through time or between RCP scenarios was then calculated. Shifts in the timing of maximum and minimum values were determined through a comparison of corresponding days.

The sum of all spatially averaged daily values for accumulation, ablation, and rainfall were calculated for each of the three time periods and respective RCP scenarios. The sum of average daily accumulation and average daily ablation were compared to determine the magnitude of change between both variables comprising mass balance through the century and between RCP scenarios. The sum of average daily ablation and average daily rainfall were combined to determine the changes in magnitude to runoff through the 21st century and for all RCP scenarios, relative to runoff calculated for the 2006-2037 time period for an RCP2.6 scenario.

Lastly, each data set was smoothed using a thirty-day moving average to remove noise and increase plot readability. Without the moving average, some daily data sets were noisy during portions of the year, and trends were more difficult to see.

3.4 Monthly time series

Monthly time series of accumulation, ablation, and rainfall were calculated from daily time series of the respective processes to better understand seasonal shifts of each data set and the impact on runoff. As such, the components of mass balance and the contributions to runoff were the focus of monthly analysis and therefore mass balance was not analyzed.

First, daily times series of accumulation, ablation, and rainfall were sorted into monthly time series after they were separated into RCP scenarios (e.g. acc_day_rcp45). For example, April includes day 1 to day 30, and March includes day 335 to day 366. Next, all GCM runs for respective RCP scenarios across all Waitaki glaciers were averaged. Daily accumulation for each month is summed to obtain total monthly accumulation in any given year in the three time periods (2006-2037, 2037-2068, and 2068-2098). For example, there are 32 different values for average accumulation in April between 2006 and 2037 (inclusive of both the first and final year). Lastly, all April values were averaged to obtain a monthly representative value for the given time period. The resulting data set for monthly accumulation is 12 months x 4 RCP scenarios for the first time period (2006-2037). This was repeated for every month, for every time period and RCP scenario, and for all accumulation, ablation, and rainfall variables. As such, each variable has three data sets representing each time period with monthly averages and corresponding RCP scenarios included in each set.

3.4.1 Standard deviation analysis

Standard deviation was calculated to show the extent of variability within the data projections on a monthly basis but also when comparing seasonal changes. Standard deviation was calculated for the daily accumulation, ablation, and rainfall data and then sorted into monthly averages. As above, accumulation, ablation, and rainfall each have three data sets representing each time period, but with monthly standard deviations and corresponding RCP scenarios included in each set.

Standard deviation was used to determine which month has the largest variability. This was completed by using standard deviations for the 2006-2037 time period and for an RCP2.6 scenario as a baseline to reference change in percent in all other RCP scenarios and time periods. The reference period and RCP was set to 100% and the standard deviation above or below this reference was plotted.

3.5 Statistical comparison of annual time series analysis

Using ablation data, average annual ablation volume and total annual ablation volume were calculated for three glaciers of varying sizes within the Waitaki catchment. Average annual ablation was calculated by summing the average daily ablation data across the given glacier. The total annual ablation was calculated by summing the daily ablation data across the given glacier and multiplying the ablation value by the number of grids that contain ice for the glacier. The ice extent within a grid is updated annually. The daily ablation values for a given year were then summed to obtain the total annual ablation. For both average annual ablation and total annual ablation, volume was calculated by multiplying the ablation values from a particular glacier by the grid resolution (100 km2).

Average annual ablation volume and total annual ablation volume calculations were completed for three glaciers: an unnamed ridge glacier (RGI number 2177) with a grid size of 15 x 9, the medium-sized Huxley Glacier with a grid size of 25 x 18, and the large Haupapa/Tasman Glacier with a grid size of 115 x 293. These glaciers were selected to test if and when peak water would be reached based on the size of a glacier, and whether total annual ablation volume and average annual ablation volume showed similar results. An RCP6.0 scenario was used for this comparison for all three glaciers, and projections were forced using climate simulations from the six GCMs described Section 3.1.

Lastly, the total annual ablation volume was calculated for all glaciers in the Waitaki catchment, and for all RCP scenarios. This calculation was completed to determine total annual ablation volume for the Waitaki Catchment and thus determine if and when peak water would occur.

Chapter 4

Results

Changes to glacier volume, glacier mass balance, accumulation, ablation, and rainfall in the Waitaki catchment between 2006 and 2098 are presented below. The results are separated into four sections that follow the outline of the Methodology Chapter. The first section presents annual time series projections of glacier volume change and the following sections explore the drivers of glacier change. The second section presents daily time series projections of mass balance, accumulation, ablation, and rainfall. The third section presents monthly time series projections of accumulation, ablation, rainfall. The last section presents the comparison between two spatial averaging methods for ablation projections of individual glaciers, and of all glaciers in the Waitaki Catchment cumulatively, to explore how peak water will change through the century.

4.1 Annual changes to ice volume

Projections of annual glacier volume change are presented in two figures that differ by the GCMs used to model future climate. The results are compared to understand how climate forcing data may influence projections of ice loss (Figure 4.1). These figures are from outputs produced by Anderson et al. (2021) but have been adapted to specifically address the Waitaki Catchment.

Figure 4.1 shows ice volume projections from 2006 to 2098 for the Waitaki catchment, using climate data from 6 GCMs that have been processed through NIWA's RCM. Projections of annual volume change in the Waitaki catchment are shown for four RCP scenarios. Figure 4.2 show ice volume projects for the same time period using climate data from sixteen statistically downscaled GCMs and three RCP scenarios.

Figure 4.1 shows that from 2006 to about 2050, there is a steady decrease in projected ice volume for each RCP scenario. There are minimal differences in volume projections between the four RCP scenarios during this period. By 2050, ice volume in the catchment is projected to decrease by 30% to 32% relative to the 2005 volume for all RCP scenarios. After 2050, projections of ice volume for each RCP scenario start diverging, resulting in notably different projections of ice volume by the end of the century. By 2098, ice volume is projected to decrease by 48% for an RCP2.6 scenario, 59% for an RCP4.5 scenario, 63% for an RCP6.0 scenario, and as much as 76% for an RCP8.5 scenario, relative to the 2005 volume.

Similar to Figure 4.1, glacier volume is projected to decrease steadily during the first half of the century with minimal differences in volume projections between RCP scenarios. By 2050, ice volume in the catchment is projected to decrease by 42% to 47% relative to the initial volume at the end of 2005. After 2050, projections diverge from one another resulting in notably different ice volumes by the end of the century, depending on the RCP scenario. Relative to the initial volume, ice volume in the catchment is projected to decrease by 52% for an RCP2.6 scenario, 67% for an RCP4.5 scenario, and as much as 86% for an RCP8.5 scenario (Table 4.1).

One notable difference between Figure 4.2 and Figure 4.1 is the volume projections by the end of the century for an RCP2.6 scenario. Volume projections for the RCP2.6 scenario level off with no further continuous decline after 2050, which is different than the RCP2.6 projection in Figure 4.1, where volume continues to decline during the second half of the century. These differences are driven by the input climate data, and represent variations in climate projections between RCMs and statistically downscaled GCMs.

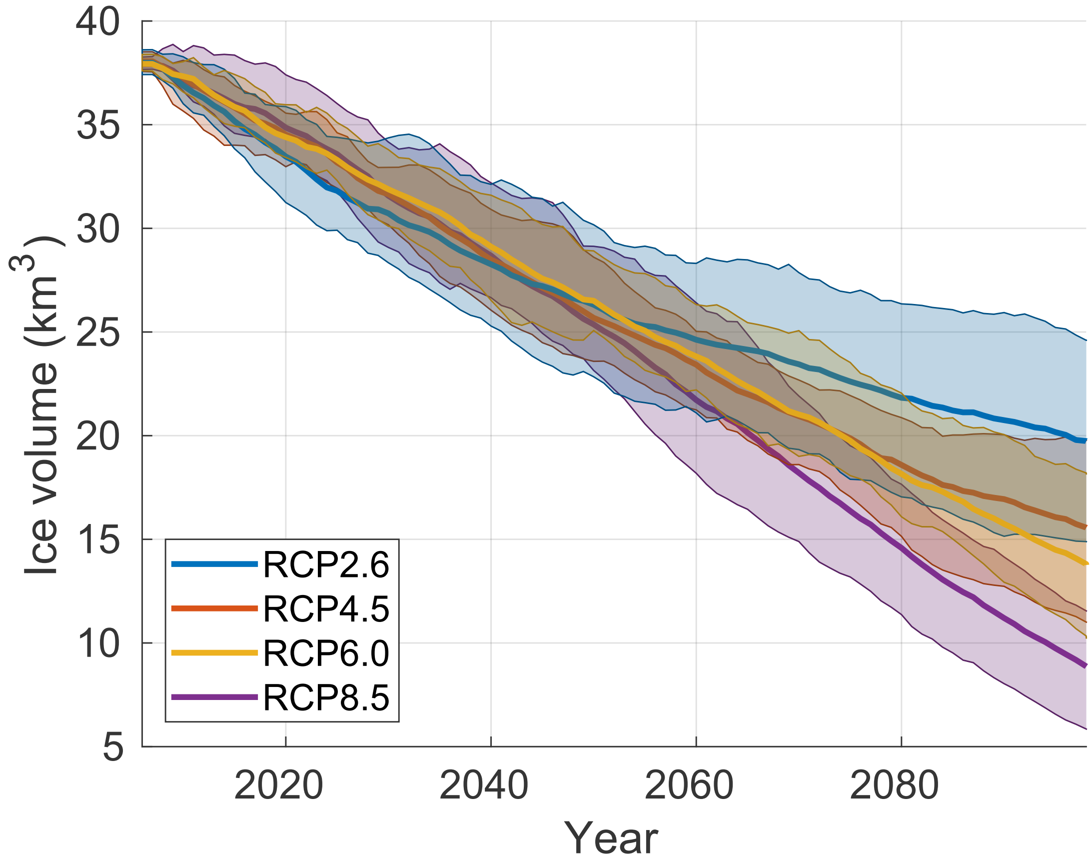

Figure 4.1: Annual glacier volume change in the Waitaki catchment from 2006 to 2098 using six RCMs generated by NIWA from respective GCMs as per Vargo et al. (2020) and Anderson et al. (2021).

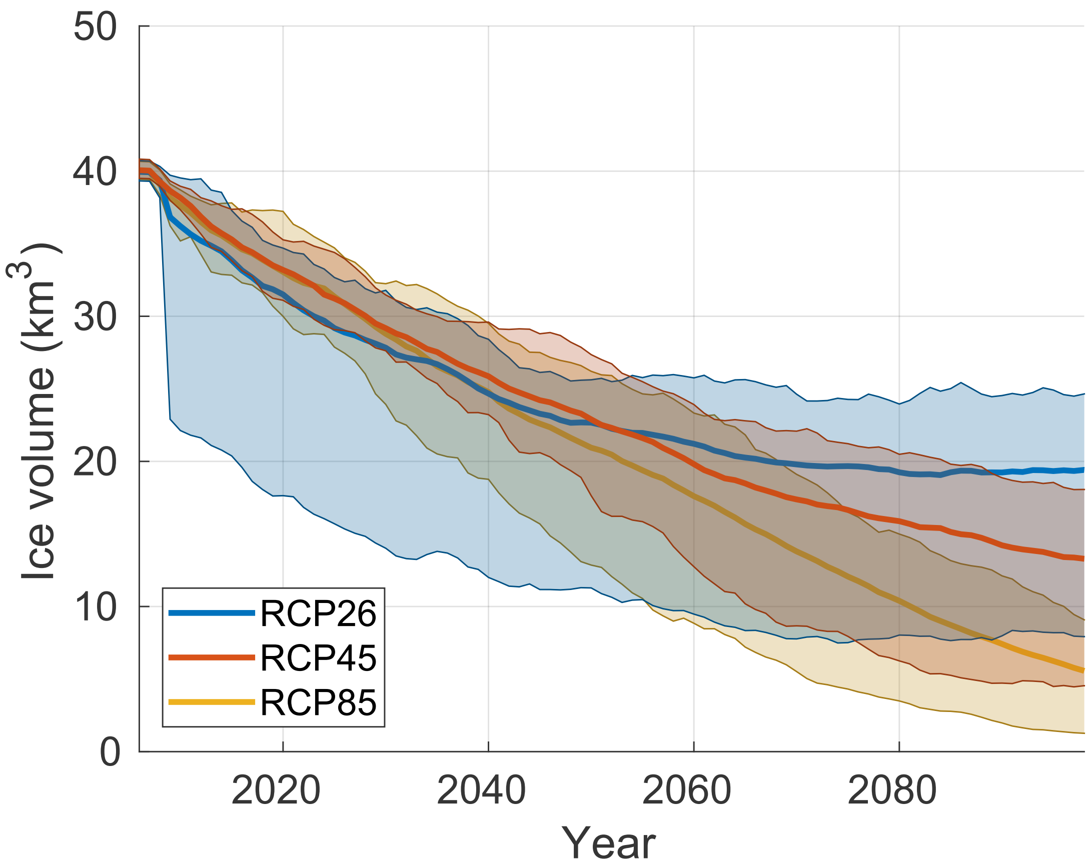

Figure 4.2: Annual glacier volume change in the Waitaki catchment from 2006 to 2098 using sixteen statistically down-scaled GCMs as per Vargo et al. (2020) and Anderson et al. (2021).

Table 4.1: Projections of glacier volume in the Waitaki catchment to 2098. Percent figures are relative to the ice volume at the end of 2005. Initial ice volume is 38.0 km^3 for the RCM mean and 40.0 km^3 for the 16 GCM mean. Volume and projected range values are approximate and have been rounded to the nearest kilometer .

Models	RCP	2050 Volume (km^3)	Projected range (km^3)	2098 Volume (km^3)	Projected range (km^3)
RCM mean	2.6	27 (70 %)	23-30	20 (52 %)	15-25
RCM mean	4.5	26 (68 %)	24-29	16 (41 %)	11-20
RCM mean	6.0	27 (70 %)	25-29	14 (37 %)	10-18
RCM mean	8.5	26 (68 %)	23-29	9 (24 %)	6-12
16 GCMs mean	2.6	23 (57 %)	11-26	19 (48 %)	8-25
16 GCMs mean	4.5	23 (58 %)	18-27	13 (33 %)	5-18
16 GCMs mean	8.5	21 (53 %)	13-26	6 (14 %)	1-9

Total ice volume in the Waitaki catchment is projected to be substantially different by 2098 compared to present day. Even with minimal warming represented by the RCP2.6 scenario, on average based on the GCMs used, only 48% to 51% of ice is projected to remain in the Waitaki relative to the 2006 volume. For an RCP8.5 scenario, on average, as little as 13% to 22% is projected to remain in the catchment. Notably, the range of projections of volume is greater by the end of the century (2098) than in the middle of the century (2050) for every RCP scenario and both sources of climate forcing data. The increase in projected volume range suggests greater uncertainty in the data, glacier response time, or inter annual climate variability, the further into the future the mass balance and ice flow models are run. Further, the 16 statistically downscaled GCMs produce a larger range of ice volume projections than the RCMs. For the following results, only the six RCMs generated by NIWA were used to force future projections of glacier change.

4.2 Daily time series

Changes in mass balance, accumulation, ablation, and rainfall were analyzed through a daily time series divided into three periods (2006-2037, 2037-2068, and 2068-2098).

4.2.1 Mass balance, accumulation, ablation, and rainfall

The following section presents mass balance projections for all Waitaki glaciers, and then the response of individual accumulation and ablation components. Finally, daily rainfall projections are presented. Data representing mass balance, accumulation, ablation and rainfall were smoothed through a 30-day moving average. The maximum and minimum daily value, and which day of the year they occurred, were obtained from each data set. These values were used to determine magnitude of change through time and between RCP scenarios. The day of the year that maximum and minimum daily values occurred were also compared to determine seasonal shifts. Lastly, the sum of daily averages are presented to show changes in magnitude for a given time period.

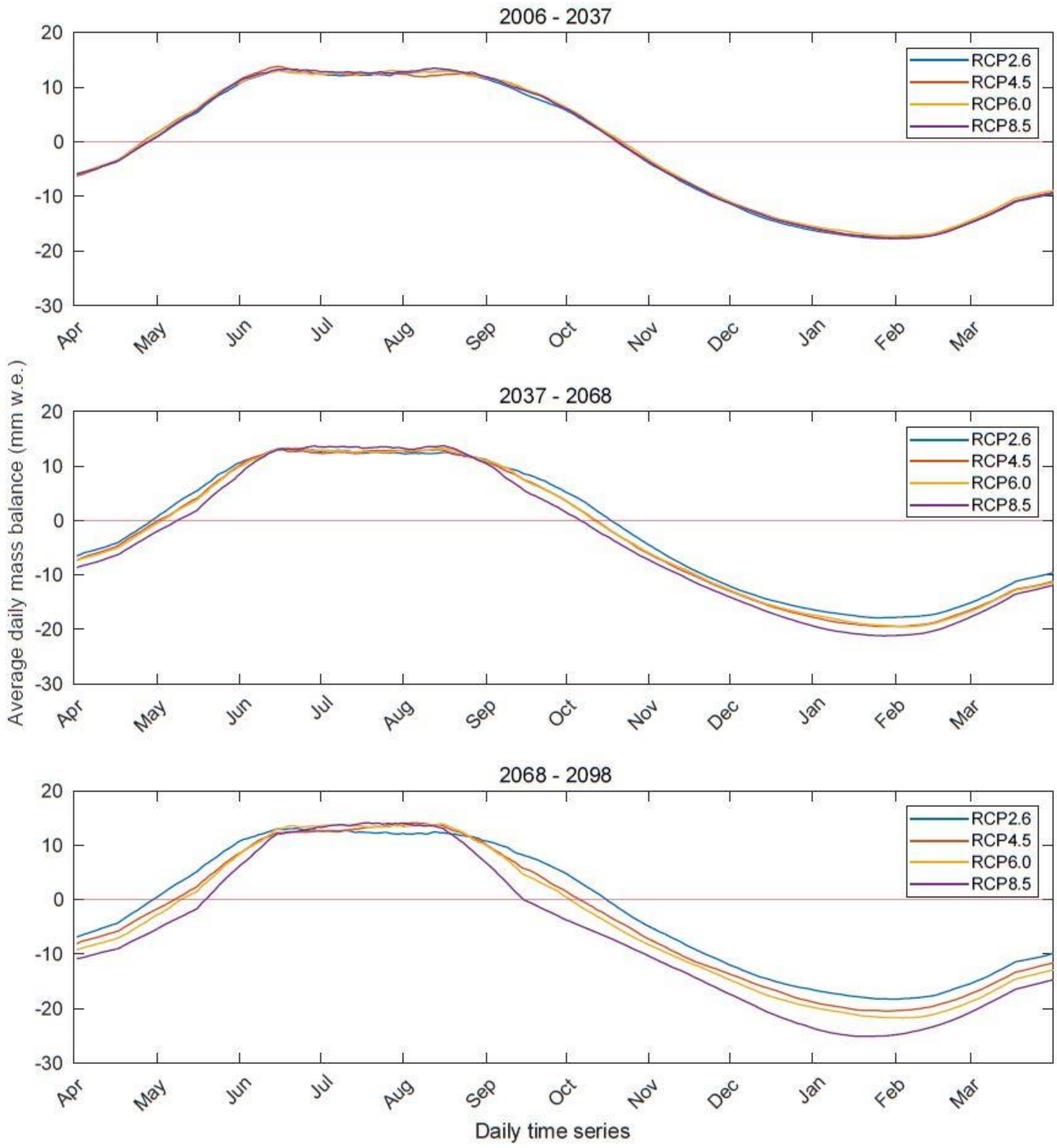

Figure 4.3: 30-day mean daily mass balance averaged for all Waitaki glaciers and averaged over three time periods (2006-2037, 2037-2068, and 2068-2098) for each RCP scenario.

Figure 4.3 shows projections of mass balance averaged for all glaciers within the Waitaki catchment for different RCP scenarios, divided into three time periods. Mass balance is largest in mid-June through mid-August (accumulation season). There is limited variability in mass balance projections through time and between RCP scenarios for mid-June to mid-August. Conversely, there are notable differences in daily mass balance projections through time and between RCP scenarios From April to early-June, and September to Match. The maximum daily mass balance value for RCP4.5, RCP6.0, and RCP8.5 stays within 11% of the maximum daily value for RCP2.6 in all respective time periods. The largest changes in mass balance between RCP scenarios are modeled in the summer months when most ablation occurs. Relative to RCP2.6, the minimum value for daily mass balance decreases by 13% for RCP4.5, 21% for RCP6.0, and 37% for RCP8.5 by the end of the century (2068-2098) suggesting more ablation is occurring with increasing RCP scenario.

Mass balance changes through time are shown for each RCP scenario in Figure 4.4. The data is the same as Figure 4.3, it is only presented differently to understand variations between years under different scenarios. For the RCP2.6 scenario, minimum and maximum daily mass balance values for the middle and last portion of the century stay within 6% of 2006-2037 values. For RCP4.5 for the 2068-2098 period, the minimum daily mass balance value decreased by 17% and the maximum daily value increased by 16% relative to 2006-2037 values. For RCP6.0 and the 2068-2098 period, the minimum daily value decreased by 27% and the maximum value stay within 15% relative to 2006-2037 values. Lastly, for RCP8.5, by 2068-2098 the minimum daily mass balance decreases by 39%, and the maximum daily value stays within 4% of 2006-2037 values.

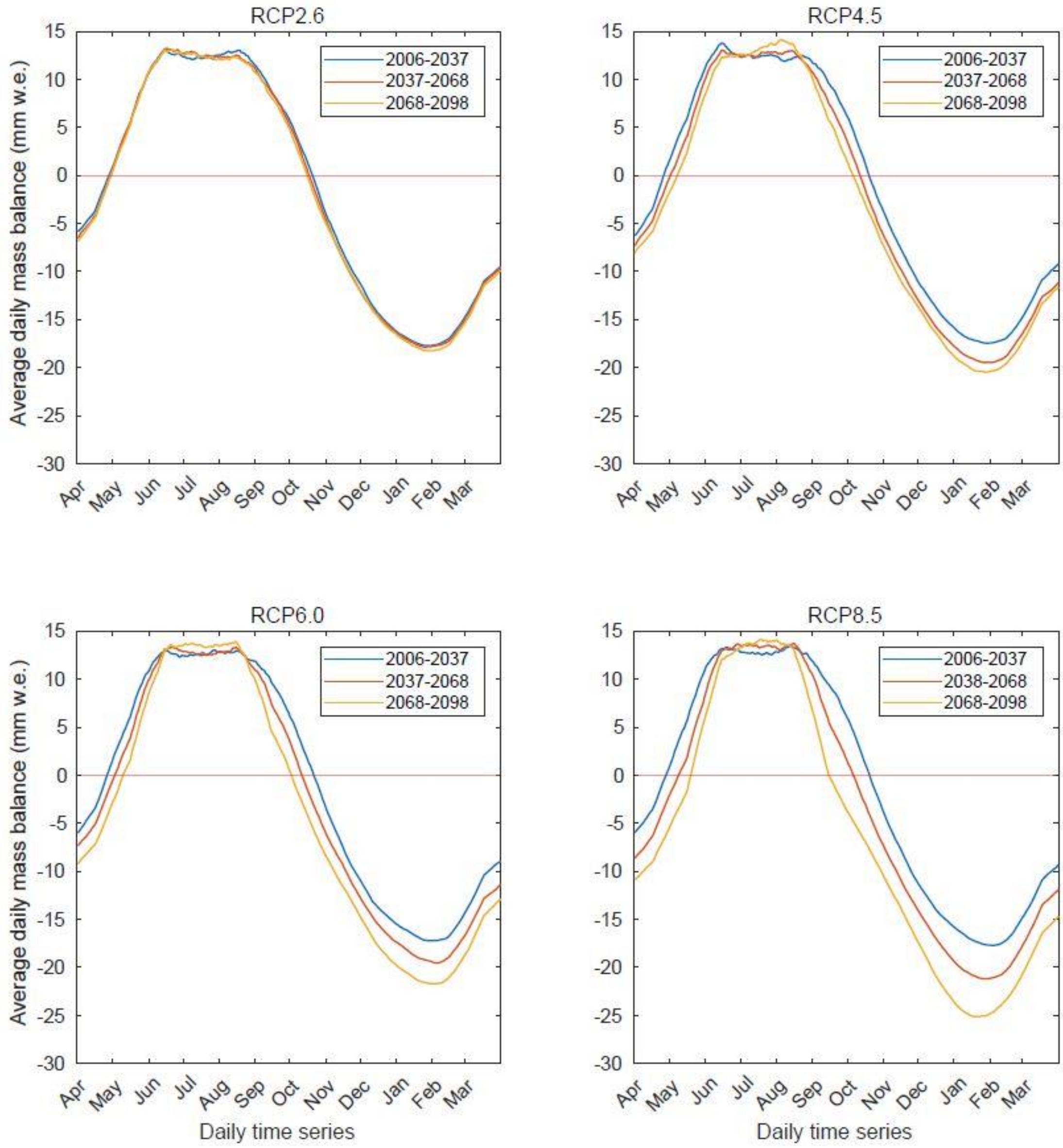

Figure 4.4: Daily mass balance averaged for all Waitaki glaciers and averaged over three time periods, organised by RCP scenario.

Daily time series of accumulation, ablation, and rainfall are shown in Figure 4.5, Figure 4.6, and Figure 4.7, respectively.

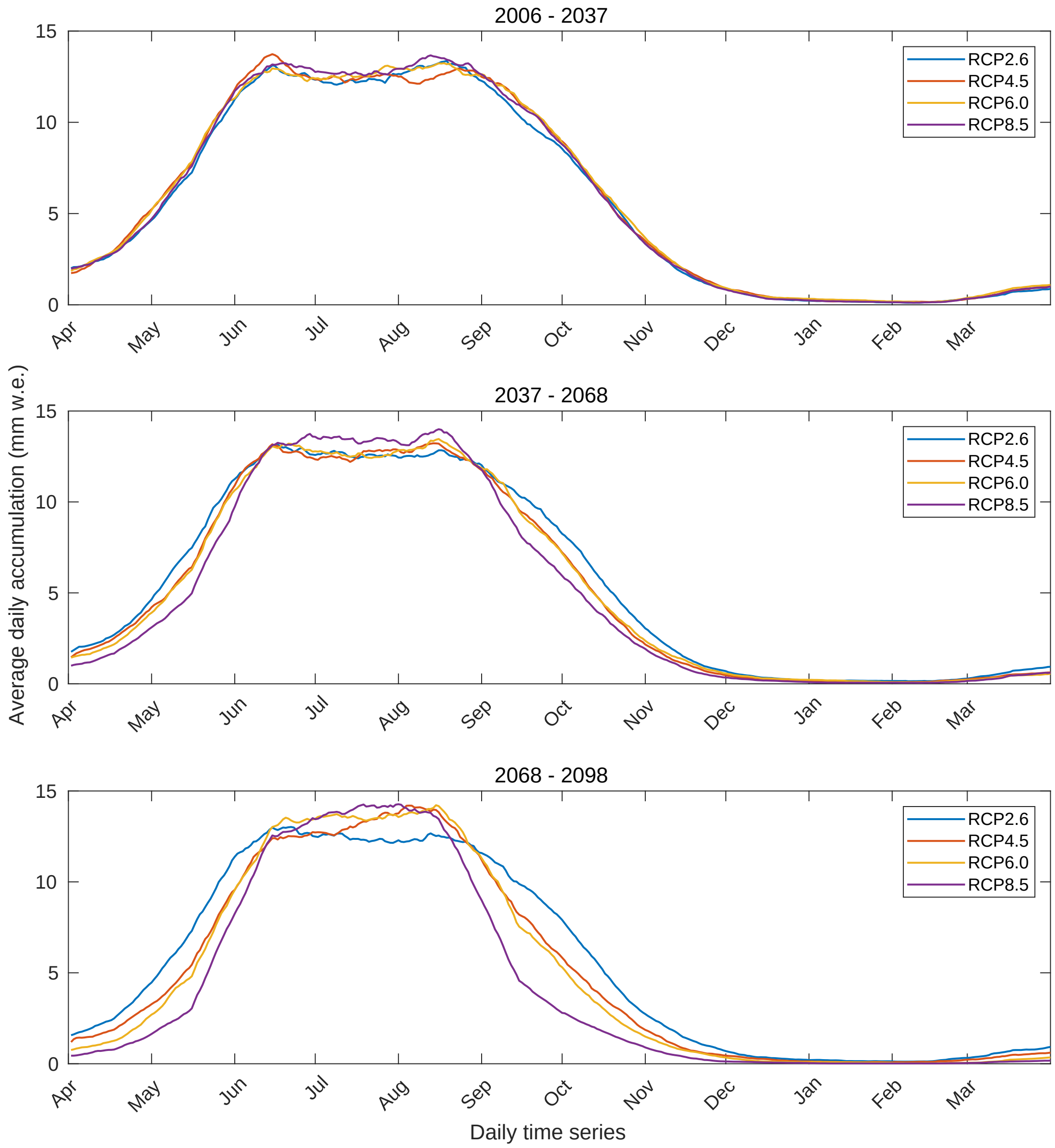

Figure 4.5: Daily accumulation averaged for all Waitaki glaciers through the 21st century for four RCP scenarios.

Most accumulation in the Waitaki catchment occurs between May and November (Figure 4.5). Variations of maximum and minimum values of average daily accumulation are not apparent as in mass balance figures, but seasonal shifts are more evident by the last time period (2068-2098). For RCP2.6, the maximum daily accumulation value for each time period (2006-2037, 2037-2068, and 2068-2098) stays within 3% of each other. For the 2068-2098 time period, the maximum daily accumulation value for RCP4.5, RCP6.0, and RCP8.5 scenarios increases between 5% and 10% relative to the RCP2.6 maximum daily value.

For the RCP2.6 scenario, accumulation starts earlier in the year and gradually increases to the plateau between June and September(Figure 4.5). For the RCP8.5 scenario, the duration of accumulation is shorter but maximum daily accumulation is 5% greater compared to the RCP2.6 scenario. Accumulation also begins later in the season and decreases earlier at the end of the winter.

Despite low values of daily accumulation in summer periods, notable changes are projected in the minimum daily average values through the century. By the 2068-2098 period and relative to RCP2.6, the minimum daily accumulation in summer decreases for all RCP scenarios, and by as much as 95% for RCP8.5. Finally, for the 2068-2098 time period and relative to RCP2.6, the total sum of daily accumulation averaged for all glaciers is projected to decrease by 8% for RCP4.5, by 10% for RCP6.0 and by 22% for RCP8.5. Comparatively, at the beginning of the century (2006-2037), the sum of daily accumulation varies only by 3% between RCP scenarios.

Conversely, at the beginning of the century (2006-2037) the sum of daily accumulation for RCP4.5, RCP6.0, and RCP8.5 is projected to stay within 3% of the sum projected for the RCP2.6 scenario.

Largest changes in glacier mass balance projections are modeled during the ablation season. In Figure 4.6, little change in ablation is projected to occur between RCP scenarios during the first time period (2006-2037). By the 2068-2098 time period (2068-2098), ablation is projected to start earlier in the year, around mid-August for RCP8.5. Ablation is projected to gradually increase between mid-August and mid-September for the RCP2.6 scenario. A similar trend occurs during the end of the ablation period where ablation decreases more gradually for an RCP2.6 scenario compared to an RCP8.5 scenario.

For RCP8.5, the maximum daily average ablation value is projected to increases by 36% when compared to the RCP2.6 value by the 2068-2098 time period. In the same time period, maximum ablation is projected to occur, on average, on 27 January for RCP2.6 and on 14 January for RCP8.5. Overall, average daily ablation is projected to be higher throughout the year later in the century when comparing RCP8.5 to RCP2.6 scenarios. For the 2068-2098 time period and relative to RCP2.6, the total sum of daily ablation averaged for all glaciers is projected to increase by 14% for RCP4.5, by 22% for RCP6.0 and by 43% for RCP8.5.

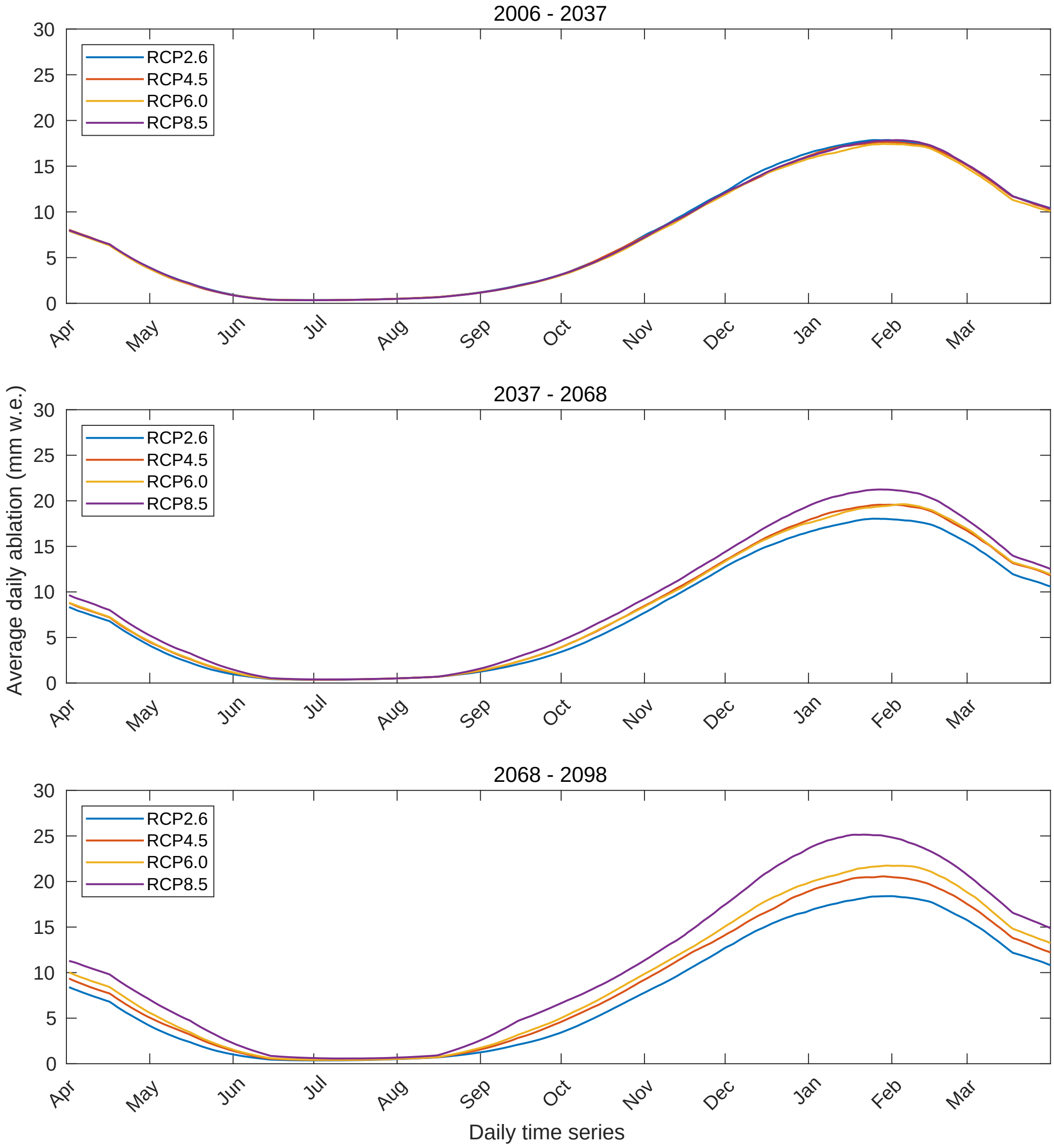

Figure 4.6: Daily ablation averaged for all Waitaki glaciers through the 21st century for four RCP scenarios.

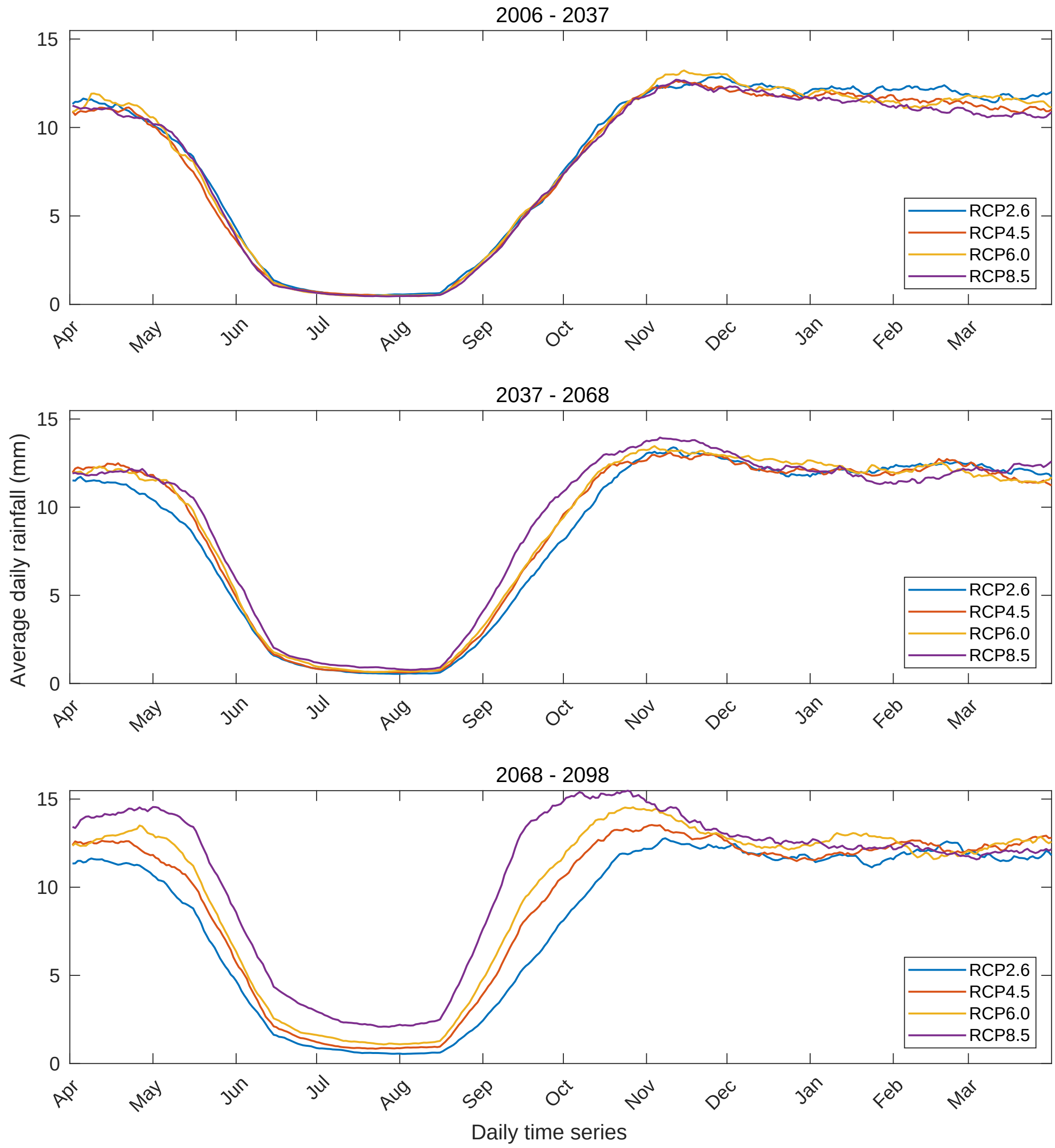

Figure 4.7: Daily rainfall averaged for all Waitaki glaciers through the 21st century for four RCP scenarios.

There is a distinct increase in average daily rainfall projected in the Waitaki catchment during winter months through the century and for all RCP scenarios 4.7. During the warmer months of November through May, average daily rainfall is projected to remain consistently high.

A peak in average daily rainfall is projected to occur during the spring and autumn months for the RCP8.5 scenario in the 2068-2098 period. This peak is less distinct with decreasing RCP scenarios. More rainfall is projected to occur in spring and autumn with increasing RCP scenarios. For the 2068-2098 period the minimum value for daily average rainfall (note that is is near zero) is projected to increase by 274% from the RC2.6 scenario to the RCP8.5 scenario. Overall increases to projected rainfall are largest for the last time period (2068-2098). Relative to RCP2.6, the sum of daily rainfall averaged across all glaciers is projected to increase by 10% for RCP4.5, by 17% for RCP6.0, and by 30% for RCP8.5.

4.2.2 Mass balance, precipitation, and runoff

Together, accumulation and ablation constitute glacier mass balance, accumulation and rainfall constitute precipitation, and ablation and rainfall constitute runoff. The daily time series of each process that respectively constitute glacier mass balance, precipitation, and runoff, are compared. Comparisons are made for each time period and for two RCP scenarios (RCP2.6 and RCP8.5) to cover the widest range of possible projections.

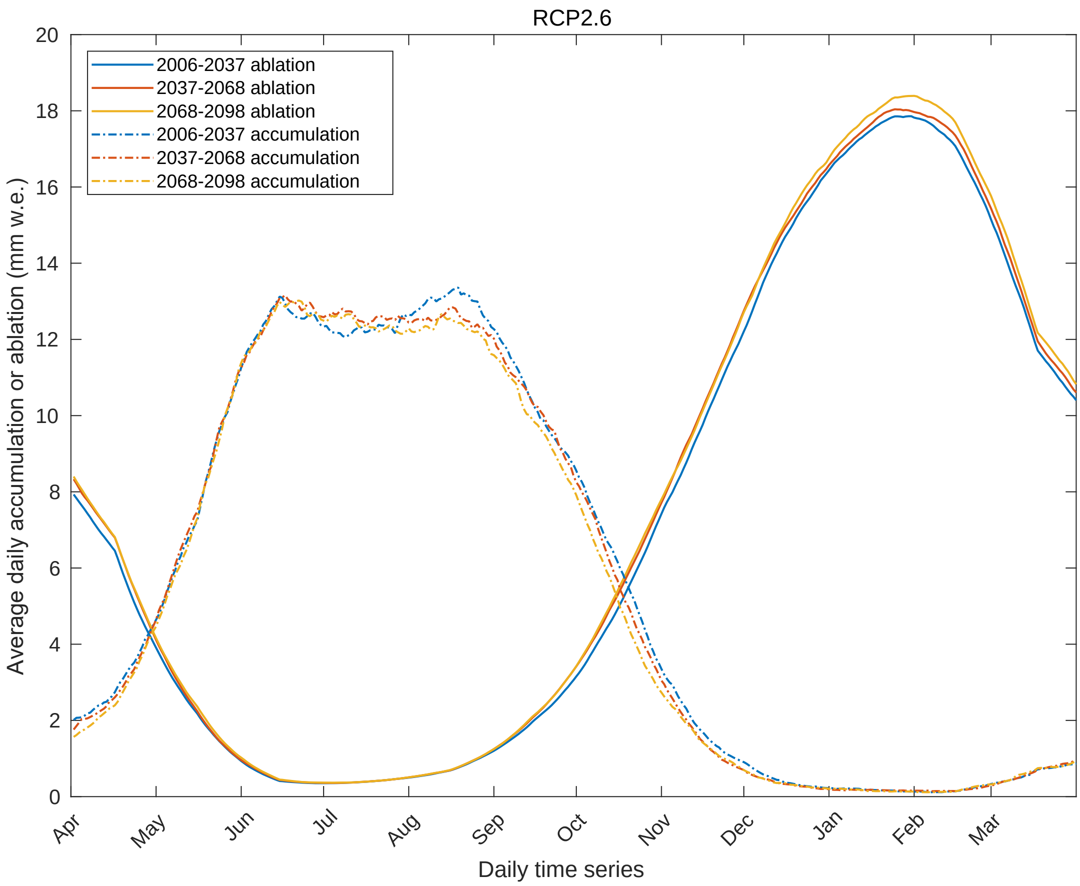

Figure 4.8: Comparison between daily accumulation and ablation averaged for all Waitaki glaciers through the 21st century for an RCP2.6 scenario.

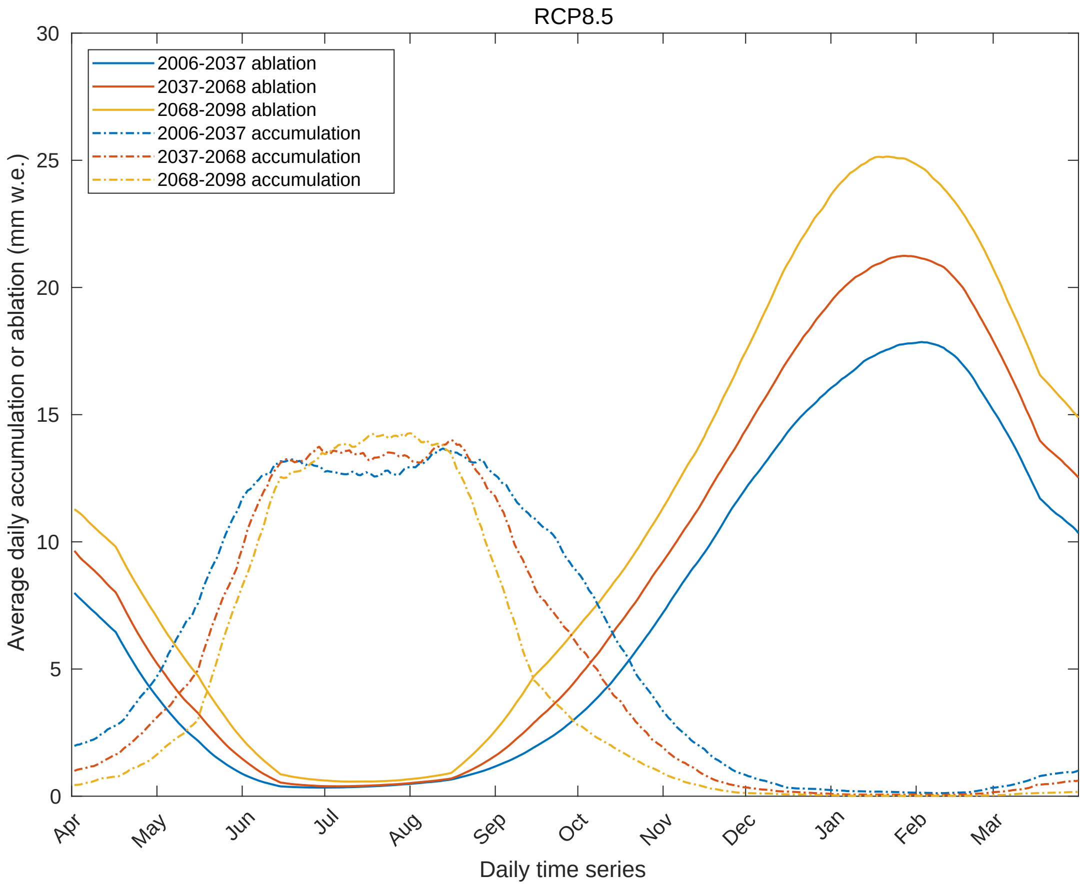

Figure 4.9: Comparison between daily accumulation and ablation averaged for all Waitaki glaciers through the 21st century for an RCP8.5 scenario.

For an RCP2.6 scenario, limited variability occurs in both accumulation and ablation processes throughout the century (Figure 4.8). The sum of average daily accumulation during the 2006-2037 period for RCP2.6 is 2083 mm per year w.e., and for ablation, the sum is 2676 mm per year w.e. For an RCP8.5 scenario, the maximum average daily accumulation increases slightly, but largest change occurs in the maximum values of ablation. The cumulative total of average daily accumulation during the 2068-2098 period for RCP8.5 is 1556 mm per year w.e., and for ablation, but the cumulative total is 3972 mm per year w.e..

There is an apparent shift in timing when either accumulation or ablation becomes dominant. In the first time period (2006-2037), accumulation is the dominant process between early-May and late-October. By the last time period (2068-2098), accumulation is only dominant between mid-May and early-September. Not only does the magnitude of ablation increase by the end of the century for an RCP8.5 scenario, the length of the accumulation season is also reduced.

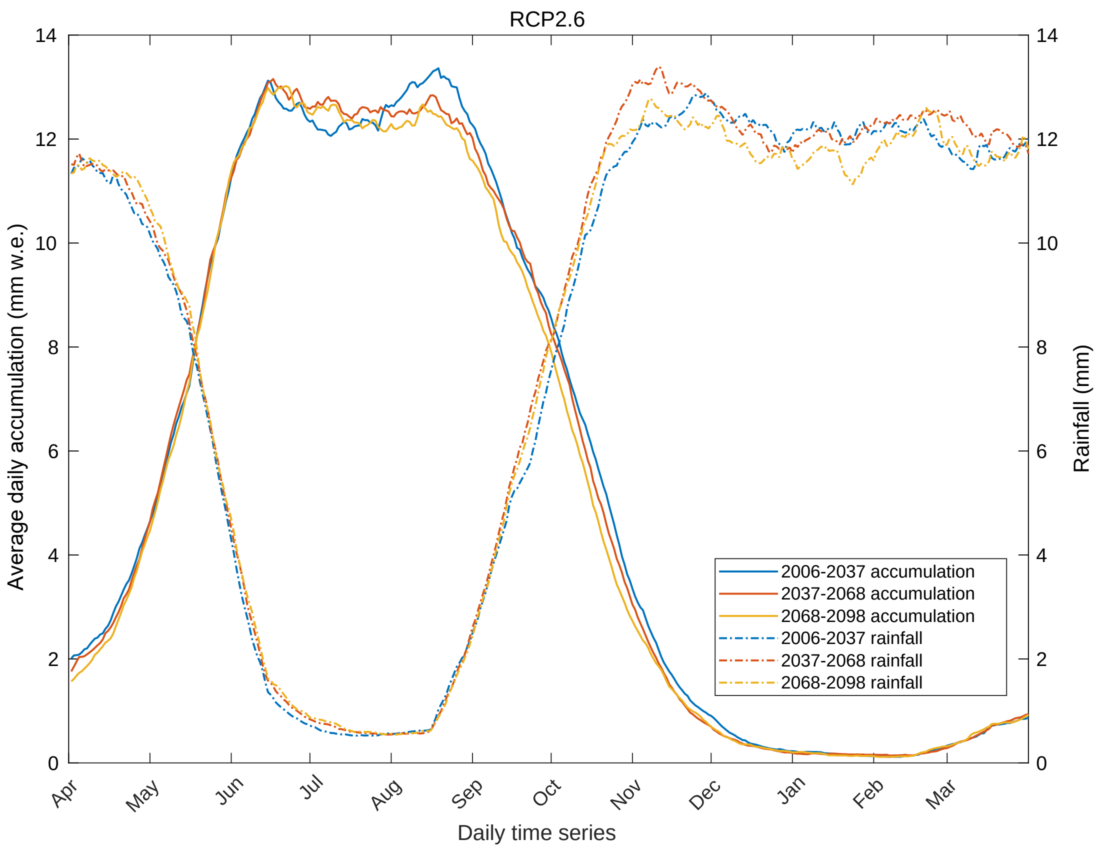

Figure 4.10: Comparison between daily accumulation and rainfall averaged for all Waitaki glaciers through the 21st century for an RCP2.6 scenario.

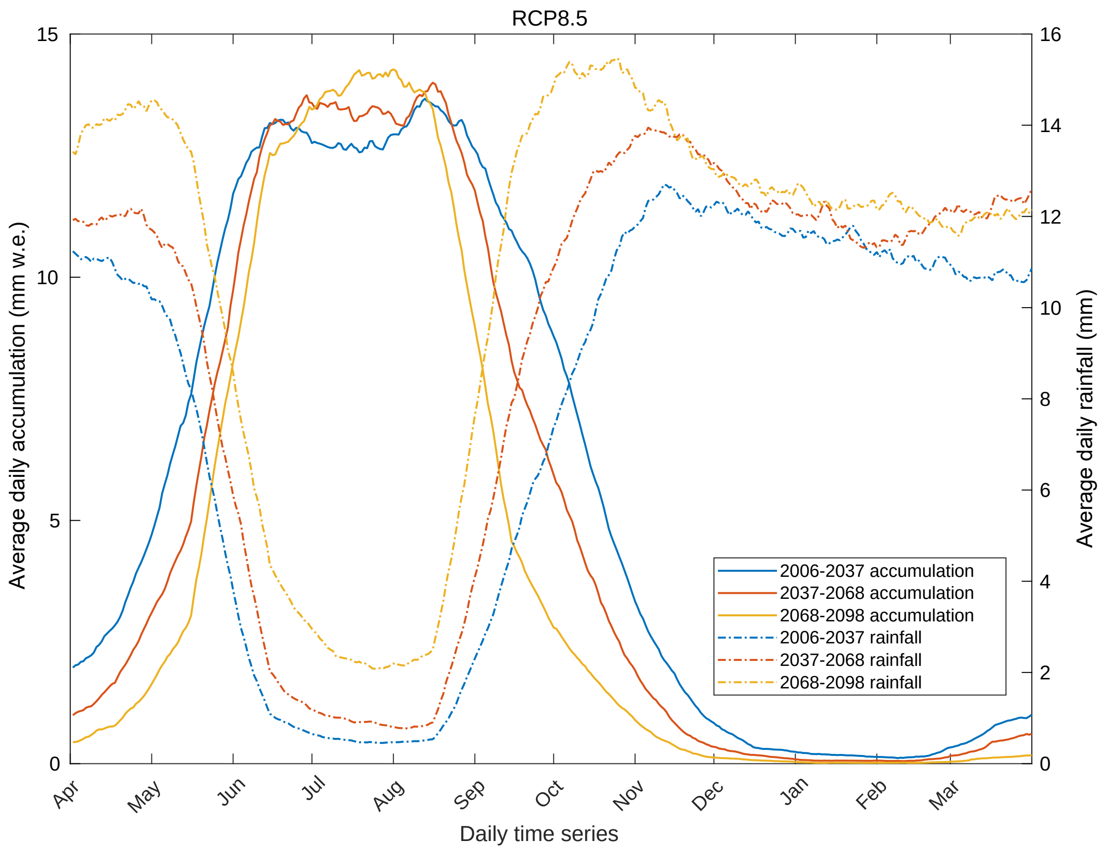

Figure 4.11: Comparison between daily accumulation and rainfall averaged for all Waitaki glaciers through through the 21st century for an RCP8.5 scenario.

Similar to previous comparisons of accumulation and ablation, the processes that compose average daily precipitation do not vary significantly through the 21st century for an RCP2.6 scenario (Figure 4.10). Accumulation is projected to be the dominant process between late-May and the start of October. The sum of rainfall averaged across all glaciers through the century is projected to stay within 3% of the 2006-2037 sum. The sum of accumulation is projected to stay within 4%.

For the RCP8.5 scenario, rainfall is projected to increase throughout the year with most notable increases occurring between March and December (Figure 4.11). As the accumulation season becomes shorter but with a larger maximum daily accumulation, rainfall is projected to become the dominant precipitation component for more of the shoulder season months. The sum of rainfall averaged across all glaciers through the century for the RCP8.5 scenario is projected to increase by 37% by 2068-2098 relative to the 2006-2037 period. The sum of accumulation is projected to decrease by 27% by the end of the century (2068-2098), relative to the start (2006-2037). While rainfall is projected to increase and ablation is projected to decrease, the sum of daily precipitation averaged across all glaciers is projected to increase by 9% by the end of the century for the RCP8.5 scenario.

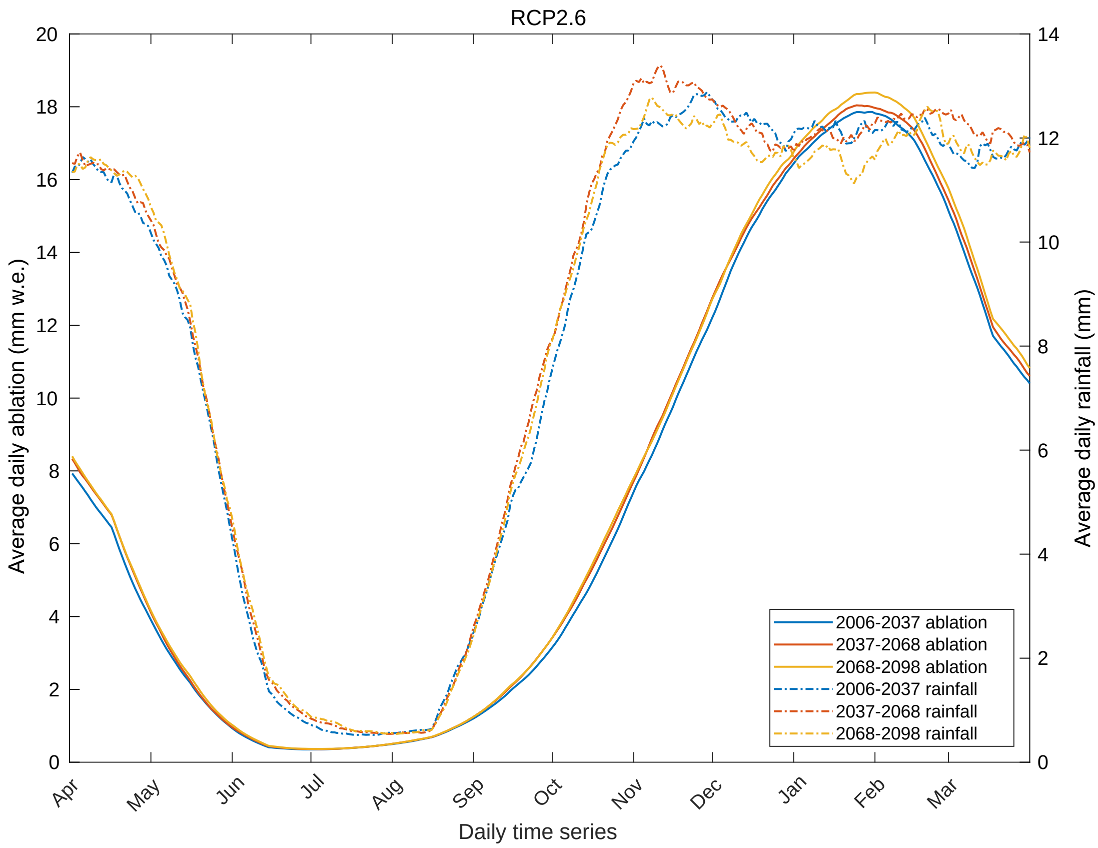

Figure 4.12: Comparison of daily ablation and rainfall averaged for all Waitaki glaciers through the 21st century for an RCP2.6 scenario.

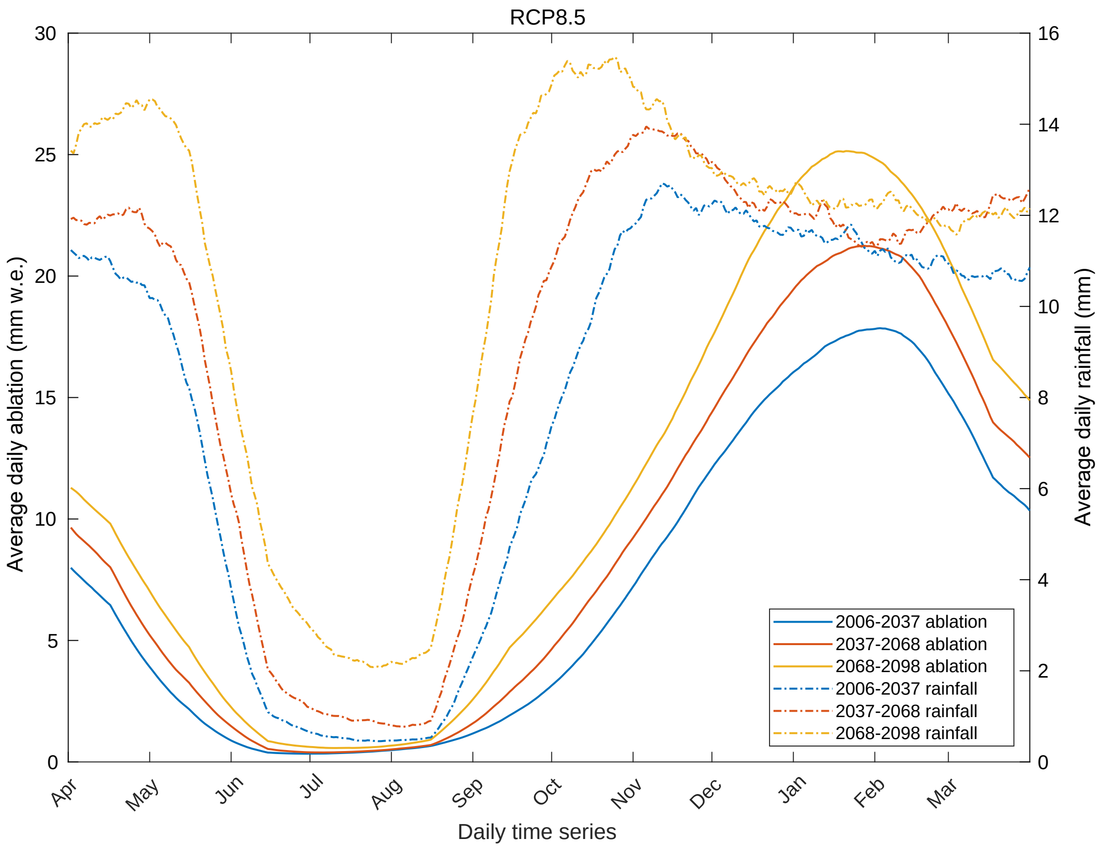

Figure 4.13: Comparison of daily ablation and rainfall averaged for all Waitaki glaciers through the 21st century for an RCP8.5 scenario.

For the RCP2.6 scenario, projections show limited variations in timing and magnitude of ablation and rainfall through the 21st century (Figure 4.12). Average daily ablation is highest in the summer, and average daily rainfall is consistently high between November and April, suggesting that runoff is largest in the warmer months with a peak in February projected. For RCP8.5, the timing of runoff contributions varies during the later portion of the century (2068-2098) with three distinct peaks in maximum contributions from either rainfall and ablation projected (Figure 4.13). Maximum contribution to runoff from rainfall is projected to occur in spring and autumn, and maximum contribution to runoff from ablation is projected to occur in the summer. Contributions to runoff from rainfall are projected to increase during the winter season through the century. The sum of daily runoff averaged across all glaciers is projected to increase by 36% by the end of the century for the RCP8.5 scenario, relative to the RCP2.6 scenario.

Finally, the percent change in sum of daily runoff averaged across all glaciers, relative to the sum in 2006-2037 for RCP2.6 is shown in Table 4.2. The 2006-2037 period for RCP2.6 was selected as the reference period because it most closely represents present-day conditions. Projected increases in average runoff by the middle of the century (2037-2068) range between 3% and 16%, depending on the RCP scenario. Average runoff is projected to increase by 3% to 39% by the end of the century depending on RCP scenario, relative to the average in 2006-2037 for RCP2.6. Minimal increases in average runoff of 2% to 3% are projected through the century if temperature stays within the range represented by an RCP2.6 scenario.

Table 4.2: Changes in the annual sum of daily runoff averaged across all Waitaki glaciers, relative to the runoff in 2006-2037 for RCP2.6

RCP	2006-2037 Δ runoff	2037-2068 Δ runoff	2068-2098 Δ runoff
2.6	0 %	+3 %	+2 %
4.5	-3 %	+9 %	+15 %
6.0	-2 %	+9 %	+22 %
8.5	-3 %	+16 %	+39 %

4.3 Monthly time series

Monthly time series of accumulation, ablation, and rainfall were calculated to further understand seasonal shifts of precipitation and runoff. Standard deviations were calculated for accumulation, ablation, and rainfall to determine the level of variability within the dataset for each month. Lastly, average monthly accumulation and rainfall were summed together to obtain total average monthly precipitation, and the same was done for ablation and rainfall to determine total average monthly runoff from glaciers in the Waitaki.

4.3.1 Accumulation, ablation, and rainfall

The first three figures (Figures 4.14, 4.15, and 4.16) show projections of average monthly accumulation, ablation, and precipitation, similar to daily time series analysis but with standard deviation included as a visual reference. The following three tables summarise the monthly values and show the extent of seasonal changes. The last three figures show an analysis of standard deviations for each process.

Monthly time series projections are similar to daily time series projections of accumulation, ablation, and rainfall processes. Projections of average monthly accumulation are highest between June and August and lowest between December and February (Figure 4.14). Notably, the standard deviation for accumulation is also largest between June and August, and lowest between December and January. This suggests there is more uncertainty around projections of months with maximum accumulation.

Monthly ablation averaged for all Waitaki glaciers is largest in January, and lowest between June and August for all RCP scenarios and time periods (Figure 4.15). Similarly, the standard deviation for ablation data shows largest variability during the summer months (December through February) when the most ablation is projected to occur, and least variability during the winter months when the least ablation is projected to occur.

Projected monthly rainfall averaged for all Waitaki glaciers is lowest in the winter months of June through August for all RCP scenarios and time periods (Figure 4.16). The standard deviation of rainfall data suggests that there is less variability or rainfall projections during these winter months than in the majority of other months. Monthly rainfall is projected to be consistently high between September and May, and the standard deviation is similarly projected to be highest during these months.

Overall, variability is largest when accumulation, ablation, and rainfall is projected to be highest through the year. Conversely, variability is lowest when accumulation, ablation, and rainfall processes are projected to be minimal. This suggests that there is more variability in the data when projecting maximum monthly averages, than when projecting minimum monthly averages for all processes.

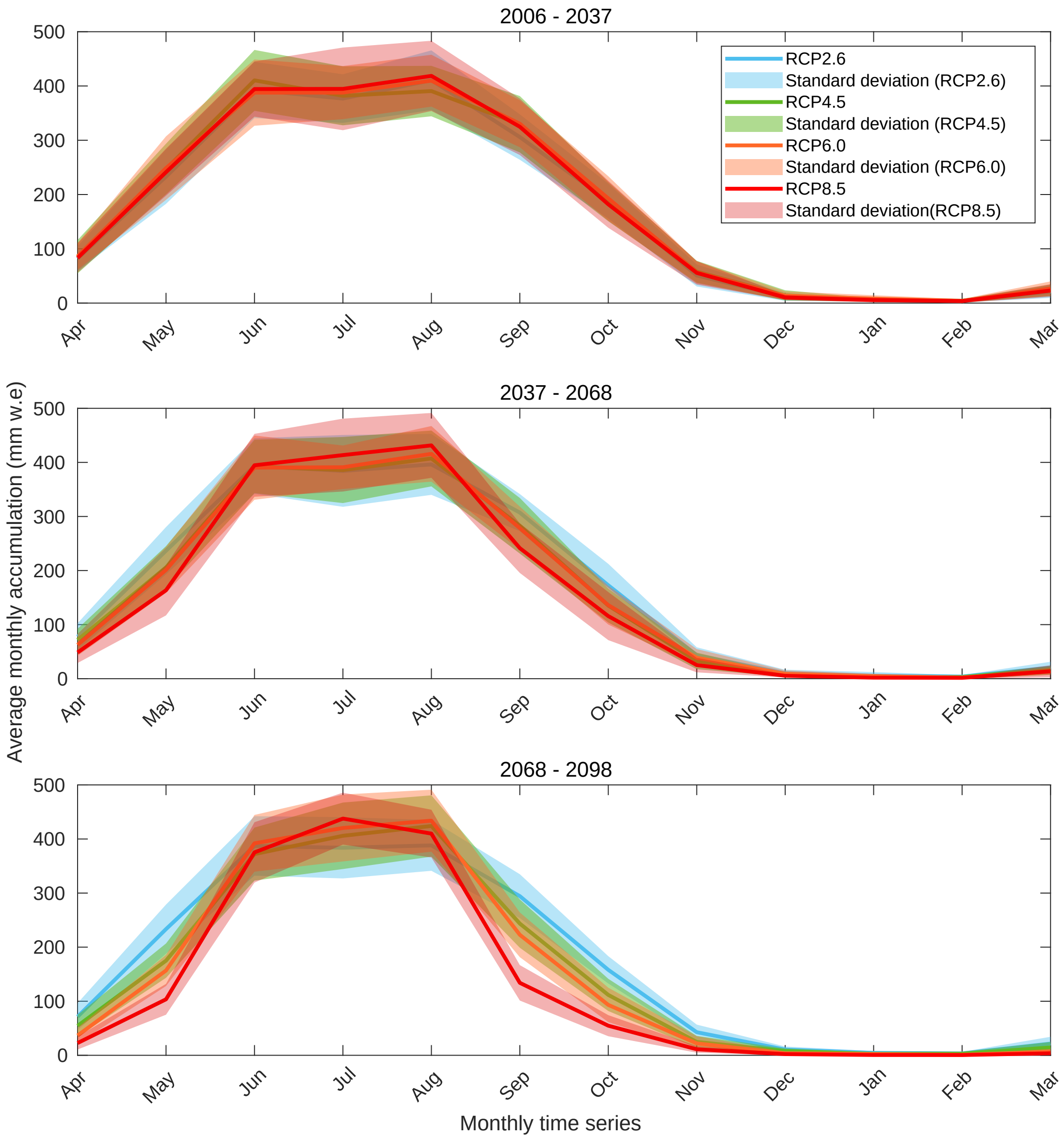

Figure 4.14: Monthly accumulation averaged for all Waitaki glaciers through the 21st century for each RCP scenario. Standard deviation included.

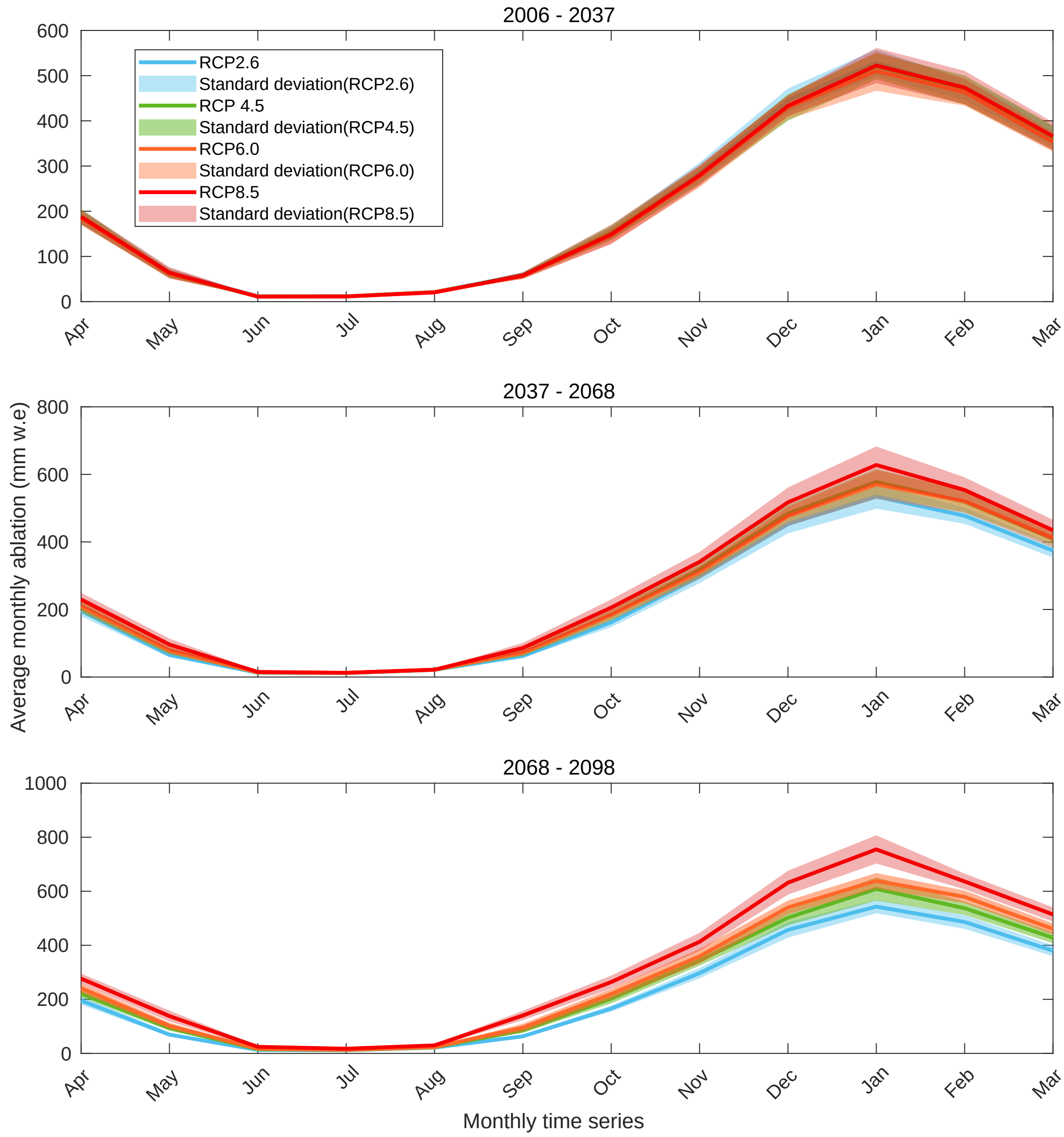

Figure 4.15: Monthly ablation averaged for all Waitaki glaciers through the 21st century for each RCP scenario. Standard deviation included.

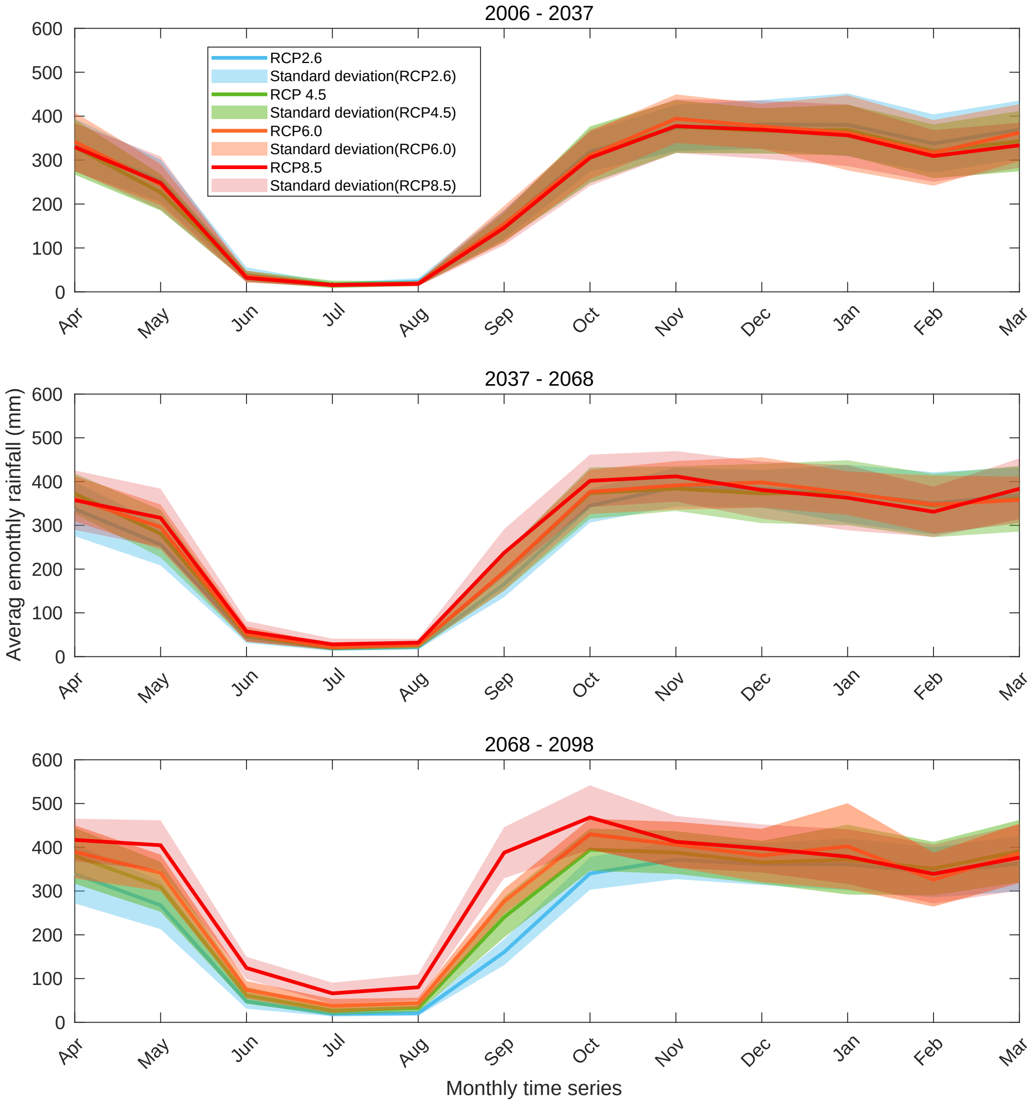

Figure 4.16: Monthly rainfall averaged for all Waitaki glaciers through the 21st century for each RCP scenario. Standard deviation included.

Changes between seasons are distinguishable through monthly time series and as such, all monthly averages for the above processes are listed below in the respective tables. The tables present changes in average monthly values between RCP extremes (RCP2.6 and RCP8.5). In some instances however, changes between other RCP scenarios may be slightly higher, but the comparison between RCP2.6 and RCP8.5 was selected because this typically represents the widest range of possible outcomes.

Projections of average monthly accumulation (Table 4.3) in the 2006-2037 period for the RCP8.5 scenario stay within 10% of all monthly accumulation values for RCP2.6 during the same time. Seasonal changes become more evident through the century. In the 2037-2068 time period, average monthly accumulation is projected to decrease in all months except for the winter season when most accumulation occurs. In the middle of the century during winter, accumulation is projected to increase from 0% to 9% between RCP2.6 and RCP8.5 scenarios. By the 2068-2098 period, accumulation is projected to decrease by up to 88% in the summer months when comparing RCP8.5 to RCP2.6. Further, accumulation is projected to decrease in all other months except for July and August, which show an increase of 14% and 6%, respectively between RCP2.6 and RCP8.5.

Similar to average monthly accumulation, changes in projected average monthly ablation are larger by the end of the century between RCP scenarios (Table 4.4). Projections for average monthly ablation show little variation in the first time period (2006-2037) but by the 2068-2098 time period, ablation is projected to increase in all months, by 31% in February to 122% in September, when comparing RCP2.6 and RCP8.5 scenarios. The largest projected increases in average monthly ablation are observed in late-autumn, winter, and early-spring. Conversely, the smallest increases in average monthly ablation is projected to occur in summer months, despite most ablation occurring during this time.

The highest degree of change out of accumulation, ablation, and rainfall processes is noted in average monthly rainfall projections Table (4.5). In the 2006-2037 period, rainfall is projected to to be lower for RCP8.5 than for RCP2.6 in every month except November. Average monthly rainfall for RCP8.5 is between 1% and 20% lower than rainfall for RCP2.6, depending on the month. In the 2037-2068 period, the difference in rainfall projections between RCP2.6 and RCP8.5 increases to 4% to 48% in all seasons except summer, which shows a decrease between 1% and 6%. By the last time period, the difference in rainfall is projected to increases during all months of the year except February where a decrease of 1% is observed. Most change between RCP2.6 and RCP8.5 occurs in the winter months with difference in rainfall ranging from 160% to 280% between the two scenarios. Notably, this pattern of change between RCP scenarios in the first time period (2006-2037) and the last time period (2068-2098) are opposite, where the difference in rainfall was initially decreasing in nearly all months to the difference in rainfall increasing in nearly all months.

Table 4.3: Average monthly accumulation (mm w.e.) through the 21st century for each RCP scenario.

Season	Month	RCP2.6	RCP4.5	RCP6.0	RCP8.5	Change from RCP2.6 to RCP8.5
2006 - 2037						
Autumn	April	82	85	86	83	1%
Autumn	May	233	247	249	241	4%
Winter	June	393	410	388	394	0%
Winter	July	377	382	388	395	5%
Winter	August	411	391	410	419	2%
Spring	September	306	330	330	325	6%
Spring	October	188	187	193	182	-3%
Spring	November	51	58	56	56	9%
Summer	December	11	14	14	10	-9%
Summer	January	6	6	8	6	-2%
Summer	February	4	4	4	4	0%
Autumn	March	21	23	27	23	10%
2037 - 2068						
Season	Month	RCP2.6	RCP4.5	RCP6.0	RCP8.5	Change from RCP2.6 to RCP8.5
Autumn	April	77	71	63	48	-38%
Autumn	May	235	207	201	163	-31%
Winter	June	395	390	394	393	0%
Winter	July	383	388	395	415	8%
Winter	August	396	407	419	430	9%
Spring	September	306	282	279	239	-22%
Spring	October	173	137	136	115	-34%
Spring	November	43	33	38	25	-42%
Summer	December	10	7	9	5	-47%
Summer	January	6	3	5	2	-67%
Summer	February	4	3	2	2	-63%
Autumn	March	21	15	13	13	-37%
2068 - 2098						
Season	Month	RCP2.6	RCP4.5	RCP6.0	RCP8.5	Change from RCP2.6 to RCP8.5
Autumn	April	71	54	37	22	-69%
Autumn	May	233	175	157	103	-56%
Winter	June	388	372	395	374	-4%
Winter	July	385	406	420	437	14%
Winter	August	390	424	433	411	6%
Spring	September	293	246	223	134	-54%
Spring	October	159	113	93	55	-65%
Spring	November	43	25	22	11	-74%
Summer	December	11	8	4	2	-80%
Summer	January	5	3	2	1	-88%
Summer	February	4	3	1	0	-86%
Autumn	March	21	14	7	4	-83%

Table 4.4: Average monthly ablation (mm w.e) through the 21st century for each RCP scenario.

Season	Month	RCP2.6	RCP4.5	RCP6.0	RCP8.5	Change from RCP2.6 to RCP8.5
2006 - 2037						
Autumn	April	188	188	185	188	0%
Autumn	May	64	61	62	64	0%
Winter	June	12	11	11	11	-6%
Winter	July	12	12	12	12	-3%
Winter	August	21	21	21	20	-4%
Spring	September	59	58	57	58	-2%
Spring	October	151	152	146	149	-1%
Spring	November	285	280	276	280	-2%
Summer	December	445	429	430	433	-3%
Summer	January	528	521	510	522	-1%
Summer	February	469	468	464	474	1%
Autumn	March	366	363	353	366	0%
2037 - 2068						
Season	Month	RCP2.6	RCP4.5	RCP6.0	RCP8.5	Change from RCP2.6 to RCP8.5
Autumn	April	196	207	209	230	17%
Autumn	May	66	77	79	96	46%
Winter	June	13	13	14	15	21%
Winter	July	12	12	12	13	5%
Winter	August	21	21	22	22	2%
Spring	September	62	71	72	86	38%
Spring	October	162	183	184	206	27%
Spring	November	297	318	310	341	15%
Summer	December	453	484	476	517	14%
Summer	January	534	578	570	628	17%
Summer	February	478	519	521	554	16%
Autumn	March	374	409	412	434	16%
2068 - 2098						
Season	Month	RCP2.6	RCP4.5	RCP6.0	RCP8.5	Change from RCP2.6 to RCP8.5
Autumn	April	196	221	241	277	41%
Autumn	May	69	94	102	138	99%
Winter	June	13	15	17	24	88%
Winter	July	12	13	13	17	46%
Winter	August	22	23	23	30	38%
Spring	September	63	85	95	140	122%
Spring	October	166	203	220	264	59%
Spring	November	297	344	359	413	39%
Summer	December	457	502	540	632	38%
Summer	January	543	609	639	755	39%
Summer	February	486	537	579	636	31%
Autumn	March	380	428	461	514	35%

Table 4.5: Average monthly rainfall (mm) through the 21st century for each RCP scenario.

Season	Month	RCP2.6	RCP4.5	RCP6.0	RCP8.5	Change from RCP2.6 to RCP8.5
2006 - 2037						
Autumn	April	334	330	342	330	-1%
Autumn	May	253	227	244	248	-2%
Winter	June	39	36	35	32	-19%
Winter	July	16	17	15	16	-5%
Winter	August	23	19	19	18	-20%
Spring	September	154	148	154	146	-5%
Spring	October	319	312	311	305	-4%
Spring	November	373	376	394	377	1%
Summer	December	381	367	377	369	-3%
Summer	January	380	368	362	356	-6%
Summer	February	338	320	316	309	-8%
Autumn	March	369	343	362	334	-10%
2037 - 2068						
Season	Month	RCP2.6	RCP4.5	RCP6.0	RCP8.5	Change from RCP2.6 to RCP8.5
Autumn	April	337	372	361	358	6%
Autumn	May	256	281	296	317	24%
Winter	June	46	48	52	58	26%
Winter	July	19	20	22	28	51%
Winter	August	22	25	27	32	48%
Spring	September	166	193	193	237	43%
Spring	October	345	374	376	402	16%
Spring	November	388	384	391	412	6%
Summer	December	384	373	398	381	-1%
Summer	January	372	375	374	363	-2%
Summer	February	350	345	348	331	-6%
Autumn	March	369	361	358	383	4%
2068 - 2098						
Season	Month	RCP2.6	RCP4.5	RCP6.0	RCP8.5	Change from RCP2.6 to RCP8.5
Autumn	April	340	381	390	417	23%
Autumn	May	268	309	341	405	51%
Winter	June	48	62	74	124	160%
Winter	July	19	27	38	66	243%
Winter	August	21	33	44	80	280%
Spring	September	160	240	276	388	142%
Spring	October	340	395	430	468	38%
Spring	November	372	388	406	413	11%
Summer	December	361	366	381	397	10%
Summer	January	361	372	402	379	5%
Summer	February	343	351	326	339	-1%
Autumn	March	363	391	387	377	4%

For accumulation, ablation, and rainfall processes, the standard deviation for each month was calculated to determine the variability of the data within monthly averages. The variability in monthly averages can provide insights into the possibility of extreme weather events occurring, or the level of certainty around projected values. The following figures (Figures 4.17, 4.18, and 4.19) show the standard deviation of accumulation, ablation, and rainfall, respectively through each RCP scenario and time period to determine which months have the highest variability in the data.

Each month in the 2006-2037 period for RCP2.6 was selected to be the standard deviation baseline. Baseline standard deviation is represented as 100% and thus variability in standard deviation for other time periods and RCP scenarios are shown relative to 100%.

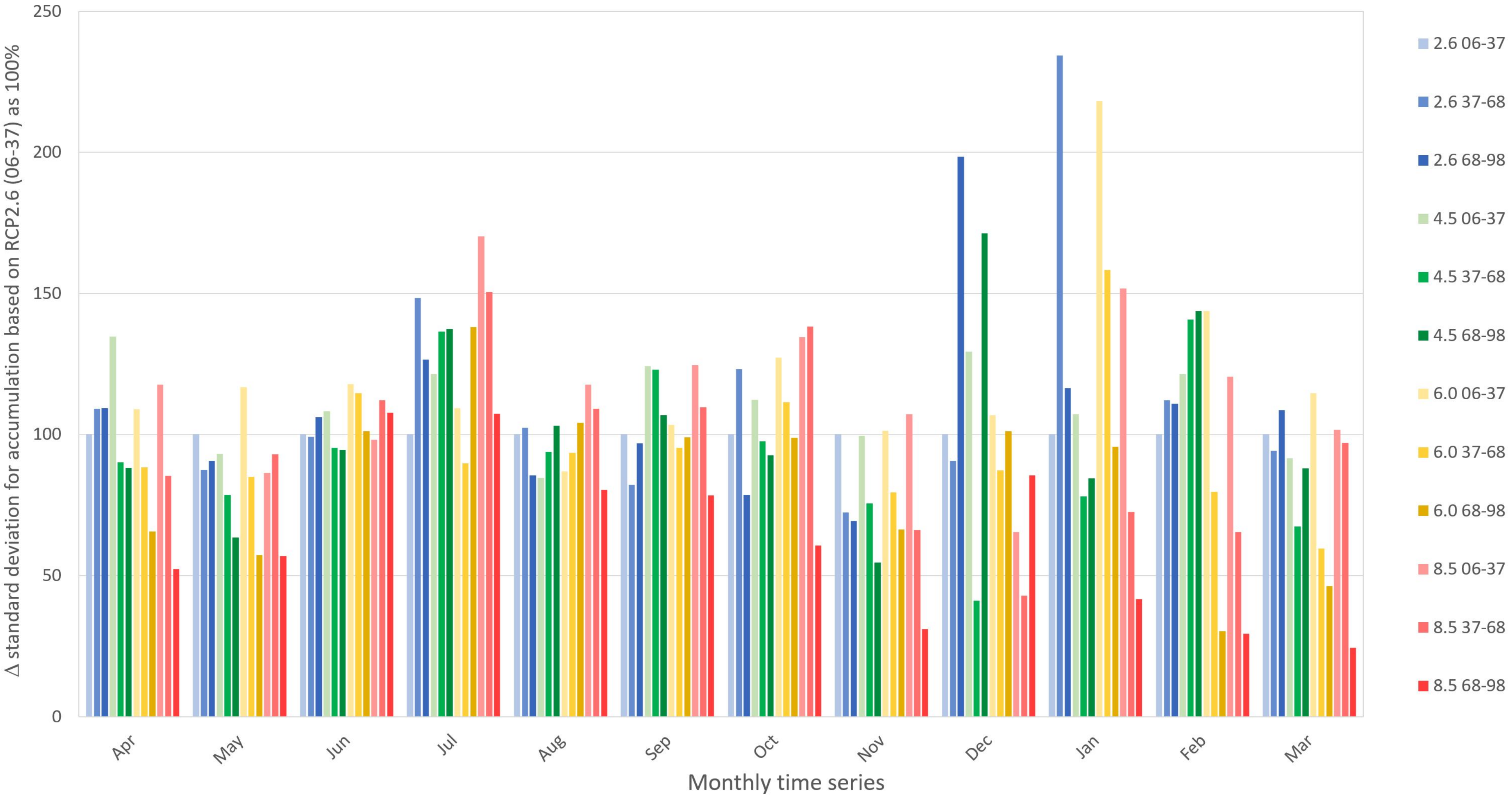

Figure 4.17: Standard deviation variability for average monthly accumulation. The time period between 2006 and 2037 for an RCP2.6 scenario was used as baseline and considered as 100%. All percent changes in standard deviation are relative to the baseline.

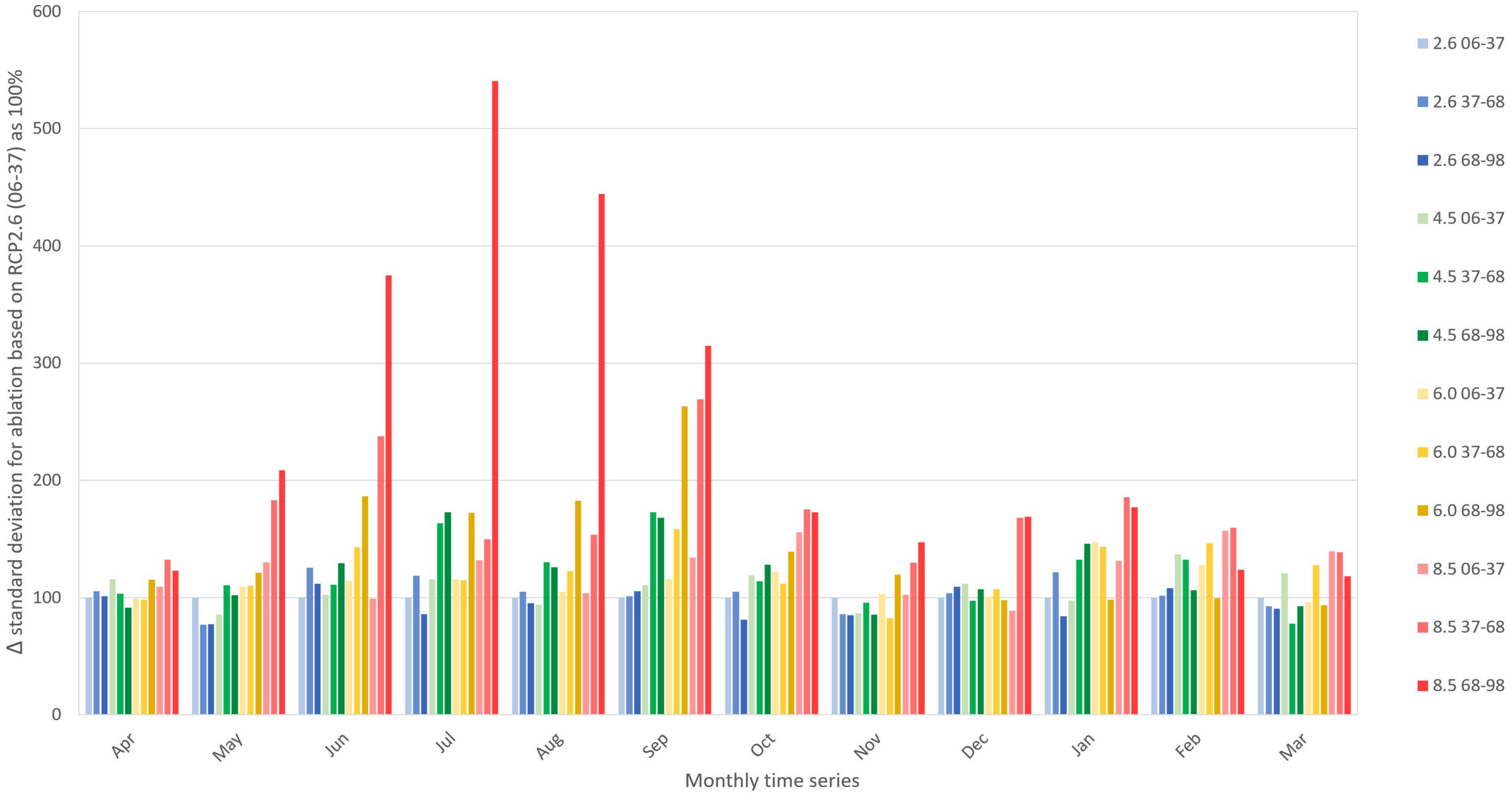

Figure 4.18: Standard deviation variability for average monthly ablation. The time period between 2006 and 2037 for an RCP2.6 scenario was used as baseline and considered as 100%. All percent changes in standard deviation are relative to the baseline.

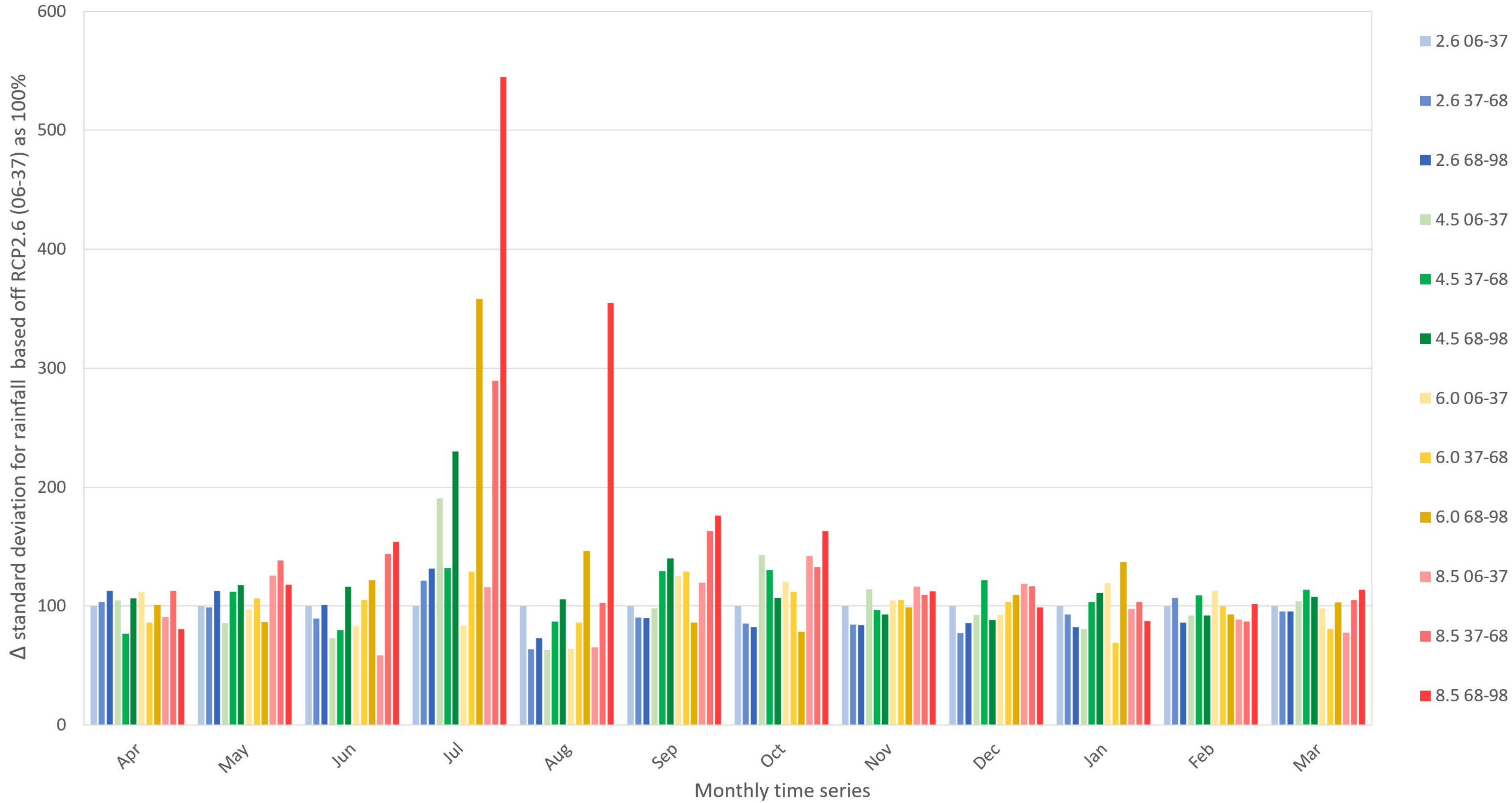

Figure 4.19: Standard deviation variability for average monthly rainfall. The time period between 2006 and 2037 for an RCP2.6 scenario was used as baseline and considered as 100%. All percent changes in standard deviation are relative to the baseline.

The variability in the standard deviation in accumulation data (Figure 4.17) shows the largest differences relative to RCP2.6 (2006-2037) occurring in January for RCP2.6 and RCP6.0, and in December for RCP2.6. There is consistently less variability in the data in the 2068-2098 period for RCP8.5 in all months except June and July when most accumulation occurs.

The variability in the standard deviation of ablation data (Figure 4.18) shows more distinctive trends compared to accumulation data. Variability tends to increase with increasing RCP scenarios, though exceptions exist for some months. The most notable result is the large increase in variability for the RCP8.5 scenario for all months, but specifically between May and September during the last portion of the century (2068-2098). While minimal ablation typically occurs in the winter months, the results show that variability of this data for these months is highest near the end of the century, suggesting uncertainty of possible ablation amounts for this RCP scenario.

Lastly, the variability in the standard deviation for rainfall data is shown in Figure 4.19. Similar to ablation, most variability in rainfall data occurs in the winter months of July and August during the later portion of the century (2068-2098) for an RCP8.5 scenario. Precipitation as rain decreases in the winter months compared to summer months, but rainfall is projected to increase most significantly in the winter months by the end of the century. This increase in variability within the data suggests higher uncertainty for the projections of rainfall during winter compared to spring, summer or autumn. Lastly, as rainfall is only projected across the changing glacier area rather than across the entire catchment, these results are specific to glacierized areas of the watershed.

4.4 Statistical comparison of annual time series analysis

The results in the above sections (Sections 4.1, 4.2, and 4.3) were calculated using spatial averages that consist of one average value for accumulation, ablation or rainfall per glacier. This section presents the comparison between the method used above by calculating spatially averaged annual ablation and total annual sum of ablation for particular glaciers. Total annual ablation volume for the Waitaki catchment is also calculated.

Subsection 4.4.1 shows projections of spatially averaged and total annual ablation volumes calculated for three individual glaciers of varying size for RCP6.0, and subsection 4.4.2 shows the total annual ablation volume of all glaciers in the Waitaki catchment for all RCP scenarios. These results aim to inform the discussion around peak water in the Waitaki catchment.

4.4.1 Annual ablation of individual glaciers

Annual ablation volume was calculated for three individual glaciers. The first glacier is an unnamed ridge glacier (RGI 2177) (Figure 4.20), the second is the Huxley Glacier (Figure 4.21), and the third is the Haupapa/Tasman Glacier (Figure 4.22).

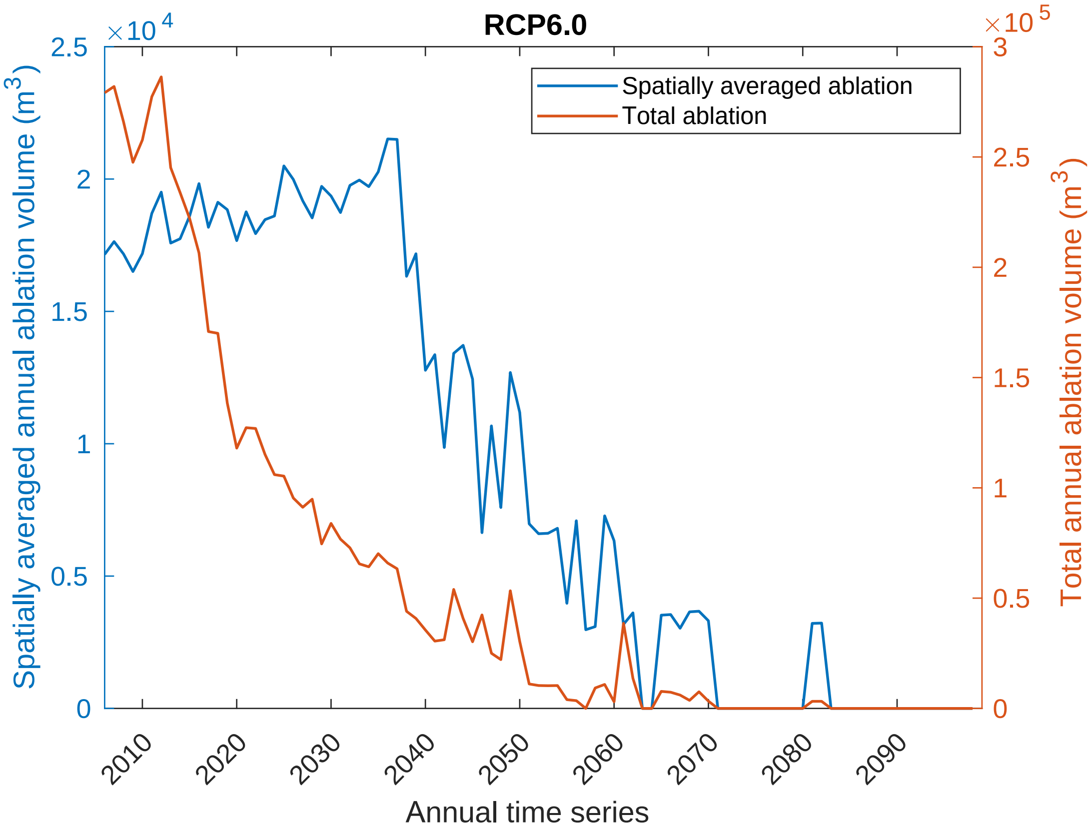

Figure 4.20: Spatially averaged annual ablation volume and total annual ablation volume of glacier 2177.

Figure 4.20 shows the spatially averaged annual ablation volume calculated for Glacier 2177 on the left axis. This spatial averaging method was also used in Sections 4.1, 4.2, and 4.3. The total annual ablation volume on the right axis represents the sum of ablation calculated, specifically accounting for decreasing glacier size.

Spatially averaged ablation volume and total ablation volume show a similar trend, with annual ablation volume projected to decrease later in the century for both methods of calculation. Spatially averaged annual ablation volume is projected to increase slightly to approximately 2040, and then decrease rapidly thereafter. Total annual ablation volume is projected to be at its highest at the beginning of the century then decrease rapidly from approximately 2015. Spatially average ablation is projected to be higher throughout the century compared to total ablation, except for approximately the first decade (2006 to 2015).

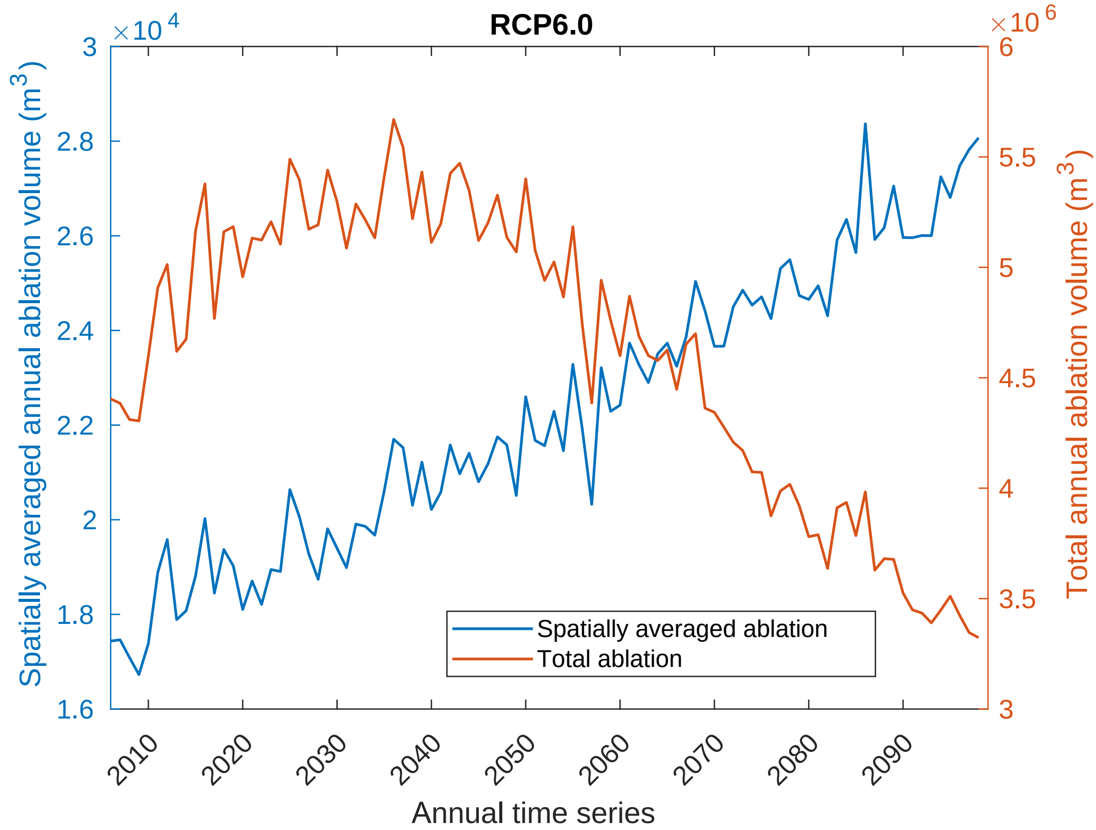

Figure 4.21: Spatially averaged annual ablation volume and total annual ablation volume of Huxley Glacier.

Spatially averaged annual ablation volume and total annual ablation volume show different trends for the Huxley Glacier (Figure 4.21) when compared to Glacier 2177 (Figure 4.20). Spatially averaged ablation volume is projected to steadily increase into the century, while total ablation volume is projected to peak around 2030-2040 before steadily decreasing again. This peak in total annual ablation volume may suggest peak water could be reached around 2030-2040 for the Huxley glacier for an RCP6.0 scenario.

Though the Huxley glacier is reducing in size, ablation is still projected to occur every year while the ice still exists in the modelled glacier grid. As the glacier recedes, total ablation is adjusted annually to account for reducing ice area. Conversely, spatially averaged ablation ablation volume is shown to continue to increase because while less overall ice exists in the glacier domain each year, projected warmer temperatures mean that remaining ice will melt more rapidly, even though there is less ice to melt.

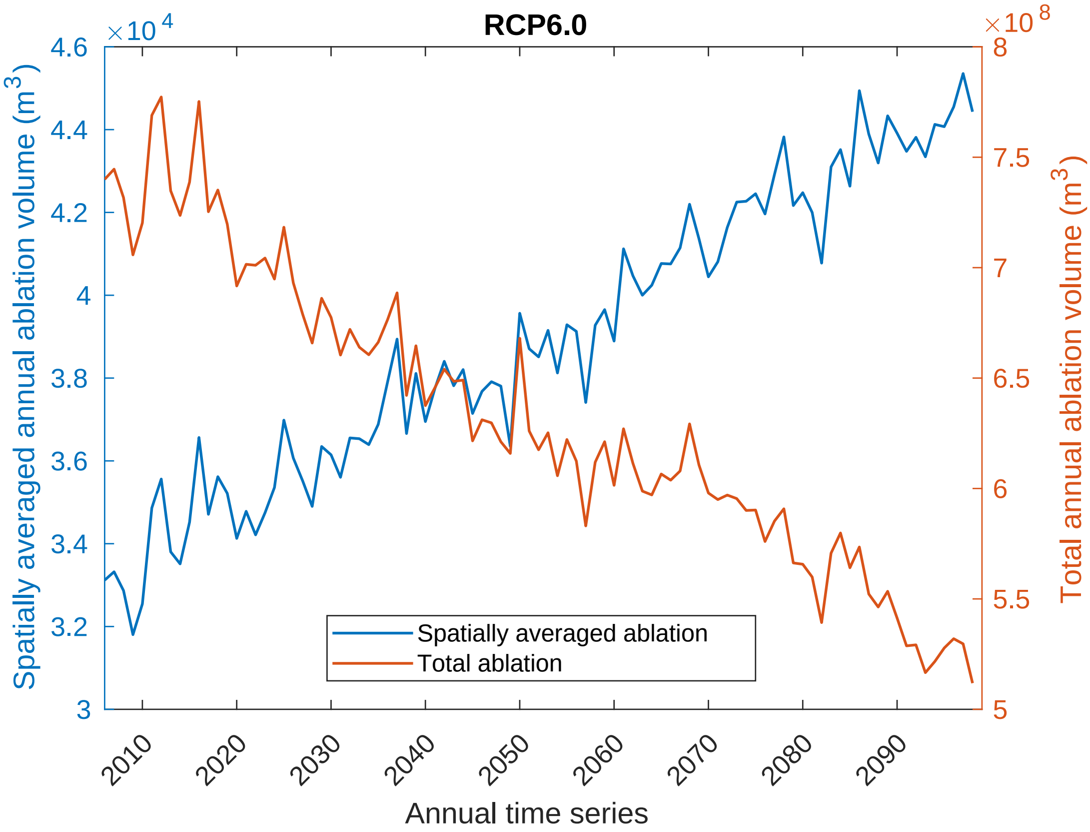

Figure 4.22: Spatially averaged annual ablation volume and total annual ablation volume of Haupapa/Tasman Glacier.

Similar to the Huxley Glacier (Figure 4.21), spatially averaged annual ablation volume for the Huapapa/Tasman Glacier (Figure 4.22) is projected to increase steadily through the century. Total annual ablation volume is projected to steadily decrease through the century. Unlike the Huxley Glacier, The Haupapa/Tasman Glacier does not show a peak in ablation volume in the total annual ablation volume plot, suggesting that peak water has already occurred in an RCP6.0 scenario, or the peak is occurring around the start of the century (2006-2020) but this cannot be confirmed without modeling total ablation further into the past.

4.4.2 Annual ablation of all Waitaki glaciers

Total annual ablation volume of all glaciers in the Waitaki catchment combined was calculated for all RCP scenarios (Figure 4.23).

Total annual ablation volume is projected to decrease for all RCP scenarios by the end of the century. The largest decrease in ablation by the end of the century is projected to occur for the RCP8.5 scenario. By the end of the century, projected ablation for the RCP4.5 and RCP6.0 scenarios are similar to each other and are both less than projections for an RCP8.5 scenario. The RCP2.6 scenario

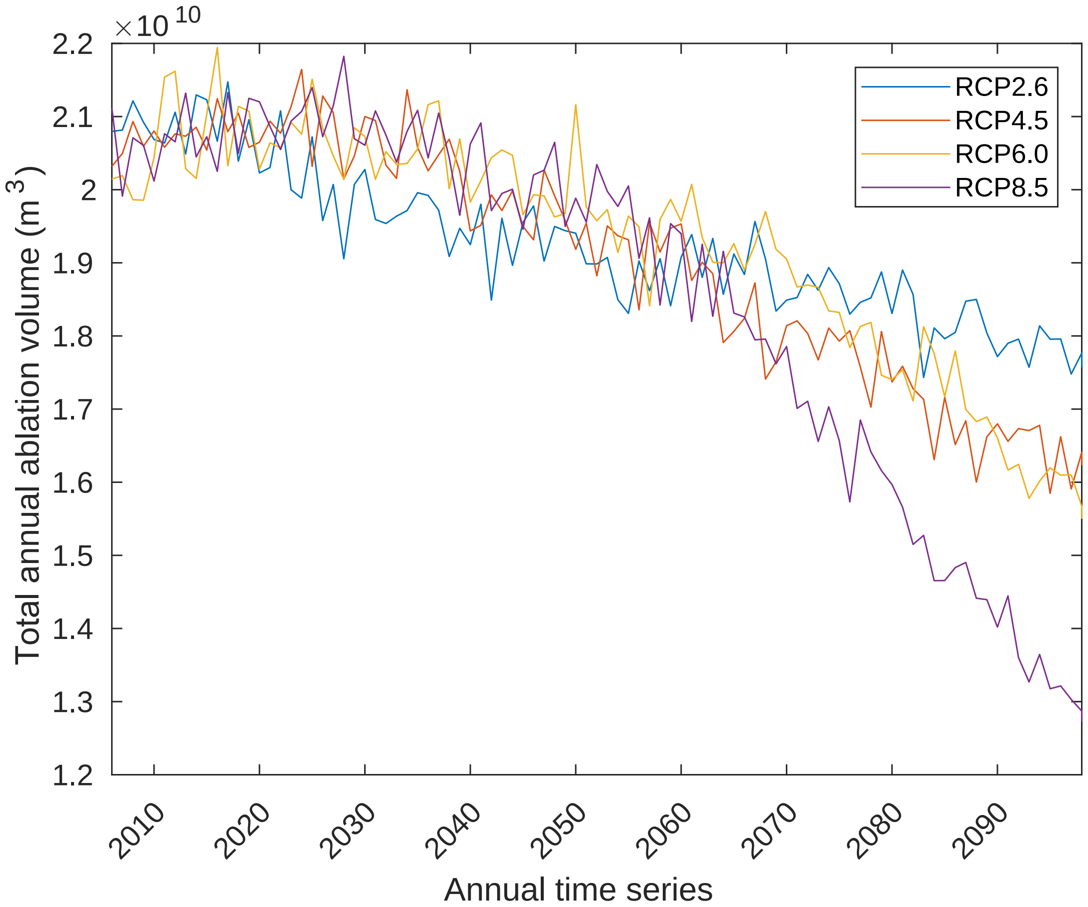

Figure 4.23: Total annual ablation volume of all glaciers in the Waitaki catchment.

shows the most gradual decrease in annual ablation by the end of the century. Projections of annual ablation for each RCP scenario notably diverge from each other around the year 2060.

A subtle peak occurs in the projected annual ablation data between roughly 2015 and 2035 for the RCP4.5, RCP6.0, and RC08.5 scenarios. The peak in projected ablation volume for the RCP2.6 scenario appears to occur slightly early, around 2006 to 2020. These results suggest that peak water is projected to occur in the Waitaki catchment in the first half of the century (before 2040) for all RCP scenarios.

4.5 Summary of key results

1. Glacier volume in the Waitaki is projected to decrease for all RCP scenarios through the 21st century. For an RCP2.6 scenario, by 2098 only 48% to 52% of glacier volume, on average, is projected to remain relative to the volume in 2006. For an RCP8.5 scenario as little as 14% to 24%, on average, is projected to remain.

2. If regional temperature stays within the range represented by the RCP2.6 scenario during the 21st century, timing and magnitude of maximum and minimum accumulation, ablation, and rainfall at the end of the century (2068-2098) is projected to be similar to the beginning of the century (2006-2037).

3. Changes in timing and magnitude of accumulation, ablation, and rainfall are projected to become larger in RCP4.5, RCP6.0 and RCP8.5 scenarios, respectively.

   - By the end of the century (2068-2098) for an RCP8.5 scenario, average accumulation is projected to decrease in every month except July and August, relative to the RCP2.6 scenario. Average accumulation is projected to decrease by as much as 88% in January and increase by as much as 14% in June. Average ablation is projected to increase in every month, and by as much as 122% in September. Average rainfall is projected to increase in every month except February. Average rainfall is projected to increase by as much as 280% for an RCP8.5 scenario, relative to an RCP2.6 scenario by the end of the century.
   - By the end of the century (2068-2098) for an RCP8.5 scenario, accumulation is projected to begin later in the autumn, and end earlier in spring relative to the RCP2.6 scenario. Increases in ablation are projected to occur later into autumn and earlier into spring. More rainfall is projected to occur later into spring, and earlier in spring for an RCP8.5 scenario, relative to an RCP2.6 scenario for the end of the century.

4. Standard deviations of accumulation, ablation, and rainfall data suggest variability of projections increase depending on month, RCP scenarios, and time period. The largest variability of accumulation projections occurs in December and January for all RCP scenarios and time periods. Variability of ablation projections is largest between May and September for RCP8.5 at the end of the century (2068-2098). Variability of rainfall projections is largest in July and August for RCP6.0 and RCP8.5 scenarios during the end of the century.

5. Peak water for glaciers in the Waitaki catchment is projected to occur at different times depending on the glacier's size. Peak water in the Waitaki Catchment, based on ablation of all glaciers in the catchment, is projected to occur before 2040 for all RCP scenarios. The peak is projected to oc-

cur slightly sooner for RCP2.6 (between the years 2006 and 2020) than for RCP4.5, RCP6.0, and RCP8.5 (between the years 2014-2035).

Chapter 5

Discussion

The Waitaki catchment is one of New Zealand's most important catchments for hydroelectricity generation and long-term water storage. In 2010, power stations in the Waitaki generated 35% to 40% of the country's electricity (Purdie and Bardsley, 2010). The three lakes in the upper catchment account for nearly 60% of New Zealand's controllable water storage (Sirguey, 2010). Additionally, the agriculture industry strongly relies on runoff from the mountainous headwaters of the Waitaki, where most of the precipitation in the catchment occurs (Kerr et al., 2011). Runoff from the headwaters of the Waitaki is generated through rainfall, snowmelt, and ice melt. As climate changes, the runoff generating processes may also change, resulting in seasonal shifts to timing, magnitude, and duration of high flow and low flow events. The Waitaki catchment holds some of the largest glaciers in the country and as such, understanding the implications of glacier retreat is an important component for long-term planning of water resource availability.

This chapter discusses the key findings in this research, starting with projections of overall changes to glacier volume in the Waitaki catchment through the 21st century. Then projected shifts in accumulation, ablation, and rainfall processes and the effects on precipitation and runoff are discussed. Lastly, possible implications of these changes on downstream environments are summarised.

5.1 The future of the Waitaki glaciers

Changes to many individual glaciers throughout New Zealand have been studied over time (Woo and Fitzharris, 1992; Cullen et al., 2017; Purdie et al., 2021) but fewer studies existed on regional-scale glacier change until recently (Chinn et al., 2012; Mackintosh et al., 2017; Vargo et al., 2020). Results from these studies suggest that New Zealand glaciers are receding. One exception was noted during the period between 1983 and 2009 where at least 58 glaciers advanced as a result of reduced air temperatures (Mackintosh et al., 2017). Future projections of regional glacier change for New Zealand are limited, with only one study by Anderson et al. (2021) published thus far that focuses on the Aoraki Mt Cook region, which includes glaciers located both east and west of the Southern Alps divide. The Waitaki catchment is included in the study as part of the Aoraki Mt Cook region. Anderson et al. (2021) found that glaciers in the study region were projected to recede through the 21st century. Projections of volume loss in the study were similar for all RCP scenarios until about 2050, after which projections of volume diverge from one another based on RCP scenario. By 2099 for an RCP2.6 scenario, a 50% decrease in volume relative to 2005 was projected for the Aoraki Mt Cook region, and as little as 8% of volume was projected to remain, relative to the 2005 volume for an RCP8.5 scenario (Anderson et al., 2021).

As this research examines the model output from the coupled mass balance and flow models used by Anderson et al. (2021), and the volume plots were altered to focus on the Waitaki Catchment, it is expected that the characteristics of volume projections are similar and thus limiting a true independent comparison of results. As such, for an RCP2.6 scenario, by 2098, on average 48% to 52% of ice is projected to remain relative to the 2005 volume, and as little as 14% to 24% on average, is projected to remain for the RCP scenario.

Several global studies of projected glacier mass balances have considered New Zealand in their models (Radić et al., 2014; Huss and Hock, 2015; Hock et al., 2019; Shannon et al., 2019; Marzeion et al., 2020). These studies cannot be directly compared to results within the Waitaki catchment because of the difference in scale, but the Aoraki Mt Cook region, which the upper Waitaki catchment is a part of, does contain 54% of the ice in New Zealand (Anderson et al., 2021), so similarities are noted between studies. While global studies show downward trends of glacier volume in New Zealand (Radić et al., 2014; Huss and Hock, 2015; Hock et al., 2019; Shannon et al., 2019; Marzeion et al., 2020), the projections of volume loss by the end of the century tend to be significantly less than what is found in this research. Projections of volume loss in the Waitaki catchment are greater per RCP scenario by the end of the century compared to projections of New Zealand glacier volume in other studies (Radić et al., 2014; Hock et al., 2019; Marzeion et al., 2020). Additionally, volume loss in New Zealand projected by the end of the century for an RCP8.5 scenario made by Shannon et al. (2019) is similar to projections in the Waitaki, but the rate of change through time is different. Shannon et al. (2019) shows the majority of ice loss in New Zealand occurs before 2050 for an RCP8.5 scenario, contrary to what is depicted in the results presented for the Waitaki.

Glaciers around the world are losing mass, and the same is projected for glaciers in the Waitaki catchment through the century based on the four RCP scenarios. The greatest uncertainty in the rate and extent of glacier mass loss stems from the uncertainty around which climate change mitigation scenario will eventuate (Marzeion et al., 2020; Anderson et al., 2021).

Change in glacier mass balance is driven by accumulation and ablation processes. Ablation must exceed accumulation for glaciers to lose mass and glaciers in the Waitaki are presently out of equilibrium and therefore receding. The results in this research suggest that volume loss will continue at a similar rate by the end of the century (RCP2.6) or become further out of equilibrium for RCP4.5, RCP6.0, or RCP8.5 by the end of the century.

5.2 Changes to ablation, rainfall, and accumulation

Changes in precipitation and runoff projected over the 21st century have been studied for several catchments on the South Island (Aqualinc Research, 2011; Poyck et al., 2011; Zammit and Woods, 2011; Caruso et al., 2017; Collins, 2020), and all studies show similar results. Annual runoff in South Island catchments is projected to increase over the century. For a "middle of the road" emission scenario based on the IPCC Fourth Assessment, which is comparable to an RCP6.0 scenario in this research, Poyck et al. (2011) found that annual runoff in the Clutha catchment, located south of the Waitaki catchment, was projected to increase by roughly 6% by 2040, and approximately 10% by 2090 relative to annual flows averaged for the 1980-1999 period. The same emission scenario and reference time period were used in a study of the Waimakariri catchment, near Christchurch (Zammit and Woods, 2011), which showed an increase in mean runoff by about 7% in 2040 and by about 10% in 2090, relative to 1980-1999. A study in of the Rangitata catchment, located adjacent and northeast to the Waitaki catchment, projected an 8% increase in mean flow by 2040, relative to 1980-1999 using the same emission scenario (Aqualinc Research, 2011). Lastly, a study by Caruso et al. (2017) suggested that increases in annual inflow to all three glacier lakes in the upper Waitaki basin is projected to range between 3% and 11% during the 2040s and the 2090s.

There are limitations to the direct comparison of runoff between the studies described above and this research. It must be noted that in this research, ablation and rainfall are only calculated from glacier domains, and not across the entire catchment like in the above studies. It is also important to note that the above studies of South Island catchments use a hydrological model (TopNet) that considers snow melt, but there is no representation of glaciers and glacier melt in the model (Poyck et al., 2011). Further, snowmelt components within the TopNet model are not directly validated due to the lack of systematic snow storage measurements within catchments (Zammit and Woods, 2011).

The results from this research of average ablation from a given glacier in the Waitaki catchment suggest slightly higher projections of annual runoff for the middle and end of the century (Table 4.2) than those of other South Island catchments, noting the limitations around such comparison. Increases in average ablation are not unexpected, as warmer temperatures through the century will promote ice to melt more rapidly from glaciers that persist. Conversely, when considering total changes in ablation volume, runoff volume is shown to decrease by the middle and the end of the century as total ice volume decreases. Decreases in overall ablation volume are discussed further in Section 5.3, Waitaki catchment peak water projections.

All studies of South Island catchments uniformly report increases in projected annual precipitation with the most significant increases occurring in the winter and spring (Caruso et al., 2017; Aqualinc Research, 2011; Poyck et al., 2011; Zammit and Woods, 2011). In this research, rainfall alone follows a similar trend, with significant increases projected during the winter and early spring, and average accumulation is projected to increase in the winter months by the end of the century. Climate projections suggest the increases in future precipitation may be a result of increases in westerly wind circulation over New Zealand, especially in the winter and spring, bringing more moisture over the South Island (Renwick et al., 2010). Additionally, increases in air temperature suggest that more precipitation will fall as rain rather than snow during the winter and spring months (Caruso et al., 2017; Poyck et al., 2011; Renwick et al., 2010).

Seasonal shifts are also apparent in runoff. Runoff in the Waimakariri catchment is projected to increase during the winter and spring by as much as 50% to 70%, whereas runoff during the summer and autumn is projected to remain the same or decrease slightly (Zammit and Woods, 2011). These same seasonal changes to runoff are projected in the Clutha catchment (Poyck et al., 2011), the Rangitata catchment (Aqualinc Research, 2011), and in the upper Waitaki basin (Caruso et al., 2017) using the TopNet model.

Again while those studies are not directly comparable to the findings in the research, similar seasonal shifts are projected for rainfall, accumulation, and ablation. For RCP6.0, similar to the scenario in the other studies of South Island catchments, at the end of the century rainfall is projected to increase by 109% in the winter, and average ablation is projected to increase by as much as 51% in the spring, relative to the RCP2.6 scenario (Tables 4.4 and 4.5). The large increases in contributions to runoff occur in winter, then spring, which has been similarly modelled in the studies of other catchments.

The results vary for summer runoff between this research and studies of other catchments. In all other catchments, summer runoff is projected to either remain the same, or decrease slightly over the century (Caruso et al., 2017; Aqualinc Research, 2011; Poyck et al., 2011; Zammit and Woods, 2011). Poyck et al. (2011) reasoned the seasonal changes in runoff were mainly due to changes in precipitation. Increases in precipitation were projected for winter and spring, whereas precipitation was projected to remain constant or decrease slightly in summer and autumn. Further, and due to rising temperatures, precipitation would fall predominantly as rain rather than snow during winter and spring (Caruso et al., 2017; Poyck et al., 2011). This research suggests that By the end of the century, rainfall in the summer months is projected to range between -1% and +10% for RCP8.5, relative to RCP2.6, whereas average ablation is projected to increase by 31% to 38% in the same months. The main reason the results vary for summer runoff between this study and other South Island catchment studies could be because the TopNet model used in other studies does not explicitly account for glacier melt. If considering only rainfall, results from this research would be comparable to other studies but when also considering ablation contributions to runoff however, results suggest that average summer runoff may continue to increase until a critical ice volume is reached in the catchment. Glacier runoff would then decrease as glaciers recede further in or disappear. This is discussed explicitly in the following section.

Despite the coarse considerations of snowmelt in the TopNet model, both Poyck et al. (2011) and Caruso et al. (2017) noted a reduction of snowmelt contributions to runoff during spring and summer flows. In the past, snowmelt and glacier melt together was estimated to contribute between 8% and 24% to annual runoff in the Waitaki basin (McKerchar et al., 1998). A study by Kerr (2013) agreed, with snow and ice melt contributions to runoff estimated at 17% for the Waitaki. Ice melt specifically was estimated to contribute about 6% to runoff into Lake Pukaki alone, in the upper Waitaki basin (Purdie and Fitzharris, 1999).

Other studies have shown that glacier melt compensates for otherwise decreasing summer runoff (Fountain and Tangborn, 1985; Young and Hewitt, 1993; Sirguey, 2010). A study of a glacierized basin in Canada by Hopkinson and Young (1998) found glaciers contributed approximately 2% to annual runoff, but in low flow years, contributions increased to 13%. In the driest month of the year, glacier runoff made up 56% of runoff. Similarly, during a drought on the South Island of New Zealand in 2005, Sirguey (2010) found that ice melt mitigated otherwise low flow volumes into the glacier lakes of the upper Waitaki basin. The greatest volume of ice is located in the Pukaki sub-catchment and contributions of glacier melt, much larger than usual, was believed to sustain runoff to within 17% of the mean annual flow into Lake Pukaki, despite precipitation being reduced by 34%.

The buffering effect of glacier melt on runoff is particularly important during drought periods, but as glaciers recede ice melt contributions mitigating low flows may become more unreliable. The following section discusses glacier melt contributions to runoff variability over the 21st century in the Waitaki catchment.

5.3 Waitaki catchment peak water projections

Reduction in glacier mass leads to increases in ice melt contributions to runoff, often only lasting for a few years or decades (Orlove, 2009). The temporary increase in ice melt contributions from receding glaciers is called "peak water". After peak water is reached, ice melt contributions steadily decrease as glaciers become smaller or disappear completely (Jansson et al., 2003; Huss and Hock, 2018).

The timing of peak water for a particular glacier will vary depending on its size. The Waitaki catchment contains glaciers of many different sizes. If climate change and glacier retreat continue, most small glaciers would disappear, while larger and high-altitude glaciers would likely eventually establish a new equilibrium state (Anderton, 1973). Haupapa/Tasman Glacier, located in the Lake Pukaki subcatchment of the Waitaki catchment, is New Zealand's largest glacier. Large glaciers such as the Haupapa/Tasman, respond very slowly to climate change and because of their great mass, they will likely continue to exist for several centuries (Fitzharris et al., 1999). In addition to Haupapa/Tasman Glacier, other large glaciers in the catchment, namely Mueller, Hooker, and Murchison glaciers (Figure 5.1), may obscure the visibility of distinct peak water that could otherwise be present if the catchment was only composed of smaller ridgeline and pocket glaciers (Bliss et al., 2014).

The variability in timing of peak water depending on glacier size agrees with the findings in this study. When calculating total ablation, described in Chapter 3.5 and for RCP6.0, the maximum total annual ablation volume is projected to occur at different times for different sized glaciers in the Waitaki catchment. Small ridgeline or pocket glaciers are likely to disappear before the end of the century with the peak in ablation possible within the first two decades of the century for an RCP6.0 scenario. The peak in total ablation for slightly larger glaciers may have yet to occur (Figure 4.21), with the Huxley glacier showing a peak around 2030-2040. Larger glaciers in the catchment such as the Haupapa/Tasman show a steady decrease in total ablation over the century, suggesting that peak water has either passed or is occurring at the start of the decade. It is difficult to differentiate between if peak water has passed or if it is presently occurring without beginning the model run from a time further into the past. Model runs beginning sometime in the last century could provide a clearer picture of when peak water could, or did occur for glaciers that presently show a steady decrease in projected total ablation volume.

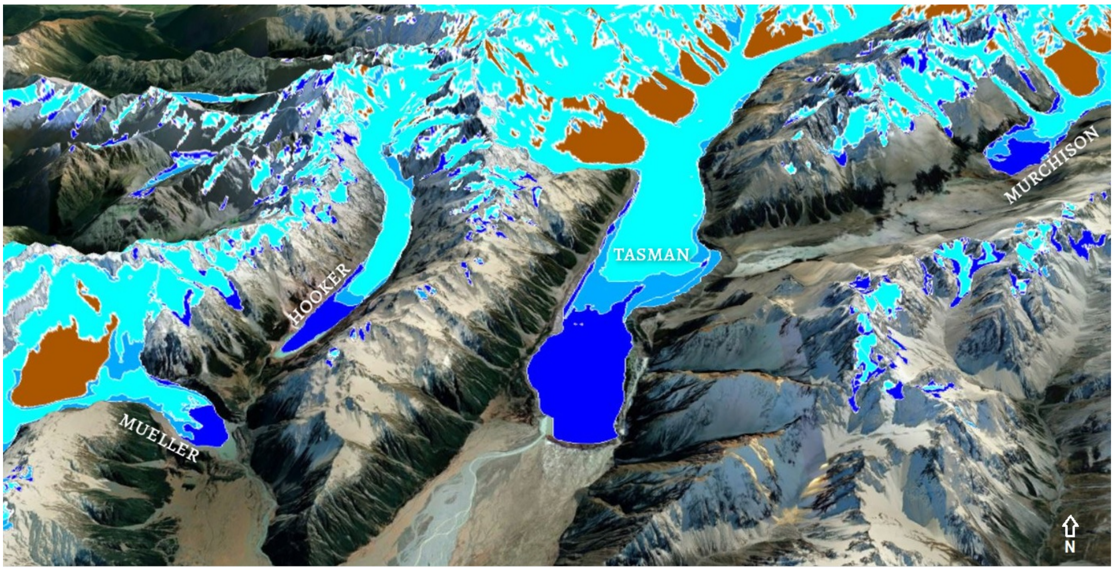

Figure 5.1: Large glaciers within the upper Waitaki catchment. Dark blue represents 1978 glacier outlines, medium blue represent 2009 glacier outlines, and light blue represent 2016 glacier outlines (Baumann et al., 2020). Brown represents rock, cliff faces, or the features that are not ice.

Peak water and the downstream hydrological response were explored in a global study by Huss and Hock (2018) using an RCP4.5 scenario for future projections of glacier change. Basins with large glaciers and high glacierization tend to reach peak water towards the end of the twenty-first century. In contrast, in basins dominated by smaller glaciers, peak water has passed or is expected to occur within the next decade. The Waitaki catchment has an extensive range of different sized glaciers and therefore peak water is more challenging to infer based on glacier size alone. This research suggests that peak water in the Waitaki catchment may occur this century, before 2040 for all RCP scenarios.

In a global study of peak water through the 21st century, Bliss et al. (2014) shows that glacier runoff in New Zealand steadily decreases through the century via three averaged time periods (2003-2022, 2041-2060, and 2080-2099) with an RCP4.5 scenario. This study considered all glaciers within New Zealand, and the lack of projected peak in runoff may be due to the inclusion of a far greater number of smaller glaciers than there are in the Waitaki. Huss and Hock (2018) included New Zealand in their global peak flow and glacier runoff, using the Clutha catchment as a representative watershed to model future glacier change for an

RCP4.5 scenario. This study showed an increase in glacier runoff in all months between December and April by 2050, and a decrease in runoff in February through April by 2090. Though the Clutha catchment holds comparatively less ice than the Waitaki catchment, results from this study regarding peak water agree with the findings by Huss and Hock (2018).

5.4 Implication on downstream environments

Runoff in the Waitaki catchment is important for hydroelectricity generation, water supply storage, and downstream agricultural uses. As most precipitation in the Waitaki occurs in the headwaters (Kingston et al., 2016), downstream services and users are dependent on runoff. Therefore, seasonal shifts and changes to peak flows or low flows are important considerations for downstream water users. Huss et al. (2017) summarises the impact of receding glaciers and reduced precipitation as snow in downstream runoff which can be considered in the context of the Waitaki catchment (Figure 5.2).

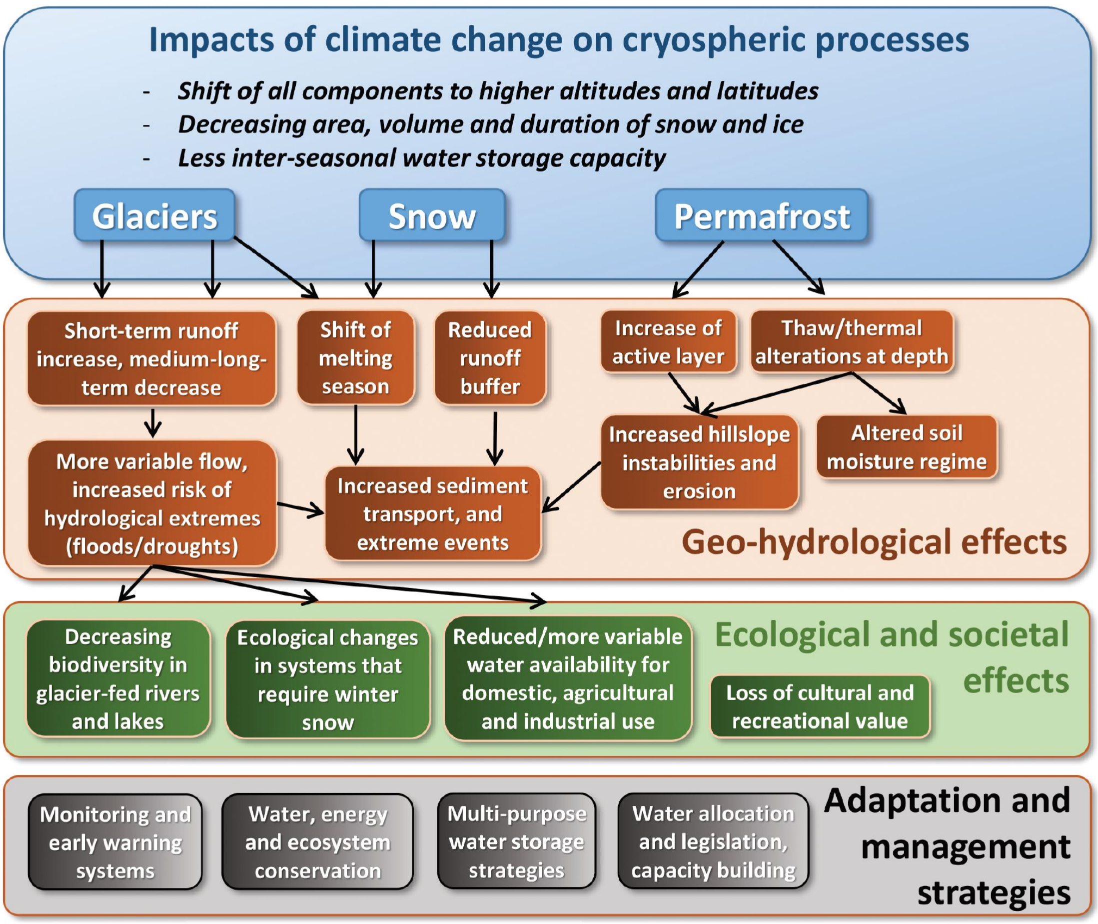

Figure 5.2: Summary of climate change impacts on glaciers and snow from (Huss et al., 2017)

Runoff from glacier melt is likely to vary through the century. The variability can result in more frequent flooding when glaciers are receding, to more frequent droughts when glacier melt contributions are reduced or disappear completely. Therefore, seasonal shifts in timing of glacier melt can exacerbate peak or low flow events (Barnett et al., 2005; Beniston, 2012; Vuille et al., 2018). Although not considered in this work, changes in snowmelt from glacier-free terrain can also influence runoff (Barnett et al., 2005; Knowles et al., 2006). Increased temperatures suggest increases in rainfall during the winter months, leading to greater runoff occurring in autumn, winter, and spring because water is not stored as snow to melt at a later time in the season. Results for the Waitaki catchment show that runoff from glaciers may increase until 2040 before decreasing thereafter for all RCP scenarios. While the initial increase in runoff can be beneficial for hydropower generation in winter when the demand is greatest, or for agriculture in the spring when water demand is highest (Aqualinc Research, 2011; Caruso et al., 2017), it also means that floods caused by peak flows may increase in magnitude and shift in timing.

The Waitaki catchment is a primary producer of hydroelectricity and therefore changes in runoff could affect generation potential. Caruso et al. (2017) noted that seasonal changes in runoff could result in generation demand being met in winter and spring with potential shortfall in summer and autumn. It is possible that shortfalls noted by Caruso et al. (2017) resulting in reduced power generation capacities could be masked by increases in ice melt in glacier runoff, ultimately reducing the number of extreme low flow events during a portion of the 21st century. It should be noted that as temperatures rise due to climate change demand for electricity may also change, such that demand for heating may decrease in the winter, and demand for cooling may increase in the summer (Renwick et al., 2010).

Agriculture, which heavily relies on water supply, is an important industry in New Zealand that has expanded and intensified over the past century (MacLeod and Moller, 2006; Moller et al., 2008). A study by Aqualinc Research (2011) projected future irrigation use in the Rangitata catchment, just north of the Waitaki basin. The study concluded that by 2040, annual irrigation would increase by approximately 6%, with the largest increases in mean monthly irrigation occurring in the summer months of December and January. Water pumping may one reason for the increase in electrical demand (Renwick et al., 2010). Caruso et al. (2017) suggested that projected increases in runoff in the Waitaki catchment during winter and early spring could result in the need to release more water from reservoirs to mitigate over-topping dams and downstream flooding. As such, stored water available for downstream agriculture and irrigation in summer and autumn would decrease when it is needed most (Caruso et al., 2017). Results from this research conversely suggest that increases in ice melt during the summer could reduce water supply issues that could affect agriculture industries and other downstream users. Once peak water passes in the Waitaki catchment, extreme low flow events will likely be of more equal concern. Results for projected increases in runoff and shifts in timing during the winter and spring when runoff is typically at its lowest do agree with findings by Caruso et al. (2017). Finally, projected increases in runoff during the summer when runoff is typically at its highest suggest that flooding risks could be increased. Increasing ice melt contributions to runoff suggest flood risk during periods with high rainfall may become more severe until peak water has passed in the catchment. The flood risks may also shift in timing as a result of large increases in rainfall and ablation projected to occur in spring.

Changes in runoff from glacier retreat could also affect biodiversity and downstream ecology (Milner et al., 2009; Finn et al., 2010), as well as loss of culture value (Allison, 2015; Carey et al., 2017) and recreational value, which is particularly important for New Zealand (McCormack, 1999; Purdie, 2013; Stewart et al., 2016). Mitigating the effect of climate change on runoff is fundamental for a more sustainable long-term water supply. Mitigation strategies may include conservation strategies to increase water supply if needed, decrease energy generation demands, and reduce the impact on downstream ecosystems and planning for extreme flooding events.

5.5 Implication of statistical analysis methods

Results in this thesis show spatially averaged and total annual ablation volume projections from specific glaciers in the Waitaki catchment. While similar trends were noted between projections of spatially average annual ablation volume and total annual ablation volume for a small glacier within the Waitaki catchment (Figure 4.20), projected annual ablation volumes for larger glaciers significantly differed between the two calculation methods (Figures 4.21 and 4.22).

Both projections of total annual ablation volume and spatially averaged ablation volume for a small Waitaki glacier showed decreases in ablation through the century, albeit at different rates. Conversely, projections of spatially averaged annual ablation volume increase over the century in a large glacier because as long as the glacier exists, an increase in temperature will result in an increase in melt despite overall less ice volume and extent through time. Projected total annual ablation volume for large glaciers decreases through the century because the calculation accounts for the overall decreasing ice volume/extent through time.

As such, the results showing average daily time series and average monthly time series of ablation, accumulation, and rainfall throughout this thesis provide some insight into how Waitaki catchment glaciers respond to climate change, but total volume changes of ablation (and accumulation) through time provide further refined insights into glacier response.

Chapter 6

Conclusion

6.1 Summary

The Waitaki catchment is one of New Zealand's most important watersheds for hydroelectricity generation and long-term water supply storage. Runoff in the catchment is generated by rainfall, snow melt, and ice melt. Some of the largest glaciers in New Zealand, such as Tasman, Mueller, Hooker, and Murchison Glaciers, are located in the Waitaki catchment. As climate changes and glaciers recede, their contributions to runoff can also change.

Using an enhanced temperature index model paired with an ice flow model, changes to accumulation, ablation, and rainfall in the Waitaki catchment are projected to 2098 for four RCP scenarios: RCP2.6, RCP4.5, RCP6.0, and RCP8.5. This study investigates how glaciers in the Waitaki catchment are projected to change over the 21st century as accumulation, ablation, and rainfall change. Lastly, the impact of these changes on the timing and magnitude of downstream runoff is explored.

The first objective of this study was to investigate the change in glacier volume in the Waitaki catchment over the 21st century. Glacier volume in the Waitaki catchment is projected to decrease over the 21st century for all RCP scenarios. From 2006 to 2050, there are minimal differences in volume projections between RCP scenarios but after 2050 projections of ice volume for each RCP scenario start diverging. By 2098, ice volume in the Waitaki catchment is projected to decrease by 48% to 52% relative to the 2005 volume for an RCP2.6 scenario. For an RCP8.5 scenario, ice volume is projected to decrease by as much as 76% to 86%.

The second objective of this study was to investigate the changes in accumulation, ablation, and rainfall processes over the 21st century. There is minimal change in average accumulation, ablation, and rainfall projections through the century for an RCP2.6 scenario. Changes in timing and magnitude are projected for all three processes for all other RCP scenarios. The increase in glacier volume loss with increasing RCP scenario is driven by seasonal changes in accumulation and ablation, as well as magnitude changes in ablation. At the end of the century (2068-2098) for RCP8.5, average ablation is projected to increase in every month, with the largest increase of 122% relative to RCP2.6 occurring in September. Seasonal shifts in ablation suggest more ice melt may occur in the spring and autumn months, relative to the RCP2.6 scenario. Conversely, average accumulation is projected to decrease in all months except winter when accumulation is typically the highest. Changes in accumulation and ablation reflect the average changes projected across a given glacier in the Waitaki catchment, despite its size. Average rainfall is projected to increase in all months by the end of the century for all RCP scenarios relative to RCP2.6, with increases by as much as 280% occurring in the winter months when rainfall is usually the lowest.

The third objective of this study was to investigate how runoff from glaciers may change. Ice melt contributions to runoff increase as glaciers recede to a point of "peak water", after which contributions decrease because glaciers either shrink or disappear completely. Different sized glaciers in the Waitaki catchment will reach peak water at different times but as a whole, peak water is projected to occur in the Waitaki catchment during the 21st century, specifically before 2040, for all RCP scenarios.

While glaciers recede, contributions to runoff from ice melt are known to mitigate low flow events and potential water shortages (Fountain and Tangborn, 1985; Young and Hewitt, 1993; Hopkinson and Young, 1998; Sirguey, 2010). The implication of projected changes to runoff suggests that temporary increases in ice melt during dry periods can reduce the number or severity of low flow events that could affect power generation, agriculture industries, and other downstream users. Projected increases in ice melt during the summer periods when runoff is typically at its highest also suggest that flood risks could increase. Once peak water passes in the Waitaki catchment and contributions to runoff from ice melt decrease, extreme low flow events may be more of a concern during dry periods with reduced rainfall.

6.2 Recommendations for future work

Understanding the impact of climate change on glacier mass balance and the implications on quantity and timing of meltwater runoff is due to the complex and dynamic nature of interactions between hydroclimatological processes (Milner et al., 2009). The challenges are further magnified when projecting these processes and interactions into the future due to the uncertainty of eventuating climate change scenarios. Further work to improve climate change projections at the end of the century would add clarity and reduce uncertainty around potential changes to runoff contributions and the implications to downstream hydrology, but this endeavour is also the most challenging improvement to achieve.

Comparing statistical analysis methods confirm variations in projections of annual ablation volume. Daily and monthly time series of spatially averaged accumulation and ablation across Waitaki glaciers provide some insights on glacier response to climate change but this study would be strengthened by using total accumulation and ablation volumes in daily and monthly time series to further refine results presented in this thesis.

Further, there are presently limited studies that explicitly consider glacier melt contributions to runoff in catchments on the South Island of New Zealand. This study focuses on accumulation, ablation, and rainfall that occurs on glaciers in the Waitaki catchment, and it does not consider the impact of climate change on runoff contributions across the whole catchment, accounting for all non-glacierized area. Coupling mass balance and ice flow models to catchment-wide hydrology models would add clarity around potential changes of runoff contributions to downstream hydrology.

Finally, further studies of the increasing or decreasing demand of hydroelectricity, or water supply for agriculture industries or other downstream users with respect to climate change in future time periods will aid in understanding the potential pressure on runoff and help to inform long-term water resource planning.

References

Ackerley, D., Dean, S., Sood, A., and Mullan, A. B. 2012. Regional climate modelling in New Zealand: comparison to gridded and satellite observations. *Weather and Climate*, 32(1):3–22.

Aizen, V. B., Aizen, E. M., and Melack, J. M. 1996. Precipitation, melt and runoff in the northern tien shan. *Journal of Hydrology*, 186(1-4):229–251.

Akhtar, M., Ahmad, N., and Booij, M. J. 2008. The impact of climate change on the water resources of hindukush–karakorum–himalaya region under different glacier coverage scenarios. *Journal of hydrology*, 355(1-4):148–163.

Allison, E. A. 2015. The spiritual significance of glaciers in an age of climate change. *Wiley Interdisciplinary Reviews: Climate Change*, 6(5):493–508.

Ambach, W. 1988. Interpretation of the positive-degree-days factor by heat balance characteristics–west greenland. *Hydrology Research*, 19(4):217–224.

Anderson, B., Mackintosh, A. N., Dadić, R., Oerlemans, J., Zammit, C., Doughty, A., Sood, A., and Mullan, B. 2021. Modelled response of debris-covered and lake-calving glaciers to climate change, Kā Tiritiri o te Moana/Southern Alps, New Zealand. *Global and Planetary Change*, page 103593.

Anderton, P. 1973. The significance of perennial snow and ice to the water resources of the South Island, New Zealand. *Journal of Hydrology (New Zealand)*, pages 6–18.

Aqualinc Research. 2011. Projected effects of climate change on water supply reliability in mid-Canterbury. *MAF Technical Paper No 2011/12.*

Arnell, N. W. 1999. Climate change and global water resources. *Global environmental change*, 9:S31–S49.

Arnold, N., Willis, I., Sharp, M., Richards, K., and Lawson, W. 1996. A distributed surface energy-balance model for a small valley glacier. i. development and testing for haut glacier d'arolla, valais, switzerland. *Journal of Glaciology*, 42(140):77–89.

Barnett, T. P., Adam, J. C., and Lettenmaier, D. P. 2005. Potential impacts of a warming climate on water availability in snow-dominated regions. *Nature*, 438 (7066):303–309.

Baumann, S., Anderson, B., Chinn, T., Mackintosh, A., Collier, C., Lorrey, A. M., Rack, W., Purdie, H., and Eaves, S. 2020. Updated inventory of glacier ice in New Zealand based on 2016 satellite imagery. *Journal of Glaciology*, pages 1–14.

Becker, A. Runoff processes in mountain headwater catchments: recent understanding and research challenges. In *Global change and mountain regions*, pages 283–295. Springer, 2005.

Beniston, M. 2003. Climatic change in mountain regions: a review of possible impacts. *Climate variability and change in high elevation regions: Past, present & future*, pages 5–31.

Beniston, M. The risks associated with climatic change in mountain regions. In *Global change and mountain regions*, pages 511–519. Springer, 2005.

Beniston, M. 2012. Impacts of climatic change on water and associated economic activities in the swiss alps. *Journal of Hydrology*, 412:291–296.

Beniston, M., Fox, D. G., Adhikary, S., Andressen, R., Guisan, A., Holten, J., Innes, J., Maitima, J., Price, M., Tessier, L., et al. 1996. Impacts of climate change on mountain regions.

Benn, D. I. and Lehmkuhl, F. 2000. Mass balance and equilibrium-line altitudes of glaciers in high-mountain environments. *Quaternary International*, 65:15–29.

Bhutiyani, M. 1999. Mass-balance studies on siachen glacier in the nubra valley, karakoram himalaya, india. *Journal of Glaciology*, 45(149):112–118.

Bliss, A., Hock, R., and Radić, V. 2014. Global response of glacier runoff to twenty-first century climate change. *Journal of Geophysical Research: Earth Surface*, 119(4):717–730.

Braithwaite, R. J. and Zhang, Y. 1999. Modelling changes in glacier mass balance that may occur as a result of climate changes. *Geografiska Annaler: Series A, Physical Geography*, 81(4):489–496.

Braithwaite, R. J., Konzelmann, T., Marty, C., and Olesen, O. B. 1998. Errors in daily ablation measurements in northern Greenland, 1993-94, and their implications for glacier climate studies. *Journal of Glaciology*, 44(148):583–588.

Braithwaite, R. J. 1984. Calculation of degree-days for glacier-climate research. *Z. Gletscherkd. Glazialgeol*, 20:1–20.

Braithwaite, R. J. 2002. Glacier mass balance: the first 50 years of international monitoring. *Progress in Physical Geography*, 26(1):76–95.

Canterbury Maps, n.d. Canterbury maps open data. `https://opendata.canterburymaps.govt.nz/`. Accessed: 2021-10-15.

Carenzo, M., Pellicciotti, F., and Burlando, P. Modeling distributed glacier ablation for climate change simulations: comparison of an energy-balance and an enhanced temperature-index model. In *AGU Fall Meeting Abstracts*, volume 2010, pages C23A–0588, 2010.

Carenzo, M. 2012. *Distributed modelling of changes in glacier mass balance and runoff*. PhD thesis, ETH Zurich.

Carey, M., Molden, O. C., Rasmussen, M. B., Jackson, M., Nolin, A. W., and Mark, B. G. 2017. Impacts of glacier recession and declining meltwater on mountain societies. *Annals of the American Association of Geographers*, 107 (2):350–359.

Caruso, B. S., King, R., Newton, S., and Zammit, C. 2017. Simulation of climate change effects on hydropower operations in mountain headwater lakes, New Zealand. *River research and applications*, 33(1):147–161.

Cherry, J. E., Knapp, C., Trainor, S., Ray, A. J., Tedesche, M., and Walker, S. 2017. Planning for climate change impacts on hydropower in the far north. *Hydrology and Earth System Sciences*, 21(1):133–151.

Chinn, T., Fitzharris, B., Willsman, A., and Salinger, M. 2012. Annual ice volume changes 1976–2008 for the New Zealand southern alps. *Global and Planetary Change*, 92:105–118.

Chinn, T. J. 2001. Distribution of the glacial water resources of New Zealand. *Journal of Hydrology (New Zealand)*, pages 139–187.

Chinn, T. 1995. Glacier fluctuations in the southern alps of new zealand determined from snowline elevations. *Arctic and alpine research*, 27(2):187–198.

Cogley, J. G., Arendt, A. A., Bauder, A., Braithwaite, R., Hock, R., Jansson, P., Kaser, G., Moller, M., Nicholson, L., Rasmussen, L. A., et al. 2010. Glossary of glacier mass balance and related terms.

Cogley, J. G. 2009. Geodetic and direct mass-balance measurements: comparison and joint analysis. *Annals of Glaciology*, 50(50):96–100.

Collins, D. B. 2020. New Zealand river hydrology under late 21st century climate change. *Water*, 12(8):2175.

Conway, J., 2019. How do clouds modify the response of mountain glaciers to climate change? `https://niwa.co.nz/freshwater-and-estuaries/research-projects/how-do-clouds-modify-the-response-of-mountain-glaciers-to-climate-change`. Accessed: 2021-05-10.

Corripio, J. G. 2003. Vectorial algebra algorithms for calculating terrain parameters from dems and solar radiation modelling in mountainous terrain. *International Journal of Geographical Information Science*, 17(1):1–23.

Cuffey, K. M. and Paterson, W. S. B. 2010. The physics of glaciers. Academic Press.

Cullen, N. J., Anderson, B., Sirguey, P., Stumm, D., Mackintosh, A., Conway, J. P., Horgan, H. J., Dadić, R., Fitzsimons, S. J., and Lorrey, A. 2017. An 11-year record of mass balance of Brewster Glacier, New Zealand, determined using a geostatistical approach. *Journal of Glaciology*, 63(238):199–217.

Dadic, R., Mott, R., Lehning, M., and Burlando, P. 2010. Wind influence on snow depth distribution and accumulation over glaciers. *Journal of Geophysical Research: Earth Surface*, 115(F1).

DeBeer, C. M., Wheater, H. S., Carey, S. K., and Chun, K. P. 2016. Recent climatic, cryospheric, and hydrological changes over the interior of western canada: a review and synthesis. *Hydrology and Earth System Sciences*, 20(4):1573–1598.

DeBeer, C. M., Sharp, M., and Schuster-Wallace, C. 2020. Glaciers and ice sheets. *World*, 215(705,739):1565.

Edenhofer, O., Pichs-Madruga, R., Sokona, Y., Farahani, E., Kadner, S., Seyboth, K., Adler, A., Baum, I., Brunner, S., Eickemeier, P., Kriemann, B., Savolainen, J., Schlömer, S., von Stechow, C., Zwickel, T., and Minx, J. C. 2014. Summary for policymakers. *Climate Change 2014: Mitigation of Climate Change. Contribution of Working Group III to the Fifth Assessment Report of the Intergovernmental Panel on Climate Change*.

Edwards, P. N. 2011. History of climate modeling. *Wiley Interdisciplinary Reviews: Climate Change*, 2(1):128–139.

Falkenmark, M. and Chapman, T. 1989. Comparative hydrology: An ecological approach to land and water resources. Unesco.

Filion, Y. 2000. Climate change: implications for canadian water resources and hydropower production. *Canadian Water Resources Journal*, 25(3):255–269.

Finn, D. S., Raesaenen, K., and Robinson, C. T. 2010. Physical and biological changes to a lengthening stream gradient following a decade of rapid glacial recession. *Global Change Biology*, 16(12):3314–3326.

Fitzharris, B., Lawson, W., and Owens, I. 1999. Research on glaciers and snow in New Zealand. *Progress in Physical Geography*, 23(4):469–500.

Forster, P., Ramaswamy, V., Artaxo, P., Berntsen, T., Betts, R., Fahey, D. W., Haywood, J., Lean, J., Lowe, D. C., Myhre, G., et al. 2007. Climate change 2007. the physcial science basis. changes in atmospheric constituents and in radiative forcing.

Fountain, A. G. and Tangborn, W. V. 1985. The effect of glaciers on streamflow variations. *Water Resources Research*, 21(4):579–586.

Francou, B., Ribstein, P., Wagnon, P., Ramirez, E., and Pouyaud, B. Glaciers of the tropical andes: indicators of global climate variability. In *Global change and mountain regions*, pages 197–204. Springer, 2005.

Gu, L., Baldocchi, D., Verma, S. B., Black, T., Vesala, T., Falge, E. M., and Dowty, P. R. 2002. Advantages of diffuse radiation for terrestrial ecosystem productivity. *Journal of Geophysical Research: Atmospheres*, 107(D6):ACL–2.

Hambrey, M. J., Alean, J., Alean, J., and Alean, J. 2004. Glaciers. volume 376. Cambridge University Press Cambridge.

Hansen, J., Sato, M., Kharecha, P., and Schuckmann, K. v. 2011. Earth's energy imbalance and implications. *Atmospheric Chemistry and Physics*, 11(24):13421–13449.

Hochstein, M. P., Claridge, D., Henrys, S. A., Pyne, A., Nobes, D. C., and Leary, S. F. 1995. Downwasting of the Tasman Glacier, South Island, New Zealand: changes in the terminus region between 1971 and 1993. *New Zealand journal of geology and geophysics*, 38(1):1–16.

Hock, R. 1999. A distributed temperature-index ice-and snowmelt model including potential direct solar radiation. *Journal of glaciology*, 45(149):101–111.

Hock, R. 2003. Temperature index melt modelling in mountain areas. *Journal of hydrology*, 282(1-4):104–115.

Hock, R. 2005. Glacier melt: a review of processes and their modelling. *Progress in physical geography*, 29(3):362–391.

Hock, R., Rasul, G., Adler, C., Cáceres, B., Gruber, S., Hirabayashi, Y., Jackson, M., Kääb, A., Kang, S., Kutuzov, S., Milner, A., Molau, U., Morin, S., Orlove, B., and Steltzer, H. 2019. High mountain areas. *IPCC Special Report on the Ocean and Cryosphere in a Changing Climate*, In press.

Hock, R., Bliss, A., Marzeion, B., Giesen, R. H., Hirabayashi, Y., Huss, M., Radić, V., and Slangen, A. B. 2019. Glaciermip–a model intercomparison of global-scale glacier mass-balance models and projections. *Journal of Glaciology*, 65 (251):453–467.

Hopkinson, C. and Young, G. J. 1998. The effect of glacier wastage on the flow of the Bow River at Banff, Alberta, 1951–1993. *Hydrological Processes*, 12(10-11): 1745–1762.

Huss, M. and Hock, R. 2015. A new model for global glacier change and sea-level rise. *Frontiers in Earth Science*, 3:54.

Huss, M. and Hock, R. 2018. Global-scale hydrological response to future glacier mass loss. *Nature Climate Change*, 8(2):135–140.

Huss, M., Bookhagen, B., Huggel, C., Jacobsen, D., Bradley, R. S., Clague, J. J., Vuille, M., Buytaert, W., Cayan, D. R., Greenwood, G., et al. 2017. Toward mountains without permanent snow and ice. *Earth's Future*, 5(5):418–435.

Huybrechts, P. Ice sheet modeling. In *Encyclopedia of the Antarctic*, pages 514–517. Routledge, 2007.

Huybrechts, P. and Oerlemans, J. 1990. Response of the Antarctic ice sheet to future greenhouse warming. *Climate Dynamics*, 5(2):93–102.

Immerzeel, W. W., Lutz, A., Andrade, M., Bahl, A., Biemans, H., Bolch, T., Hyde, S., Brumby, S., Davies, B., Elmore, A., et al. 2020. Importance and vulnerability of the world's water towers. *Nature*, 577(7790):364–369.

IPCC, n.d. The intergovernmental panel on climate change. `https://www.ipcc.ch/`. Accessed: 2021-06-26.

IPCC Data Distribution Centre, n.d. What is a gcm? `https://www.ipcc-data.org/guidelines/pages/gcm_guide.html`. Accessed: 2021-06-25.

Jakeman, A. and Hornberger, G. 1993. How much complexity is warranted in a rainfall-runoff model? *Water resources research*, 29(8):2637–2649.

Jansson, P., Hock, R., and Schneider, T. 2003. The concept of glacier storage: a review. *Journal of Hydrology*, 282(1-4):116–129.

Jóhannesson, T., Sigurdsson, O., Laumann, T., and Kennett, M. 1995. Degree-day glacier mass-balance modelling with applications to glaciers in iceland, norway and greenland. *Journal of Glaciology*, 41(138):345–358.

Kaser, G., Großhauser, M., and Marzeion, B. 2010. Contribution potential of glaciers to water availability in different climate regimes. *Proceedings of the National Academy of Sciences*, 107(47):20223–20227.

Kerr, T. 2013. The contribution of snowmelt to the rivers of the South Island, New Zealand. *Journal of Hydrology (New Zealand)*, pages 61–82.

Kerr, T., Owens, I., and Henderson, R. 2011. The precipitation distribution in the Lake Pukaki catchment. *Journal of Hydrology (New Zealand)*, 50(2):361–382.

Kiehl, J. T. and Trenberth, K. E. 1997. Earth's annual global mean energy budget. *Bulletin of the American meteorological society*, 78(2):197–208.

Kingston, D. G., Webster, C. S., and Sirguey, P. 2016. Atmospheric circulation drivers of lake inflow for the Waitaki River, New Zealand. *International Journal of Climatology*, 36(3):1102–1113.

Kirchner, N., Ahlkrona, J., Gowan, E. J., Lötstedt, P., Lea, J. M., Noormets, R., von Sydow, L., Dowdeswell, J. A., and Benham, T. 2016. Shallow ice approximation, second order shallow ice approximation, and full stokes models: A discussion of their roles in palaeo-ice sheet modelling and development. *Quaternary Science Reviews*, 147:136–147.

Kirkbride, M. P. and Warren, C. R. 1999. Tasman Glacier, New Zealand: 20th-century thinning and predicted calving retreat. *Global and Planetary Change*, 22(1-4):11–28.

Knowles, N., Dettinger, M. D., and Cayan, D. R. 2006. Trends in snowfall versus rainfall in the western united states. *Journal of Climate*, 19(18):4545–4559.

Kulkarni, A. V. 1992. Mass balance of himalayan glaciers using aar and ela methods. *Journal of Glaciology*, 38(128):101–104.

Kustas, W. P., Rango, A., and Uijlenhoet, R. 1994. A simple energy budget algorithm for the snowmelt runoff model. *Water Resources Research*, 30(5): 1515–1527.

Laha, S., Kumari, R., Singh, S., Mishra, A., Sharma, T., Banerjee, A., Nainwal, H. C., and Shankar, R. 2017. Evaluating the contribution of avalanching to the mass balance of himalayan glaciers. *Annals of Glaciology*, 58(75pt2):110–118.

Lang, H. Forecasting meltwater runoff from snow-covered areas and from glacier basins. In *River flow modelling and forecasting*, pages 99–127. Springer, 1986.

Laumann, T. and Reeh, N. 1993. Sensitivity to climate change of the mass balance of glaciers in southern norway. *Journal of Glaciology*, 39(133):656–665.

Le Meur, E. and Vincent, C. 2003. A two-dimensional shallow ice-flow model of glacier de saint-sorlin, france. *Journal of Glaciology*, 49(167):527–538.

Leong, D. and Chesterton, J. Waitaki catchment, hydrological information. Report commissioned by the Ministry for the Environment for consideration by the Waitaki Catchment Water Allocation Board 582, Ministry for the Environment, Wellington, New Zealand, 2005.

Lindsey, R. 2009. Climate and earth's energy budget. *NASA Earth Observatory*, 680.

Mackintosh, A. N., Anderson, B. M., Lorrey, A. M., Renwick, J. A., Frei, P., and Dean, S. M. 2017. Regional cooling caused recent New Zealand glacier advances in a period of global warming. *Nature Communications*, 8(1):1–13.

MacLeod, C. J. and Moller, H. 2006. Intensification and diversification of New Zealand agriculture since 1960: An evaluation of current indicators of land use change. *Agriculture, ecosystems & environment*, 115(1-4):201–218.

Manabe, S. 1969. Climate and the ocean circulation: I. the atmospheric circulation and the hydrology of the earth's surface. *Monthly weather review*, 97(11):739–774.

Marzeion, B., Hock, R., Anderson, B., Bliss, A., Champollion, N., Fujita, K., Huss, M., Immerzeel, W. W., Kraaijenbrink, P., Malles, J.-H., et al. 2020. Partitioning the uncertainty of ensemble projections of global glacier mass change. *Earth's Future*, 8(7):e2019EF001470.

McCormack, T. 1999. *Glacier advance: the development of tourism at Franz Josef Glacier, 1865-1965*. PhD thesis, University of Otago.

McKerchar, A., Pearson, C., and Fitzharris, B. 1998. Dependency of summer lake inflows and precipitation on spring soi. *Journal of Hydrology*, 205(1-2):66–80.

Meehl, G. A., Boer, G. J., Covey, C., Latif, M., and Stouffer, R. J. 2000. The coupled model intercomparison project (cmip). *Bulletin of the American Meteorological Society*, 81(2):313–318.

Meier, M. F. and Tangborn, W. V. 1961. Distinctive characteristics of glacier runoff. *US Geological Survey Professional Paper*, 424:14–16.

Meier, M. F. 1969. Glaciers and water supply. *Journal-American Water Works Association*, 61(1):8–12.

Milner, A. M., Brown, L. E., and Hannah, D. M. 2009. Hydroecological response of river systems to shrinking glaciers. *Hydrological Processes: An International Journal*, 23(1):62–77.

Ministry for the Environment, 2018. Climate change projections for New Zealand: atmosphere projections based on simulations from the IPCC Fifth Assessment, 2nd edition. Technical report.

Moller, H., MacLeod, C. J., Haggerty, J., Rosin, C., Blackwell, G., Perley, C., Meadows, S., Weller, F., and Gradwohl, M. 2008. Intensification of New Zealand agriculture: implications for biodiversity. *New Zealand Journal of Agricultural Research*, 51(3):253–263.

Mullan, B., Porteous, A., Wratt, D., and Hollis, M. 2005. Changes in drought risk with climate change. *Prepared for Ministry for the Environment (NZ Climate Change Office) and Ministry of Agriculture and Forestry. NIWA Client Report: WLG2005–23.(National Institute of Water and Atmospheric Research, Wellington).*

Oerlemans, J. and Fortuin, J. 1992. Sensitivity of glaciers and small ice caps to greenhouse warming. *Science*, 258(5079):115–117.

Oerlemans, J. and Klok, E. L. 2004. Effect of summer snowfall on glacier mass balance. *Annals of Glaciology*, 38:97–100.

Orlove, B. 2009. Glacier retreat: reviewing the limits of human adaptation to climate change. *Environment: Science and Policy for Sustainable Development*, 51(3):22–34.

Østrem, G. 1975. Erts data in glaciology—an effort to monitor glacier mass balance from satellite imagery. *Journal of Glaciology*, 15(73):403–415.

Østrem, G. and Brugman, M. 1966. Glacier mass balance measurements. Department of Mines and Technical Surveys, Glaciology Section.

Paul, F., Machguth, H., Hoelzle, M., Salzmann, N., and Haeberli, W. 2008. Alpinewide distributed glacier mass balance modeling. *Darkening peaks: glacier retreat, science, and society*, page 111.

Pielke, J. R., Burgess, M. G., and Ritchie, J. 2021. Most plausible 2005-2040 emissions scenarios project less than 2.5 degrees c of warming by 2100.

Poyck, S., Hendrikx, J., McMillan, H., Hreinsson, E. Ö., and Woods, R. 2011. Combined snow and streamflow modelling to estimate impacts of climate change on water resources in the Clutha River, New Zealand. *Journal of Hydrology (New Zealand)*, pages 293–311.

Purdie, H., Kerr, T., Rack, W., and Lorrey, A. 2021. Rolleston glacier: First decade of mass balance measurement and the implications of climate change on mass balance monitoring.

Purdie, H. 2013. Glacier retreat and tourism: Insights from New Zealand. *Mountain Research and Development*, 33(4):463–472.

Purdie, J. and Bardsley, W. E. 2010. Seasonal prediction of lake inflows and rainfall in a hydro-electricity catchment, Waitaki river, New Zealand. *International Journal of Climatology: A Journal of the Royal Meteorological Society*, 30(3): 372–389.

Purdie, J. and Fitzharris, B. 1999. Processes and rates of ice loss at the terminus of Tasman Glacier, New Zealand. *Global and Planetary Change*, 22(1-4):79–91.

Quincey, D. J. and Glasser, N. F. 2009. Morphological and ice-dynamical changes on the Tasman Glacier, New Zealand, 1990–2007. *Global and Planetary Change*, 68(3):185–197.

Radić, V., Bliss, A., Beedlow, A. C., Hock, R., Miles, E., and Cogley, J. G. 2014. Regional and global projections of twenty-first century glacier mass changes in response to climate scenarios from global climate models. *Climate Dynamics*, 42(1-2):37–58.

Rasouli, K., Pomeroy, J. W., Janowicz, J. R., Carey, S. K., and Williams, T. J. 2014. Hydrological sensitivity of a northern mountain basin to climate change. *Hydrological Processes*, 28(14):4191–4208.

Reeh, N. 1991. Parameterization of melt rate and surface temperature in the greenland ice sheet. *Polarforschung*, 59(3):113–128.

Renwick, J., Mladenov, P., Purdie, J., McKerchar, A., and Jamieson, D. 2010. The effects of climate variability and change upon renewable electricity in New Zealand. *Climate change adaptation in New Zealand: Future scenarios and some sectoral perspectives*, pages 70–81.

RGI, 2017. Randolph Glacier Inventory, A Dataset of Global Glacier Outlines: Version 6.0: Technical Report, Global Land Ice Measurements from Space, Colorado, USA. Digital Media. doi:10.7265/N5-RGI-60.

Rignot, E., Mouginot, J., and Scheuchl, B. 2011. Ice flow of the antarctic ice sheet. *Science*, 333(6048):1427–1430.

Rummukainen, M. 2010. State-of-the-art with regional climate models. *Wiley Interdisciplinary Reviews: Climate Change*, 1(1):82–96.

Salinger, J., Gray, W., Mullan, B., and Wratt, D., 2004. Atmospheric circulation and precipitation.

Schaefli, B., Manso, P., Fischer, M., Huss, M., and Farinotti, D. 2019. The role of glacier retreat for swiss hydropower production. *Renewable energy*, 132:615–627.

Seddik, H., Greve, R., Zwinger, T., Gillet-Chaulet, F., and Gagliardini, O. 2012. Simulations of the greenland ice sheet 100 years into the future with the full stokes model elmer/ice. *Journal of Glaciology*, 58(209):427–440.

Shanley, C. S., Pyare, S., Goldstein, M. I., Alaback, P. B., Albert, D. M., Beier, C. M., Brinkman, T. J., Edwards, R. T., Hood, E., MacKinnon, A., et al. 2015. Climate change implications in the northern coastal temperate rainforest of north america. *Climatic Change*, 130(2):155–170.

Shannon, S., Smith, R., Wiltshire, A., Payne, T., Huss, M., Betts, R., Caesar, J., Koutroulis, A., Jones, D., and Harrison, S. 2019. Global glacier volume projections under high-end climate change scenarios. *The Cryosphere*, 13(1): 325–350.

Sicart, J.-E., Pomeroy, J., Essery, R., and Bewley, D. 2006. Incoming longwave radiation to melting snow: observations, sensitivity and estimation in northern environments. *Hydrological processes*, 20(17):3697–3708.

Sirguey, P. J. B. 2010. *Monitoring snow cover and modelling catchment discharge with remote sensing in the Upper Waitaki Basin, New Zealand*. PhD thesis, University of Otago.

Soruco, A., Vincent, C., Francou, B., Ribstein, P., Berger, T., Sicart, J., Wagnon, P., Arnaud, Y., Favier, V., and Lejeune, Y. 2009. Mass balance of glaciar zongo, bolivia, between 1956 and 2006, using glaciological, hydrological and geodetic methods. *Annals of Glaciology*, 50(50):1–8.

Stenborg, T. 1970. Delay of run-off from a glacier basin. *Geografiska Annaler: Series A, Physical Geography*, 52(1):1–30.

Stewart, E. J., Wilson, J., Espiner, S., Purdie, H., Lemieux, C., and Dawson, J. 2016. Implications of climate change for glacier tourism. *Tourism Geographies*, 18(4):377–398.

Stocker, T., Qin, D., Plattner, G.-K., Tignor, M., Allen, S., Boschung, J., Nauels, A., Xia, Y., Bex, V., and Midgley, P. 2013. Summary for policymakers. *Climate change 2013: The physical science basis. Working Group I contribution to the Fifth assessment report of the Intergovernmental Panel on Climate Change.*

Taylor, K. E., Stouffer, R. J., and Meehl, G. A. 2012. An overview of cmip5 and the experiment design. *Bulletin of the American meteorological Society*, 93(4): 485–498.

Touzé-Peiffer, L., Barberousse, A., and Le Treut, H. 2020. The coupled model intercomparison project: History, uses, and structural effects on climate research. *Wiley Interdisciplinary Reviews: Climate Change*, 11(4):e648.

Trenberth, K. E., Fasullo, J. T., and Kiehl, J. 2009. Earth's global energy budget. *Bulletin of the American Meteorological Society*, 90(3):311–324.

Trenberth, K. E., Fasullo, J. T., and Balmaseda, M. A. 2014. Earth's energy imbalance. *Journal of Climate*, 27(9):3129–3144.

Van Vuuren, D. P., Edmonds, J., Kainuma, M., Riahi, K., Thomson, A., Hibbard, K., Hurtt, G. C., Kram, T., Krey, V., Lamarque, J.-F., et al. 2011. The representative concentration pathways: an overview. *Climatic change*, 109(1): 5–31.

Vargo, L. J., Anderson, B. M., Dadić, R., Horgan, H. J., Mackintosh, A. N., D., K. A., and Lorrey, A. M. 2020. Anthropogenic warming forces extreme annual glacier mass loss. *Nature Climate Change*, 10(9):856–861.

Vergara, W., Deeb, A., Valencia, A., Bradley, R., Francou, B., Zarzar, A., Grünwaldt, A., and Haeussling, S. 2007. Economic impacts of rapid glacier retreat in the Andes. *Eos, Transactions American Geophysical Union*, 88(25): 261–264.

Viviroli, D. and Weingartner, R. 2004. The hydrological significance of mountains: from regional to global scale. *Hydrology and earth system sciences*, 8(6):1017–1030.

Viviroli, D., Archer, D. R., Buytaert, W., Fowler, H. J., Greenwood, G. B., Hamlet, A. F., Huang, Y., Koboltschnig, G., Litaor, M., López-Moreno, J. I., et al. 2011. Climate change and mountain water resources: overview and recommendations for research, management and policy. *Hydrology and Earth System Sciences*, 15(2):471–504.

Vuille, M., Carey, M., Huggel, C., Buytaert, W., Rabatel, A., Jacobsen, D., Soruco, A., Villacis, M., Yarleque, C., Timm, O. E., et al. 2018. Rapid decline of snow and ice in the tropical andes–impacts, uncertainties and challenges ahead. *Earth-Science Reviews*, 176:195–213.

Wilcox, B. P., Seyfried, M. S., and Matison, T. H. 1991. Searching for chaotic dynamics in snowmelt runoff. *Water Resources Research*, 27(6):1005–1010.

Wild, M., Folini, D., Schär, C., Loeb, N., Dutton, E. G., and König-Langlo, G. 2013. The global energy balance from a surface perspective. *Climate dynamics*, 40(11-12):3107–3134.

Woo, M.-k. and Fitzharris, B. 1992. Reconstruction of mass balance variations for Franz Josef Glacier, New Zealand, 1913 to 1989. *Arctic and Alpine Research*, 24(4):281–290.

Woo, M.-K. and Liu, C. 1994. Mountain hydrology of canada and china: A case study in comparative hydrology. *Hydrological processes*, 8(6):573–587.

Young, G. and Hewitt, K. 1993. Glaciohydrological features of the Karakoram Himalaya: measurement possibilities and constraints. *IAHS Publications-Publications of the International Association of Hydrological Sciences*, 218:273–284.

Zammit, C. and Woods, R. 2011. Projected climate and river flow for the Waimakariri catchment for 2040s and 2090s. *NIWA Client Report CHCH2011*, 25:52.